2002

Development of catalytic processes for aromatic amides and carboxylic acids

Yujun Song
Louisiana State University and Agricultural and Mechanical College, ysong2@lsu.edu

DEVELOPMENT OF CATALYTIC PROCESSES FOR AROMATIC AMIDES AND CARBOXYLIC ACIDS

A Thesis

Submitted to the Graduate Faculty of the
Louisiana State University and
Agricultural and Mechanical College
in partial fulfillment of the
requirements for the degree of
Master of Science in Chemical Engineering

In

The Department of Chemical Engineering

by
Yujun Song
B.S., Nanjing University of Chemical Technology, 1992
M.S., Beijing University of Chemical Technology, 1997
December 2002

Acknowledgements

Many thanks are due to many people who have assisted me in the completion of this project. Thanks to EagleView Technologies and MGK Co. for providing the funding for my research. My advisor, Dr. Kerry M. Dooley, has been an inspiration; his endless knowledge and motivation were irreplaceable. I would also like to thank my committee members, Dr. Thomas J. Cleij and Dr. F. Carl Knopf, Kathy Hart, Dana Doucet and Dr. Karen Xu were very helpful in providing previous experimental data and in catalyst preparation. Lastly, I would like to thank my wife, family, and friends for their continual support and advice over the past two years.

Table of Contents

List of Tables

List of Figures

List of Schemes

Abstract

New catalysts were prepared and studied for: (1) a model amidation with a hindered amine, diethylamine (DEA), to N,N'-diethyltoluamide (DEET); (2) the oxidation of m-xylene (MX) to DEET's alkylaromatic precursor, m-toluic acid (MTA). The catalysts were further characterized on the basis of surface area, ligand or metal contents by thermogravimetric methods, acid site contents by 1-propylamine temperature-programmed desorption, and chemical structure by FT-IR.

Thermodynamic analyses showed that the amidation to produce DEET from MTA and DEA was an equilibrium limited reaction with equilibrium constants (K_e) less than 41 at temperatures below 320°C. The kinetics on silica-supported titanium (IV) (triethanolaminato)-isopropoxide (Tyzor TE), calcium hydroxyapatites and silica supported tungsten heteropolyacids were studied using a continuous reactor. Although both supported acid and weak base catalysts can selectively catalyze the amidation reaction, both porous hydroxyapatites and heteropolyacids on silica proved to be superior to merely supporting the Ti-amine complexes currently used as homogeneous catalysts. These acidic catalysts were more active, more stable in the presence of a gas phase, and, unlike previous heterogeneous catalysts examined for this reaction, can be used with near stoichiometric feeds. The best results (about 65-70% MTA conversion and 93-97% DEET selectivity) were obtained using supported tungsten heteropolyacids at a WHSV of 3-9 h^{-1} using a feed of molar ratio DEA/MTA/DEET = 1/1/0.4 at 300ºC and low pressure. This catalyst can last at least 24 h without regeneration and showed no sign of apparent deactivation in 11 days of operation if there were periodic overnight air treatments at 450ºC.

The kinetics of soluble Co, Co/Mn, Co/Mn/Br, and Co/Mn/Ce catalysts for m-xylene oxidation were studied using two kinds of semi-batch reactors. Xylene oxidation was also tested in supercritical-CO_2 solution using a supported Co-imide complex as a catalyst. When the oxidation was performed in a large stirred autoclave at P_{O2} = 0.51 MPa and 170ºC, using Co/Mn/Ce as catalysts, and in the presence of recycle aldehyde/alcohol mixture, the best results (68% MX conversion, 76% MTA selectivity, less than 2% CO_x selectivity and about 4% selectivity to the heavy products) were obtained in 15 h. A Ce-salt promoter can effectively substitute for corrosive bromide salts, and recycle alcohol/aldehyde mixture can substitute for an acetic acid solvent. Both MX reaction rate and MTA selectivity increased with temperature, but so did the selectivities to heavier products and CO_x. The optimum temperature was ~160-170ºC. Both the MX reaction rate and MTA selectivity also increased with the partial pressure of oxygen. A P_{O2} of at least 0.5-0.6 MPa appeared necessary. The addition of ~ 5 wt.% water has effects similar to acetic acid addition, namely an increase in both reaction rate and MTA selectivity.

Chapter 1: Introduction and Review of Literature

1.1 Amide Synthesis

1.1.1 Goals and Project Summary

The amidation reaction is a typical SN_2 reaction, or the bimolecular acylation of an electrophilic acid with a nucleophilic amine. The general reaction is:

$$R_1COOR_2 + R_3NR_4(R_5) \rightarrow R_1CONR_4(R_5) + R_2OR_3 \qquad (1\text{-}1)$$

Different R_1, R_2, R_3, R_4, R_5 can result in different kinds of amides and amide derivatives, which can be used to synthesize polyamides, dyes, adhesives, repellents, herbicides, antioxidants, pharmaceuticals, sewage treatment agents, and soil conditioning agents.

Thermodynamically, the reaction is endothermic in the gas phase and the equilibrium constant is not very large. It is 34 at 300°C, 41 at 320°C calculated from the empirical equation Ke = exp(8.81-3019.25) (de Vekki and Mozzhukhina, 1997). However, economic and other problems such as the selectivity limit the reaction temperature because higher temperatures mean higher operation costs and more by-products. Kinetically, different reagents have different reaction activation energies. For active reagents, the reaction activation energy is very low (such as $\phi COCl$ with ϕNH_2, Ea~5.4 kJ/mol) (Pan, 1983). The reaction can be carried out quickly at moderate conditions (Pan, 1983). For reactions of high activation energy (such as $CH_3(CH_2)_7COOH$ with $CH_3(CH_2)_7NH_2$, E_a=100.4 kJ/mol), the reaction rate constant is only 1.0 L/mol•s even at 185°C (Pan, 1983). If a suitable catalyst can be found to reduce activation energies, the reaction can be carried out at higher reaction rates. In addition, it

is necessary that the catalyst be regenerated economically to reduce the cost of the product and to minimize waste.

In this project, catalysts to make N, N-diethyl-toluamide (DEET) from m-toluic acid (MTA) and diethylamine (DEA) were studied. DEET is an amide of interest because it is the chief compound in repellents for mosquitoes and other bloodsucking insects. Because the reaction mechanism of other amidations using hindered amines may be similar, the catalysts used in similar amidations may be useful in the synthesis of DEET. Generally, amidation can be classified as non-catalytic amidation and catalytic amidation. These reactions are summarized here.

1.1.2 Non-Catalytic Amidation

For amidation without catalysts, the key to a high rate of reaction is to prepare an active agent to make the activation energy low. For example, in order to prepare DEET, m-toluyl chloride could be synthesized by the reaction of m-toluic acid with a chlorinating agent such as bis(trichloromethyl)carbonate. Then m-toluyl chloride reacted with diethylamine to synthesize DEET at 0°C (LeFevre, 1990). Diphenyl(2,3-dihydro-2-thioxo-3-benzoxazolyl) phosphonate (A) is also an active agent which can react with a carboxylic acid (B) such as benzoic acid at room temperature to form 3-benzoylbenzoxazoline-2-thione (D) in 90% yield, which could undergo aminolysis smoothly to prepare the desired amide in high yield at mild conditions (Ueda, et al., 1988). This procedure could be expressed as the following two-step reaction (1-2):

$$A + B \xrightarrow{\text{base}} D \xrightarrow{R'NH_2} RC(=O)NHR' \qquad (1\text{-}2)$$

Aliphatic dicarboxylic acid can react with polyalkylenepolyamine to form polyamidopolyamine at 25°C. After that, highly active polyamidopolyamine reacted with epicholrohydrin to form amides at 45-55°C (Toshiyuki, 1989).

1.1.3 Catalytic Amidation

Amides could also be prepared by carbonylations of amines with CO, catalyzed by transition metal complexes. In preparing formamides, Co, Ni, and Fe carbonyls were active at greater than 200°C and CO pressure between 7.6-20.3 MPa (Dombek and Angelici, 1977). $[RhCl(CO)_2]_2$ was used as a catalyst precursor with a large excess of phosphine (Durad and Lassau, 1969). In N-benzylformamide synthesis, the conversion was 82% with a selectivity of 45% when the amidation was conducted at 200°C and 4.9 MPa for 6 h (Tsuji, et al., 1986). Several other attempts had been made to prepare N-substituted alkanamides from amines, olefins and carbon monoxide, so-called hydroamidation. Cobalt carbonyl (Crowe and Elmer, 1956; Imyanitov, et al, 1966) or nickel cyanide complexes (Reppe and Kroper, 1951) were typical catalysts. However, all these reactions were carried out under very severe conditions. $[Ru(CO)_2(OCOCH_3)]_n$ $[HRu(CO)_3]_n$ and $Ru_3(CO)_{12}$ (Rempel et al, 197) were effective catalysts for carbonylation of amines to formamide derivatives under quite mild conditions (1 bar CO, 75°C). $Ru_3(CO)_{12}$ (Tsuji et al, 1986) was also used as a catalyst precursor for the carbonylation of amines to formamides and the hydroamidation of olefins. In N-Benzylformamide synthesis, 83% conversion and 93% selectivity were obtained at 120°C at a CO pressure of 3.9 MPa. However the catalyst/amine ratio was very great. The key intermediate in these reactions was generated by intermolecular nucleophilic attack of the amine on the metal carbonyl ligands (Angelici, 1972), or by an intramolecular 1,2-shift

reaction between coordinated CO and an amine (Tkatchenko, 1982). Catalysts could be recovered when the hydridocarbamoyl complex forms an N-substituted formamide by reductive elimination.

Acryl amides could be prepared from vinyl chloride, CO, and an amine using a complex of a platinum group metal and a phosphine (Nicholas, 1985). The reaction was conducted at 60°C under autogenous pressure (>0.35 MPa). This catalyst could also be coated on a polymer or metal oxide supports to form a kind of heterogeneous catalyst (Nicholas, 1994). In the reaction to prepare N,N-dimethylacrylamide, acetonitrile was used to prevent irreversible adsorption of dimethylamine hydrochloride on the catalyst. The carbonylation of 4-chloro-N-phenylphthalimide with CO and aniline could be catalyzed using a Pd phosphine complex at 120°C under 0.65 MPa CO (Perry and Wilson, 1996). The reaction was rapid, more so if NaI was added to the solution.

A catalyzed amidation that is not a carbonylation is amidation of a nitrile. The reaction could be depicted as follows.

$$R_1CN + HNR_2R_3 + H_2O \xrightarrow{\text{Cat.}} R_1CONR_2R_3 + NH_3 \qquad (1\text{-}3)$$

Water provided the oxygen in the reaction. Catalysts were soluble Ru salts and neutral Mo complexes. The experimental results showed that Ru catalysts were better, especially Ru hydrides. In the synthesis of BuNHCOMe, the conversion was 100% with the selectivity 93% at 160°C under Ar (Shun-Ichi Murahashi, et al., 1986). But no evidence proved that this type of catalyst could be regenerated.

The amidation reaction of a carboxylic acid or ester with a primary or secondary amine is the main method used to prepare amides; it has been studied intensively. In DEET synthesis, the commercial catalysts are titanium alkyl and acetyl complexes,

chelated with amines (Hull, 1979). The commercial name for such catalysts is Tyzor® (E.I. du Pont). These catalysts are relatively low cost, with high selectivity and high conversions, and low corrosion for stainless steel. The reaction can be conducted at 220-235°C at autogeneous pressure for about 24 h with a feed composition MTA/DEA = 1/1 mole ratio and a catalyst (Tyzor TE) ratio of 1 g/mol MTA. The conversion of m-toluic acid to DEET was about 90% with 91-95% selectivity when water was removed continuously.

DEET synthesis was also studied (de Vekki and Mozzhukhina, 1997) using a strong acid, $HClO_4$, with the reaction at equilibrium. The following empirical equation for the equilibrium constant was obtained, Ke = exp (8.81-3019.25/T), from experimental data at temperatures in the range from 260 to 320°C. Calculation of the thermodynamically possible degree of conversion shows that with a MTA/DEA molar ratio of 1:1 between 260-320°C it is 83.8-86.5%. The enthalpy of reaction (ΔH_r) was assessed from the heats of combustion of the organic compounds in the gaseous state, and amounts to 20 ± 5 kJ/mole (Ravdel, 1981). Heats of combustion were calculated from available empirical formulae (Ravdel, 1981).

Arylboronic acids with electron-withdrawing substituents, $R\text{-}ArB(OH)_2$, have been used as catalysts in amidation reactions. With fluoroalkyl-substituted aromatics, 99% conversion with 74% selectivity was obtained in the reaction of cyclohexanecarboxylic acid and benzylamine (Ishihara, et al, 1996). These Lewis acid catalysts are based on the fact that the carboxylic acid can be converted to a more reactive acyloxyboron intermediate in situ. Dibutyltin ($Bu_2Sn{=}O$) has been reported as a catalyst for the synthesis of N-(4-anilinophenyl)-methacrylamide by amidation of methyl

methacrylate with phenothiazine at 75-80°C (Parker and Schulz, 1989). Compounds of tin or zinc containing a metal-nitrogen bond, which could be derived from halides or alkyoxides, can be used to catalyze the amidation reaction of acrylate esters. High conversions and high selectivities in synthesis of acryl amides could be obtained at 50-150°C using 1.5-2 wt% of these catalysts in the total solution. However, there was no evidence showing that these catalysts could be reutilized after reaction.

Heterogeneous catalysts have also been studied for amide synthesis. A boron phosphate catalyst was used in the synthesis of DEET from MTA and DEA giving an 88% conversion with 88% selectivity to DEET with a 1:4 MTA:DEA molar ratio feed (van Stryk, 1965). The reaction was conducted in a plug-flow reactor at 275-285°C and atmosphere pressure with a contact time of 0.5-1.5 min. Alumina -supported inorganic acids also gave conversions up to 90% when the pKa range of the initial acids used was 6.5-7.5 (de Vekki and Mozzhukhina, 1997). For 1-5 wt% Sn/SiO_2, the conversion was 78-90% at 260-320°C (de Vekki and Mozzhukhina, 1997). The catalytic activities of mildly acidic calcium hydroxyapatites [$Ca_{10-x-y}H_{x+y}(PO_4)_6(OH)_{2-x-y}$ $((x+y) \leq 2)$] were also evaluated; the pH had to be kept at ~5.5 when preparing this catalyst by precipitation. For these catalysts with excess amine feeds (MTA/DEA = 1/3-1/7), the optimum temperature for DEET synthesis was 300-320°C, with a WHSV (weight hour space velocity) from 0.3-1.3 h^{-1}. Under these conditions, a 90-95% MTA conversion was achieved and the selectivity exceeded 90% with E_a = 39 kJ/mol. This catalyst was said to be stable for 720 h.

Taurates (substituted 2-aminoalkane sulfuric acids) salts can react with carboxylic acids at 180-205°C in the presence of 30-40% water, catalyzed by boric acid, ZnO and/or

MgO (Day, 1996). The conversion of sodium N-methyltaurate can be greater than 97%. Other partially dehydrated metal (Zr, Ti and Sn) hydroxides have been used as amidation catalysts (Tabako, et al., 1987). The metal hydroxides were prepared by co-precipitation from metal oxychlorides or chlorides. The calcinations were usually at temperatures ~300°C for about 3 h. The amidation reaction could be performed in either liquid or gas phase. In N-butylacetamide synthesis catalyzed by partially dehydrated zirconium hydroxide with molar ratio 5/1 amine/acid, the yield was 54% and 100% after 2 h and 5 h, respectively.

Triphenylantimonydicarboxylates ($Ph_3Sb(O_2CR)_2$, where R=Me, CF_3, Ph, and CH_2NH-Z) can react with amines ($R'NH_2$) to prepare amides and triphenylstibine oxide. Triphenylantimonydicarboxylates could be regenerated by triphenylstibine oxide reacting with the corresponding acid (Nomura, et al., 1986). In N-n-Hexylacetamide synthesis, the yield reached 87% at 50°C in 10 h.

According to the above literature summary, strongly acidic (but not superacidic) solid catalysts with both Lewis and Brønsted sites may be good catalysts for amidation. Example materials include γ-zirconium phosphate (Alberti, et al, 2001), tungstophosphoric acids (HPA) (Kozbevnikov, 1995), and molybdophosphoric acids (Pizzio et al., 2001). The Brønsted acid strengths of the latter catalysts can be adjusted by substituting Cs^+ ions for protons. They can also be supported on high surface area carriers (such as mesoporous silica) to get high surface area catalysts (Wang, et al, 2001).

1.2 Catalytic Oxidation of Alkylaromatics

1.2.1 Goals and Project Summary

The main reaction of xylene oxidation using O_2 is:

$$2\ C_6H_4(CH_3)_2 + 3\ O_2 \rightarrow 2\ C_6H_4(CH_3)(COOH) + 2\ H_2O \qquad (1\text{-}4)$$

The direct oxidation of hydrocarbons with air or oxygen is commercially important for the production of oxygenated compounds from relatively cheap petroleum and natural gas feedstock. Oxidation reactions can be performed both in vapor- and in liquid-phase. Because of economic advantages - higher yield, improved selectivity, milder reaction conditions and advent of novel coordination complex catalysts - normally associated with liquid-phase oxidation, recent trends indicate a shift to liquid-phase processes (Raghavendrachar and Ramachandran, 1992).

There are lots of patents on homogeneous liquid-phase oxidation of p-xylene (PX) to 1,4-benzenedicarboxylic acid (TPA), a polyester feedstock. Only one patent is related to the production of m-toluic acid (MTA) (Grane, 1974), and only one patent is for making p-toluic acid (PTA) with a heterogeneous catalyst (Chisem et al, 1998). There are patents on making all isomers of toluic acid from mixed xylenes, or on making p-toluic acid alone (Hirose et al, 1982; Takeda et al, 1983). Based on the similar oxidation mechanism involving electron transfer / hydrogen abstraction (Parshall, 1992) for all of these processes, the literature on the catalytic oxidation of mixed xylenes can be a guide for the catalytic oxidation of MX to MTA. MTA itself is an important raw material for amide production.

The aim of this project was to select suitable catalysts and perform experiments to determine their applicability for MTA production. Most of the literature for toluene oxidation uses the same catalyst - soluble Co or Mn salts, typically in combination (Chavan, et al, 2000). Normally the solution is acidified (e.g., low-molecular weight carboxylic acids as solvents) in order to dissolve the salts and any promoters (e.g., NaBr). The promoters presumably aid in electron transfer, especially in the initiation step to form

a radical cation from the parent alkylaromatic (Hronec et al, 1985; Spirina et al, 1987; Raghavendrachar and Ramachandran, 1992). The main side reaction is that of xylene and oxygen to form the more oxidized phthalic acid:

$$C_6H_4(CH_3)_2 + 3\ O_2 \rightarrow C_6H_4(COOH)_2 + 2\ H_2O \qquad (1\text{-}5)$$

According to previous work (Hirose et al, 1982; Takeda et al, 1983; Cao and Servida, 1994), except for the tolualdehyde and methylbenzylalcohol that can be further oxidized to the desired acid, the remaining by-products are primarily monomethyl terephthalate, methoxycarbonylbenzyl alcohol, benzoate-type compounds, formylbenzoic acid and its methyl ester, and other unidentified acids or aldehydes. Reducing the selectivity to these by-products is another goal of this project.

Typically, highly acidic solutions, e.g., acetic acid (HAc), and bromide salts are applied in the effective catalytic oxidation of PX (Takeda, et al, 1983; Raghavendrachar and Ramachandran, 1992; Toru and Kazuo, 1993; Chavan, et al, 2000). Acidic waste cannot be avoided in the separation of the acidic solvents and products, and the combustion of the solvent can happen at the normal reaction temperatures; catalyst recovery is also difficult. Systems with high bromide contents require more exotic materials of construction for the reactor (Raghavendrachar and Ramachandran, 1992). Therefore, developing a new process using minimal amounts of catalyst without solvents and bromide salts was also a goal of this project.

1.2.2 Liquid Phase Catalytic Oxidation by Homogeneous Catalysts

A typical process consists of homogeneous oxidation of PX to TPA or PTA in HAc using soluble Co and/or Mn salts activated by promoters (e.g., bromide salts, aldehydes) that overcome the problems of acid decarboxylation by rapid electron transfer

from cobalt to promoter to peroxy radical. The process is typically conducted at ~120-200˚C and 1.0-3.0 MPa (Brill, 1960; Patton and Seppi, 1970; Digurov et al, 1970; Nakaoka et al, 1973; Hanotier and Hanotier-Bridoux, 1981; Hirose et al, 1982; Takeda et al, 1983; Partenheimer, 1990; Raghavendrachar and Ramachandran, 1992; Masashi et al, 1999). Oxidation reaction conditions in HAc solvent are summarized in Table 1.1. From the Table, it is seen that the yield to TPA and other effective products could reach 85~97% in < 3 h by using a correct combination of Co, Mn, bromide, Ce and/or Zr salts. Other liquid phase catalytic oxidation systems of alkylaromatics are listed in Table 1.2. From this table, it is seen that 68% yield of MTA could be obtained using 185 ppm tris(2,4-pentanedionato)cobalt(III) ($Co(Acac)_3$, or $C_{15}H_{21}CoO_6$) in 60 min. However, it was a two-step process. An isobutane oxidant had to be prepared first. When using cobalt(II) naphthenate ($Co(NA)_2$, $C_{22}H_{14}CoO_4$) (0.19 mmol per mol xylene) 10% yield PTA could be obtained in 135 min. With Co/Mn salts promoted by bromides, the yield to effective products can be 97.8% with 62% selectivity to PTA in 180 min, even without acidic solvents (Hirose et al, 1982).

When there are separate aqueous and organic phases existing in a catalytic oxidation system, and the mass transfer between the two phases becomes rate determining, a phase transfer catalyst (PTC) may improve the reaction rate by improving the mass transfer rate between phases. Usually there are three kinds of PTCs, quaternary onium salts, crown ethers, and polyethylene glycols. In the oxidation of 2,6-dimethylpyridine to 2,6-pyridinedicarboxylic acid (Iovel and Shymanska, 1992), 18-crown-6 was employed as PTC. With SeO_2 as the main catalyst, the yield was 49-57.5%, and with $KMnO_4$ the yield was 60%. In the oxidation of 4-chlorotoluene to 4-

chlorobenzoic acid, $RuCl_3(H_2O)_3$ was the main catalyst (~1 wt% of the total solution) and NaOCl solution (20 wt%) was employed as oxidizer (Sasson,1998). At 25°C, atmosphere pressure, and pH 9-10, the yield to sodium 4-chlorobenzoate, was 92% in 2 hours when the phase transfer catalyst tetra-n-butylammonium bromide was employed.

1.2.3 Liquid and Supercritical Phase Catalytic Oxidation by Heterogeneous Catalysts

In the catalytic oxidation of aromatics, there were some heterogeneous catalysts developed recently, as summarized in Table 1.3. From Table 1.3, it is seen that the conversion of PX could approach 100% with 99% selectivity to TPA when the oxidation was performed in $MeCO_2H$/water solution using $CoMn_2$(O)-Y ($[CoMn_2(\mu_3\text{–}O)(MeCO_2)_6(py)_3]^n$ (n=+1 or 0) inside the cage of zeolite HY as the catalyst (Chavan et al, 2001). When the oxidation of 2,6-di-tert-butylphenol was conducted in supercritical CO_2 using Co(salen) as the catalyst, the conversion also reached 95% with 85% selectivity to 2,6-di-tert-butyl-1,4-benzoquinone (DTBQ) (Musie et al, 2001).

1.2.4 Mechanism and Kinetics of Aromatics Oxidation to Acids

Generally, liquid-phase oxidation of alkylaromatics by O_2 catalyzed by Co(II/III) and promoted by bromides, aldehydes or ketones starts with the formation of free radicals. When reacted with oxygen, the radicals form hydroperoxides. Depending on the reaction conditions, the reaction proceeds to give alcohols, aldehydes, ketones, acids and finally oxides of carbon and water. Initiation of the oxidation of alkyl aromatics can be explained in terms of 2 mechanisms: (1) the electron-transfer mechanism in which electron transfer occurs from arene to a Co(III) complex producing an arene radical cation, which in turn forms an alkybenzyl radical by proton loss; (2) the abstraction mechanism, where a benzylic hydrogen is abstracted by bromine, metal atoms, $RO^{\cdot}$ or

$ROO^{\cdot}$ radicals (Fig. 1.1) (Raghavendrachar and Ramachandran, 1992). The CH_3-C_6H_5-$CH_2^{\cdot}$ Radicals produced then react with O_2 to form alkylperoxy radicals. The alkylperoxy radicals decompose to alcohol, aldehyde and finally toluic acid (Parshall, 1980). The further oxidation of PTA without acid solvents is initiated predominantly by the hydrogen abstraction mechanism, because Co(III) cannot oxidize PTA (high oxidation potential) by electron transfer. However, in acid solution, electron transfer between PTA and Co(III) acetate can happen (Kashima and Kamiya, 1974).

Mechanism I

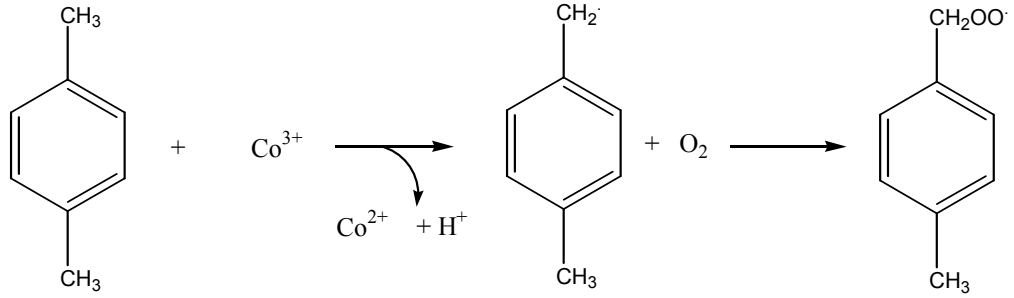

(1-6)

Mechanism II

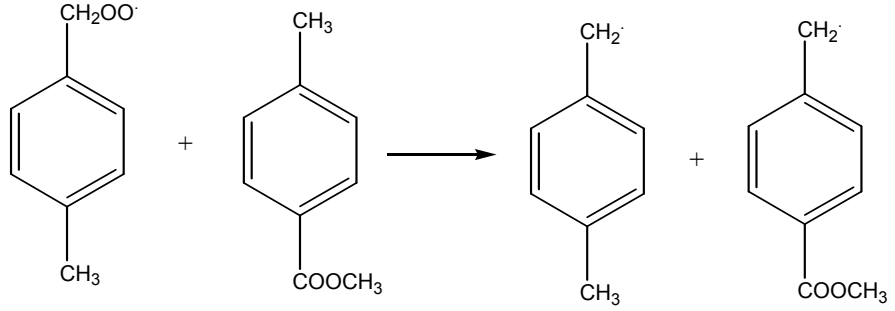

(1-7)

Fig. 1.1. Electron-transfer and hydrogen-abstraction mechanisms in coordination of p-xylene and p-methyl toluate (Parshall, 1980).

Normally Mn(III) and Co(III) without promoters are not powerful enough to initiate the free-radical reaction by electron transfer. The combined effect of Co and Mn is only to decompose hydroperoxides to yield free radicals. The initiation mechanism is

predominantly hydrogen abstraction from methyl groups by bromine atoms (Saffer et al., 1958). Fig 1.2 illustrates the cycle of bromine. Co and Mn ions also oxidize bromide to bromine, ensuring the availability of bromine atoms for initiation. When the reaction is conducted in acetic acid with $Mn(OAc)_2$, carboxymethyl radicals ($^{\cdot}CH_2COOH$) can be obtained from decomposition of the Mn salt. These radicals can abstract protons from methylbenzenes initiating the desired oxidation, or they can add to aromatic rings.

Partenheimer (2001) studied the structure of metal/bromide (Co/Mn/Br) catalyst in acetic acid/water mixtures and its significance in autoxidation. He suggested that dissolution of the metal salts in acetic acid/water mixtures resulted in significant changes in their coordination chemistry. The predominant species present in anhydrous acetic acid are non-charged $[M(HAc)_4(OAc)_2]_n$ (n=1 or 2). When water is added to the system, acetic acid ligands are replaced by aqua ligands to form $[M(HAc)_m\ (H_2O)_{4-m}(OAc)_2]_n$ species. In anhydrous acetic acid, the bromide is coordinated but coordination rapidly decreases as the water concentration increases. The predominant species is the ion-paired bromide salt: $[M(HAc)_m(H_2O)_{5-m}(OAc)]_n(Br)$. Heteronuclear metal dimers can occur with mixed Co(II)/Mn(II), and the homogeneous Co/Mn/Br catalyst is composed of a large number of different coordination compounds. A solvent ligand such as acetic acid can be displaced by equally weak ligands (peroxo radicals, peroxides, peracids). The bromide ion is in the second coordination sphere where it can be reduced by Mn(III) or Co(III) more rapidly than a bromide free in solution.

When using Co catalyst and paraldehyde promoter in acetic acid solutions to oxidize PX with air, a free radical chain mechanism was proposed in which the first step

was reaction of paraldehyde (PA) with oxygen to form peroxidic compounds which promote Co(II) ion oxidation to Co(III) ion (Eq 1-8-13, Nakaoka et al, 1973).

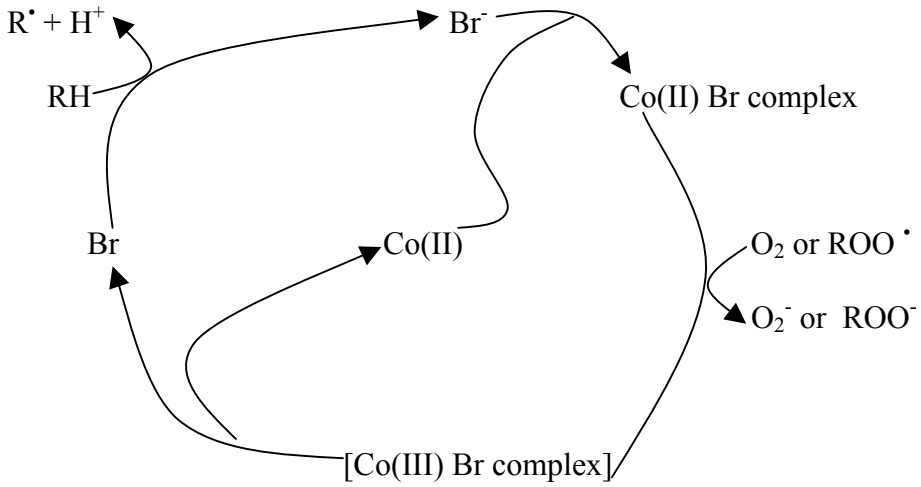

Fig. 1.2. Bromine cycle in a bromide-promoted oxidation of a hydrocarbon (Parshall, 1980).

$$PA + O_2 + Co^{2+} \longrightarrow X^{\bullet} + Co^{3+} \qquad (1\text{-}8)$$

$$H_3C\text{-}C_6H_5\text{-}CH_3 + Co^{3+} \longrightarrow H_3C\text{-}C_6H_5\text{-}CH_2^{\bullet} + H^+ + Co^{2+} \qquad (1\text{-}9)$$

$$H_3C\text{-}C_6H_5\text{-}CH_3 + X^{\bullet} \longrightarrow H_3C\text{-}C_6H_5\text{-}CH_2^{\bullet} + XH \qquad (1\text{-}10)$$

$$H_3C\text{-}C_6H_5\text{-}CH_2^{\bullet} + O_2 \longrightarrow H_3C\text{-}C_6H_5\text{-}CH_2OO^{\bullet} \qquad (1\text{-}11)$$

$$H_3C\text{-}C_6H_5\text{-}CH_2OO^{\bullet} + Co^{2+} \longrightarrow H_3C\text{-}C_6H_5\text{-}CHO + OH^- + Co^{3+} \qquad (1\text{-}12)$$

$$H_3C\text{-}C_6H_5\text{-}CHO + O_2 \longrightarrow H_3C\text{-}C_6H_5\text{-}COOH \qquad (1\text{-}13)$$

According to mechanism I, after the establishment of the steady state, the rates of different substituted toluenes follow the same rate equation (Kamiya and Kashuima, 1972; Hendriks et al, 1978; Czytko and Bub, 1981), using Co(III) salts in acetic acid solution:

$$Rate = k\frac{[Co^{3+}]^2[RCH_3]}{[Co^{2+}]} \qquad (1-14)$$

Hronec et al (1985) studied the kinetics and mechanism of high temperature (e.g. 160˚C) liquid-phase oxidation of a PX and PTA mixture in the presence of water catalyzed by Co^{3+} salts. Their proposed mechanism suggested the presence of radical species $RCH_2O_2^{\bullet}$, $RCO_2^{\bullet}$, $RCO_3^{\bullet}$, and reaction (1-15) as the rate-determining step. The activation energy for PX oxidation was found to be 93 kJ/mol.

$$RCH_2O_2^{\bullet} + RCH_3 \longrightarrow RCH_2^{\bullet} + RCH_2OOH \quad (1\text{-}15)$$

Kinetics data, based on the maximum oxygen adsorption rates, were consistent with the rate law:

$$-\frac{dO_2}{dt} = k\frac{[Co]^{0.19}}{[PTA]^{0.21}}\cdot[PX]^2 \qquad (1-16)$$

This equation was applicable to high PTA concentrations, which prevented the formation of Co-peroxide (1-17, 1-18) or Co-peracid (1-19, 1-20) complexes by coordinating with the metal center more strongly. The reactions (1-17) to (1-20) are often the rate-controlling steps (Scott, 1970; Hendriks et al, 1979).

$$RCH_2OOH + Co^{2+} \leftrightarrows [RCH_2OOH\cdots Co^{2+}] \qquad (1\text{-}17)$$

$$[RCH_2OOH\cdots Co^{2+}] \rightarrow RCH_2O^{\bullet} + OH^- + Co^{3+} \qquad (1\text{-}18)$$

$$RCO_3H + Co^{3+} \leftrightarrows [RCO_3H\cdots Co^{3+}] \qquad (1\text{-}19)$$

$$[RCO_3H\cdots Co^{3+}] \rightarrow RCO_3^{\bullet} + H^+ + Co^{2+} \qquad (1\text{-}20)$$

At lower PTA concentrations in the presence of water, PTA prevented catalyst precipitation to insoluble hydroxy derivatives by coordination with $OH^{\bullet}$ (Hronec et al, 1985). The conversion of PX increased markedly. Water and other solvents present in the system could displace ligands from the coordination sphere of the metal complex, influencing the rate of initiation and the reactivity of the radical species by forming

radical complexes (Zaikov and Maizus, 1968; Czytko and Bub, 1981). However, water influences the rate only at low concentration because of its limited solubility in PX. It also helps to dissolve the catalyst if only one phase exists. The complexes [$RCH_2^{\bullet}\cdots H_2O$] have lower reactivity than $RCH_2^{\bullet}$ or $RCO^{\bullet}$ for the termination reaction with Co^{3+}, but [$RCO^{\bullet}\cdots H_2O$] can decompose to RCHO and $^{\bullet}OH$ to terminate; the overall rate increases. At high water concentrations, two phases are formed and water does not further affect the oxidation rate (Hronec and Ilavský, 1982).

In the liquid-phase oxidation of PX catalyzed by $Co(OAc)_2$ and NaBr, the oxidation rate of PX to PTA was proportional to the concentrations of PX, catalyst and promoter (Digurov et al, 1970). The reaction was independent of the oxygen partial pressure in the range 0.02-0.1 MPa. The oxidation rate of PTA to TPA was also first order with respect to catalyst concentration, but half-order with respect to oxygen partial pressure, and independent of bromine ion concentration (Digurov et al, 1970). When using paraldehyde (PA) as promoter in acetic acid, the reaction rate was proportional to the oxygen pressure, and approximately second order in PA. From Hronec and Ilavsky (1987), in the case of cobalt oxide as catalyst, the rate was second order in PX concentration and first order in catalyst, but only 0.1 order in O_2 partial pressure. Cao and Servida (1994) studied the kinetics of PX oxidation catalyzed by cobalt naphthenate promoted by p-tolualdehyde/methyl benzoate. The results showed that the reaction was first order in the reactants and zero order in O_2 if the O_2 flux to the liquid was larger than its maximum rate of consumption.

It is obvious from the above studies on the kinetics that the liquid-phase oxidation of xylenes is a very complicated process. It is determined by the interactions between

chemical reactions and transport processes, which are affected by the catalysts, promoters, solvents and operating conditions. Particularly, the reaction rate is related to the O_2 supply rate. When there is adequate O_2 supply, the reaction is positive order in the reactant (usually first order) and zero order in O_2.

Table 1.1. Liquid Phase Catalytic Oxidation to Aromatic Carboxylic Acids in Acetic acid (HAc) Solution

Catalysts[1] and Mol Ratios	Promoters (mol ratio)	Solvent (mol ratio)	T (°C)	P (MPa)	O_2 or air	Reactant	Product	Sel. (%)	Yield %	Time min	Ref.
$Co(NA)_3/Mn(OAc)_2$, Mn/Co=0-2 (Co+Mn) = 12800-44000 ppm PX	Br^- / (Co+ Mn) = 1/(1-7)	HAc/PX = 1.8 - 4.4	195-205	2.8	air	PX	TPA	>90	>85.5	120	Saffer and Barker, 1958
Co(OAc), 0.09-0.15/ PX	No	HAc / PX = 0.27	100-130	1.0	air	PX	TPA	-	~95	-	Ichikawa et al., 1970
Co(OAc), 0.0375/ PX	Paraldehyde/PX = 0.33	HAc/PX = 2	120	1.5-3.0	O_2	PX	TPA	-	91~97	180	Nakaoka et al., 1973
Co/Mn/Ce or Co/Mn/Zr=(1-20)/(70-98)/(1-10); total metal %, 6250-125000ppm based on DMBA	Br^- /total metal = 0.8 – 5	$(HAc+H_2O)$/ DMBA = 3-10, HAc/H_2O = 0.7 – 9	180-240	2.0	air	DMBA	TMA	-	~91	60	Masashi et al., 1999

[1]Naphthenate, NA; acetylacetonates, Acac; acetate, OAc; 2,4-dimethylbenzaldehyde, DMBA; trimellitic acid, TMA; 1,4-Benzenedicarboxylic acid, TPA.

Table 1.2. Other Liquid Phase Catalytic Oxidations to Aromatic Carboxylic Acids

Catalysts[1] (mol ratio)	Promoters (mol ratio)	Solvent (mol ratio)	T/°C	P MPa	O_2 or air	Reactant	Products	Sel. (%)	Yield %	Time (min)	Ref.
Co(Acac), 185ppm based on MX	-	-	130-140	2.7-4.1	Isobutane oxidate[2] + air	MX	MTA and IPA	76 MTA, 21 IPA	68 MTA	60	Grane, 1974
Co(OAc)/Mn(Oac), Co/Mn= 99.2/0.8-70/30, 500-2500ppm metal/PX	Br^-/(Co+Mn) <1.5/1	-	180-210	4.91	Air	PX	PTA and other products[3]	62 PTA	98	180	Hirose et al., 1982
Co/Mn= 4-100, (Co+Mn) =500-1250ppm /PX	Li(OAc)+ LiX/M = 0.3-3	-	160-190	2.0	Air	PX	PTA and other products[3]	-	90-93	150	Tekeda et al., 1983
5.7 mmol Cobalt alkanote +2.5 mmol Mn(OAc)/mol PX	PTA/PX = 1.3	Water/PX = 3.3	185	2.0	Air	PX	TPA	-	66	330	Hronec et al., 1985
$CoBr_2$, Co =10-200 ppm/ aromatic aldehyde	No	Ketone/ ald.= 4-10	30-80	2.0-5.0	Air	Aromatic ald.	Aromatic carboxylic acid	68-98	58-87	80~180	Toru et al., 1992, 1994
$Co(NA)_2$ Co = 0.19 mmol/mol PX	Toluald./ X=0.11/4	MBzOAc/ X = 1	110-130	0.02-0.1	O_2	PX	PTA	58	10	135 [4]	Cao and Servida, 1994
MnO_2, 0.03 mol/mol BA	No	Benzene/BA = 11	25	0.1	O_2	BA	PBA	88	86	60	Yoshiaki, 1995

[1] Acetylacetonate, Acac; benzaldehyde, BA; methylbenzoate, MbzOAc; xylene, X; peroxybenzoic acid, PBA; isophtahlic acid, IPA; aldehyde, ald..

[2] Isobutane oxidate prepared by non-catalyst oxidation by isobutene with air at 134°C, 2.97 MPa AT residence time = 6 h.

[3] Other desired products include monomethyl terephthalate, TPA, p-methylbenzyl alcohol, p-methoxycarbonylbenzyl alcohol, benzoate-type compounds, p-tolualdehyde, and p-formylbenzoic acid and its methyl ester.

[4] CSTR reactor, time is the average retention time.

Table 1.3. Liquid and Supercritical Phase Oxidation of Aromatics by Heterogeneous Catalysts

Catalysts[1] (mol ratio)	Promoters (mol ratio)	Solvents (mol ratio)	T/°C	P MPa	O_2 or air	Reactants	Products	Sell %	Yield %	Time min	Ref.
Cr(III)(salen). Cr^{3+}% = 0.10 mol/g, Cr^{3+}/PX=0.037mmol/mol	-	-	138	0	air	PX	PTA	-	29	1440	Chisem et al, 1998
Co(salen*)/DTBP=1mol/20 mol	Methylimidazole/ DTBP=1.28/20	SC-CO_2	70	20.7	O_2/ DTBP =75/1	DTBP	DTBQ	85	81	1260	Musie et al, 2000
$Co_{0.5}H_6PMO_8V_4O_{40}^{4-}$/ DTBP = 1mol/ 7.5 mole	-	Chloroform	60	-	O_2	DTBP	DTBQ	56	56	60	Kolesnik et al, 2000
Co_3O_4/D027 (Co% = 2.6 mmol/g), Co/p-cresol =0.017 mol/mol	-	Methanolic NaOH (19wt%), P-cresol/ methanol = 0.063mol/mol	75	0	air	p-cresol	p-HBA	96.7	92.6	480	Gao, et al, 2001
$CoMn_2$(O)-Y, (Co+Mn)= 8.7 mmol/mol PX	Br^-/PX=0.052/1	H_2O/$MeCO_2H$/PX =20/40/1	200	3.8	air	PX	TPA	99.4	99.4	240	Chavan et al, 2001
Cobalt(III) /SBA-15 (Co%= 1.27mmol/g), Co/PX = 5.2mmol/mol	-	-	130	0.2	O_2% = 50%	PX	TPA	62.6	59.5	960	Burri et al, 2002

[1] Cr(III)(salen), prepared from the reaction of Cr(III) acetate with the product of salicylaldehyde and 3-aminopropyl(trimethoxy)silane; [{N,N'-bis(3,5-di-tert-butylsalicylidene)-1,2-cyclohexanediaminato(2-)}cobalt(II)], Co(salen*); 2,6-di-tert-butylphenol, DTBP; 2,6-di-tert-butyl-1,4-benzoquinone, DTBQ; copolystyrene-divinylbenzene acidic cation exchange resin, D027; p-hydroxybenzadehyde, p-HBA; Trinuclear, μ_3-oxo mixed metal acetate complex $[CoMn_2(\mu_3\text{-}O)(MeCO_2)_6(py)_3]$ encapsulated in zeolite HY, $CoMn_2$(O)-Y; mesoporous silica with pore size 260-300Å, SBA-15.

Chapter 2: Experimental

2.1 Catalyst Preparation

In continuous minireactor kinetics experiments, 8 catalysts were used for the synthesis of DEET. They were Davison Silica Gel 57, supported Titanium (IV) (triethanolaminato)-isopropoxide (Tyzor TE) with different loadings (4.6 mol% Tyzor TE/TiO_2 and 11.4 mol% Tyzor TE/Al_2O_3), calcium hydroxyapatites with different Ca/P ratios (HEA00 and HEA01), supported 12-tungstophosphoric acid (HPA, $H_3PW_{12}O_{40}.nH_2O$) (YJ01), and supported cesium-exchanged tungstophosphoric acid (CsHPA) of different cesium loadings (YJ03 and YJ10).

Prior to performing any kinetics studies, the catalysts were calcined in the reactors in flowing air or nitrogen. All catalysts were calcined at 450-550^oC in air except supported Tyzor TE that was calcined in N_2 at the desired reaction temperature (250-300 ^oC).

2.1.1 Catalysts for Synthesis of DEET

Davison 57 Silica Gel was obtained from W. R. Grace (amorphous, 8 mesh) and was pelletized and sieved to 20-40 mesh before usage.

Supported Tyzor TE (Aldrich, 80 wt% solution in 2-propanol) catalysts of different loadings were prepared using a wet impregnation method. A desired quantity of porous support (Al_2O_3, Vista Chemical Company, 1.6 mm; TiO_2, 85 wt% TiO_2/15 wt% Al_2O_3, LeRoche Chemical Company) was weighed out and dried at 300 ^oC under vacuum (<10^{-4} MPa) overnight. A desired quantity of Tyzor TE dissolved in extra isopropanol (99.5%, Aldrich) solution (0.89 mmol Tyzor/ 1mL isopropanol for TiO_2 support; 5.37

mmol Tyzor/mL isopropanol for Al_2O_3 support) was injected into the flask with the support (0.58 mmol Tyzor/g TiO_2; 1.2 mmol Tyzor/g Al_2O_3), under N_2. The catalyst was then dried under vacuum at 50 ^oC for 40 min, then 250 ^oC overnight.

Calcium hydroxyapatite catalysts (HEA00 and HEA01) were prepared according to the procedure of Bett et al. (1967). The general formula of hydroxyapatite is $Ca_{10-x-y}H_{x+y}(PO_4)_6(OH)_{2-x-y}$ ($x+y \leq 2$). It was made by titrating concentrated phosphoric acid (85%, Mallinckrodt) into saturated calcium hydroxide. The CaO (reagent, J.T. Baker) was dissolved into CO_2 free DI water to get a saturated $Ca(OH)_2$ solution. The volume of H_3PO_4 required to give a desired Ca/P ratio was slowly stirred into the $Ca(OH)_2$ at ambient temperature under N_2. The gelatinous sediment was filtered and washed several times until the washings were approximately pH 7.0. The precipitate was dried at 175 ^oC overnight and calcined in air at 500 ^oC for 1 h. The final white crystalline solids were pelletized and sieved to 20~40 mesh.

Silica-supported tungstophosphoric acid (YJ01) was obtained from ExxonMobil research (40 wt% HPA on silica gel). Supported cesium tungstophosphoric acid catalysts (YJ03 and YJ10) were prepared according to a two-step impregnation method (Wang et al., 2001). First, MCM-41 with ~500-1100 m^2/g surface area was prepared according to the procedure of Beck et al. (1992) and Kresge et al. (1992). The molar ratio of reactants is 1.0 TEOS (tetraethyl orthosilicate, Aldrich, 98%)/0.28 C_{16}TMABr (cetyltrimethylammonium bromide, Aldrich)/0.29TMA(OH) (tetramethyammonium hydroxide, 25% water solution)/80 water. After mixing the C_{16}TMABr (98.1 mmol, 34 g) with TMA(OH) (101.6 mmol, 34.8 mL) and water (100 mL), and TEOS (350.4 mmol, 75.8 mL) with water (356 mL), the two solutions were mixed and stirred for at least 30

min. The mixture was heated to 100 ^{o}C for 20 h with periodic water addition and stirring. The gel was filtered, dried at 70^{o}C overnight, extracted (1 g gel /15 mL 37% HCl /135 mL EtOH) for 24 h at 70 ^{o}C, filtered again, and dried at 100 ^{o}C overnight. MCM-41 was then treated with 0.1N HNO_3 (1 g/10 mL) for 20 min at 80 ^{o}C, dried under vacuum at 110 ^{o}C, then calcined at 540 ^{o}C for 1 h in 100 mL/min air flow to remove NO_3^-. Two batches of MCM-41 were prepared. MCM-41 of 575 m^2/g surface area was used to prepare YJ03 and MCM-41 of 1080 m^2/g surface area was used to prepare YJ10. Cs_2CO_3 (Aldrich, 99.9%) was impregnated into MCM-41 by aqueous incipient wetness, then the catalyst was dried at 110 ^{o}C overnight and calcined at 500 ^{o}C for 2 h. HPA (ALFA, Reagent Grade, Na 2%) dissolved in a solvent (1g HPA/1mL solvent; water for YJ03 and 1-butanol for YJ10) was impregnated using a similar incipient wetness technique. The catalyst was dried at 110 ^{o}C overnight and calcined at 300 ^{o}C in 100 mL/min air flow for 2 h.

2.1.2 Catalysts for Synthesis of m-Toluic Acid

In m-xylene oxidation experiments, both homogeneous and heterogeneous catalysts were studied for the synthesis of m-toluic acid (MTA). The homogeneous catalysts are based on cobalt salts and manganese salts with different promoters, such as cerium, or bromide salts. The heterogeneous catalysts are supported Co(salen) (salen = salicylidenaminato) (Fig. 2.1) and Co(DMBA) (DMBA = 4-dimethylaminobenzaldehyde) (Fig. 2.2) immobilized on silica aerogels or MCM-41. For Co(salen) and Co(DMBA) we employed a sol-gel immobilization method (Murphy et al., 2001). An example procedure for Co(salen) was to dissolve 6.0 mmol $Co(O_2CCH_3)_2.4H_2O$ (J. T. Baker, 99.2%) into 25 mL ethanol (95%, Fisher Scientific)

(solution A), and 12.0 mmol APTMS (aminopropyltrimethoxysilane, Research Chemicals, 97+%) and 12.0 mmol salicylaldehyde (Research Chemicals, 98%) into 50 mL ethanol (solution B). Then B was added into A with stirring, followed by 150 mmol TEOS, added slowly. After stirring for 1 h at ambient temperature, 15 mL 1 M HCl was added dropwise. The solution became gelatinous after reacting for 2 days. After adding some ethanol, 5 mmol triethanolamine (dissolved in 20mL ethanol) was added. After 2 h, a gel formed again. Then the solution was stirred for ~2 weeks. The gel was filtered under vacuum, washed with lots of ethanol, then washed with 90% $CHCl_3$/10% pyridine solution, and dried at 100 ^oC under vacuum for 24 h (Murphy et al, 2001).

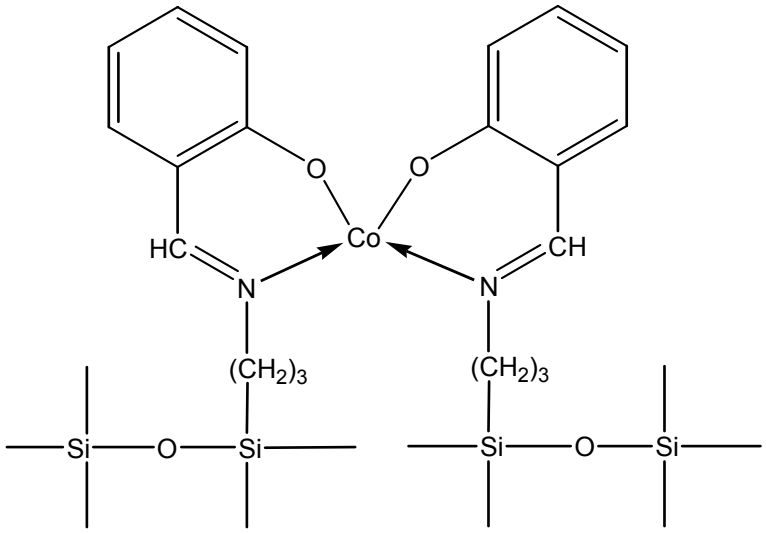

Fig. 2.1. Proposed structure of supported Co(salen)

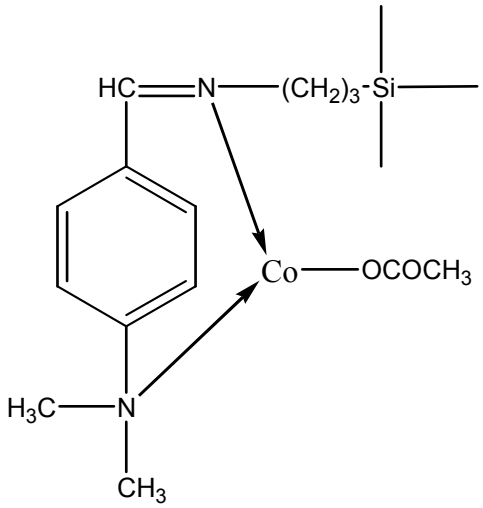

Fig. 2.2. Proposed structure of supported Co(DMBA)

In the preparation of supported Co(DMBA), the molar ratios of reactants were 0.12 C_{16}TMABr / 1.0 NaOH / 230 H_2O / 0.85 TEOS / 0.15 APTMS. To make 14 g Co(DMBA), 0.018 mol C_{16}TMABr was added to 600 mL water, AND 7.5M NaOH solution was added dropwise until the solution became clear. Then the silanes (TEOS, 127.5 mmol, APTMS, 22.5 mmol) and the $Co(OCCH_3)_2$ (22.5 mmol) were added slowly. After reacting for 12 h, the gel was washed four times using 800 mL water, then vacuum dried at 60 ^oC for 12 h, then added to methanol (1g/10mL) and 640 mmol DMBA (Reagent, ALFA). Then some dried 3Å molecular sieve (2g/10 mL) was added, and the mixture was reacted for >12 h. The 3 Å molecular sieves were filtered out, and the (aminopropyl) silica was filtered and washed using lots of methanol. It was then added to a $(Co(O_2CCH_3)_2.4H_2O$ solution (5 mmol metal salt/25 mL ethanol), and reacted with stirring for 24 h. The gel was dried under vacuum at 100^oC for 24 h.

2.2 Continuous Flow Reactor Experiments

The experiments for the synthesis of DEET were performed in a fixed bed reactor, an Autoclave Engineers 316 stainless steel tube (1.25 cm ID, 15 cm length) with stainless

steel high-pressure fittings at inlet and outlet. Typical catalyst loads were 0.5 or 2.0 g. Quartz wool and glass beads were placed above and below the catalyst bed. The reactor was heated by means of an external clamshell furnace (Teco F5). Reactor temperatures were varied between 250-320^{o}C; pressures were varied between 0-3.5 MPa. The temperature was controlled using a 1/16" internal K thermocouple in contact with the catalyst bed, by a PID controller (Eurotherm 818), and was held within ±1^{o}C of the set point. The pressure was controlled with a diaphragm-type backpressure regulator (Grove Mitey Mite). A schematic of the flow reactor is shown in Figure 2.3.

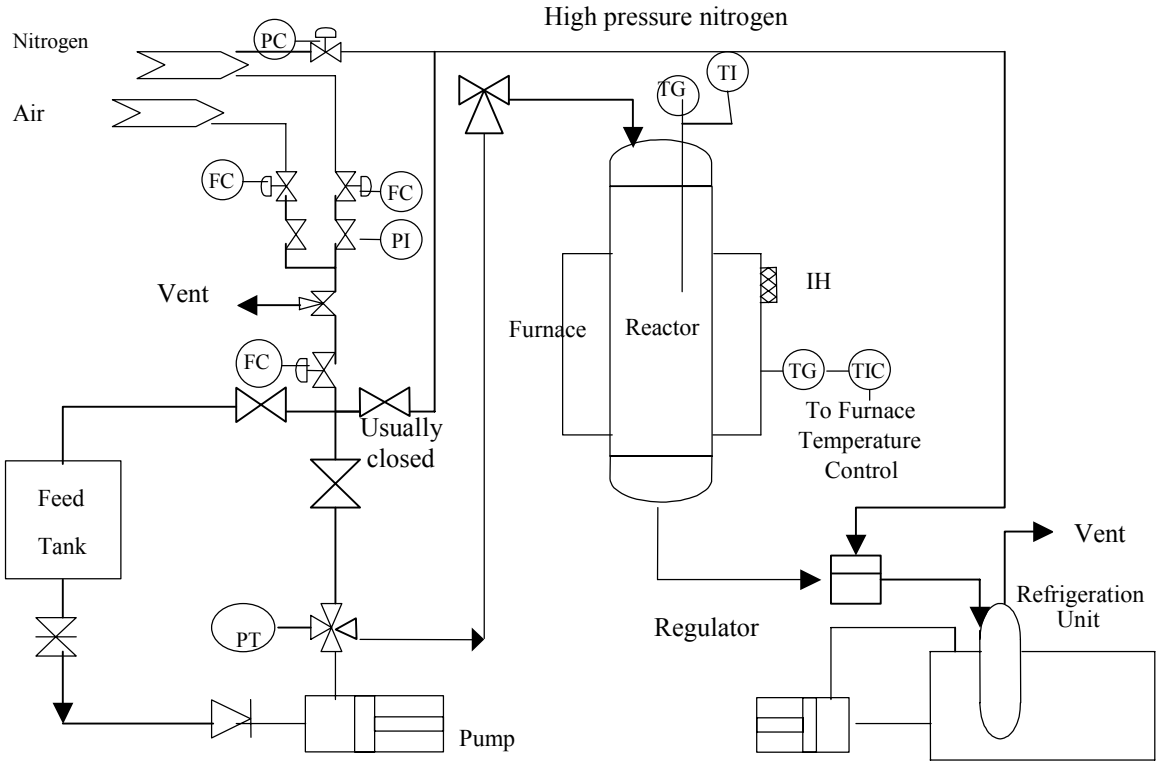

Fig. 2.3. Schematic of continuous flow reactor

The reactor was operated in downflow mode. A stainless steel plunger pump (Eldex B-100-S-4) was used to feed the reactants from a calibrated feed burette.

Adjusting the stroke length of the pump controlled the flow rate. The feed stream near the reactor inlet and the product stream to the backpressure regulator were heated using electrical heating tapes kept at 200-270^{o}C. The feed tank was kept under a slight nitrogen purge. The products from the reactor were collected in a glass receiver cooled near to 0 ^{o}C by means of a recycling cooling bath.

Prior to starting the feed pump, the reactor was purged with N_2 for 15 min. Upon observation of liquid exiting the reactor, the backpressure was applied. It took the reactor approximately 10 min to reach a pressure of 2.05 MPa. Grab samples of product were taken throughout the day from the exit line at the cooling bath.

To shut down the reactor, the pump was stopped, the inlet heating tape turned off, the high pressure vented, and the system was purged with N_2 for at least 15 min. After purging, the N_2 was sometimes replaced by air through the three-way valve to regenerate the catalyst for at least 5 h but no more than 12 h.

2.3 Semibatch Reactor Experiments

The synthesis of MTA was conducted in semibatch stirred autoclaves, either 500 mL (Autoclave Engineers, SR-ZC-500) or 20 mL (Autoclave Engineers, SR-BC-OG). In both cases a vent valve was used to adjust the gas (air or O_2) flow. Reactor temperatures were varied between 150-200^{o}C. The temperature was measured using a 1/16" internal K or J thermocouple in contact with the liquid. Temperatures of both reactors were controlled by PID controllers, and held within ± 1^{o}C of the set point. Reactor pressures were varied between 0-5.46 MPa. The reactor pressure was controlled directly by the pressure regulator on the cylinder. A refrigerated condenser after the vent valve was used

to return xylene to the reactor from the exhaust gas. A schematic of the system is shown in Figure 2.4.

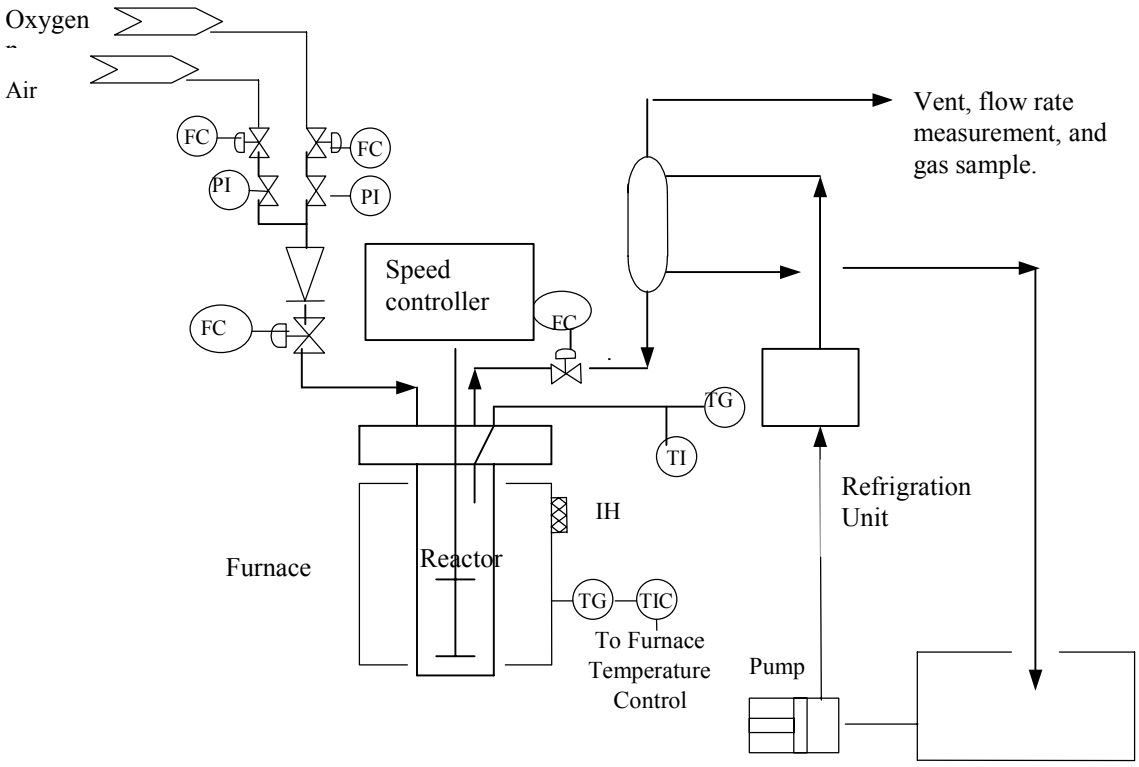

Fig. 2.4. Schematic of semibatch reactor

2.4 Analysis of Feed and Product Samples

Feeds for the synthesis of DEET were prepared from MTA (Aldrich, 99%), diethylamine (DEA, Aldrich, 99.5+%), and DEET itself (MGK, 95+%). Feed mixtures were analyzed by GC before use. Product samples of ~0.1 mL were collected and diluted with 9 volumes of 10% (vol) toluene in methanol. Toluene was the internal standard. They were stored in a refrigerator until they could be analyzed by GC. The organic phase was analyzed using a Varian 3400GC fitted with a flame ionization detector (FID). An

Alltech Econocap EC-1 column (30 m × 0.32 mm) was used. Peak identifications were made using a similar GC column in an H-P 5900 GC with mass-selective detector (H-P 5972) (Dooley, 1998). Details of the GC analyses are summarized in Appendix A.

Calibration curves (four points) were prepared for DEA, MTA and DEET. The calibration slope of DEA was also used for trimethyamine (TEA) and N,N-diethyl,1-butanamine (1-BA). The calibration slope of DEET was also used for 3-methylbenzonitrile (MTN), ethyl-m-methylbenzoate (EMB), N-ethyl, m-toluamide (ETA), N,N-diethylbenzamide (DBA), o-DEET, p-DEET, trimethylbiphenyls (TMB), N-butyl,N-ethyltoluamide (BTA) and heavier compounds (C). Compound identifications had been made previously by GC/MS (Dooley, 1998).

For the synthesis of MTA, feeds were prepared from m-xylene (Aldrich., 99%), the recycled liquid aldehyde/alcohol/acid products, and/or water, and/or acetic acid (HAc, J. T. Baker, 99.9%). There are liquid, solid, and gas product samples in this reaction. Liquid samples of ~0.1 mL and solid samples of ~0.1 g were diluted with 9 volumes of 1 wt% benzoic acid (Aldrich., 99.5%) in 50/50 (vol) methanol/ethanol. Benzoic acid was the internal standard. Samples were analyzed by an HP5890 fitted with a flame ionization detector (FID). An Alltech Supelco EC-1 column (30 m × 0.53 mm ID) was used. Peak identifications were made using a similar GC column in an H-P 5900 GC with mass-selective detector (H-P 5972) (Dooley, 2000a). Details of the GC analyses are given in Appendix A.

Calibration curves (four points) were prepared for m-xylene, m-tolualdehyde, m-methybenzyl alcohol, isophthalic acid and MTA. The calibration slope of m-xylene was also used for xylene isomers. The calibration slope of m-tolualdehyde was also used for

benzaldehyde. The calibration slope of m-methybenzyl alcohol was also used for m-cresol. The calibration slope of terephthalic acid was also used for an unknown oxygenated compound (A) of molecular weight 166. The calibration slope of MTA was also used for $C_{16}H_{16}O_2$ and a second unknown oxygenated compound (C) of molecular weight 240.

Gas samples were collected in Tedlar sample bags (17.8 × 17.8 cm, Alltech), and were used to quantify the CO and CO_2 produced. Samples were analyzed by an HP 5890A GC equipped with a thermal conductivity detector (TCD). A Porapak Q column (Supelco, 1.07 m × 3.18 mm ID) was used. Details of the GC analyses are summarized in Appendix A.

2.5 Catalyst Characterization

Catalyst surface areas were determined by multipoint N_2 adsorption measurements (BET method) using an Omnisorp 360 static adsorption apparatus. The samples except Co(salen) and Co(DMBA) were dried under vacuum at ~300^{o}C overnight. The drying temperatures for Co(salen) and Co(DMBA) were <100 ^{o}C TO prevent complex decomposition. Approximately 0.1-0.5 g samples were used in the BET experiments, with the amount depending on the expected surface area of the catalyst.

For thermogravimetric analysis (TGA, Perkin-Elmer TGA 7), the catalysts were ground to pass through a 100-mesh sieve. A 12-17 mg sample was loaded in the platinum microbalance pan at 50ºC. Temperature programs for different catalysts were run using 100 mL/min of He or 50 mL/min air + 50 mL/min He. The following sequence of treatments was performed for coke analyses: (1) the sample was dried in He (100 mL/min) by programming from 50-550 ^{o}C at 5 ^{o}C/min with a final hold of 30 min and

hold at 550 ^{o}C; (2) the sample was oxidized in gas mixture (50 mL/min air + 50 mL/min He) at 550 ^{o}C for 120 min. The raw data were differentiated using a C++ program (Massgraph).

Investigation of total strong acid and strong Brønsted acid contents of the catalysts used for DEET synthesis was by temperature-programmed desorption of 1-propanamine (1-PA) using the TGA. The following sequence of treatments was typically performed: (1) the sample was dried in He (100 mL/min) by programming from 50-575 ^{o}C at 10 ^{o}C/min with a final hold of 10 min; (2) 1-PA was delivered by bubbling 50 mL/min of He through the liquid at ambient temperature with adsorbtion for 10 min at 50 ^{o}C; (3) desorption was conducted in He by programming from 50-550 ^{o}C at 5 ^{o}C/min.

The chemical structures of some of the supported catalysts (Co(salen) and Co(DMBA)) were analyzed by FT-IR (Mattson, MI Gold) in diffuse reflectance (DRIFTS) mode. The cell was a DRIFTS Collector II (Spectra-Tech). The number of scans was 1024 and the nominal resolution was 4 cm^{-1}. The type of detector used was the MCT (cooled) detector. Before the sample was scanned, the pressure was less than 7×10^{-7} MPa.

Chapter 3 Results and Discussion

3.1 N,N-Diethyl-Toluamide (DEET) Synthesis by Catalytic Amidation from m- Toluic Acid and Diethylamine

3.1.1 Thermodynamic Analysis of DEET Synthesis

The main reaction in DEET synthesis from MTA and DEA is shown in equation (3-1). The principal side reaction is that of MTA and DEA to form N-ethyl-toluamide (ETA) and ethanol (EtOH), equation (3-2).

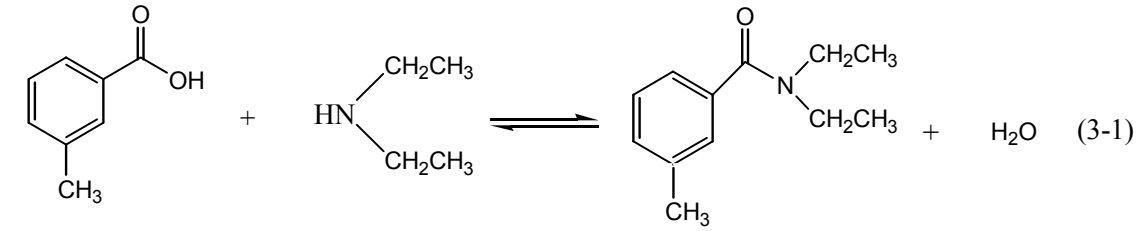

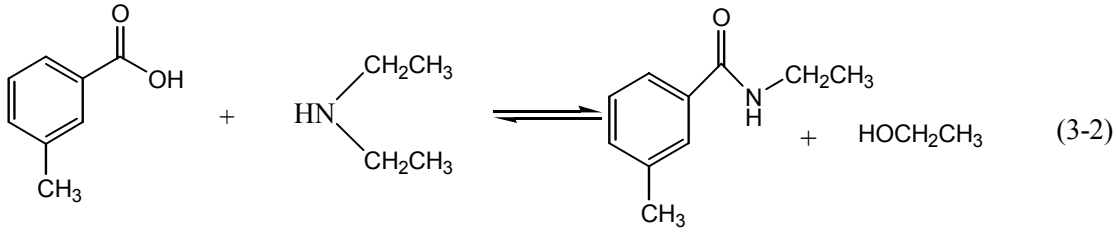

To gain a thermodynamic understanding of the reactions, the ΔH_{rxn}, ΔG_{rxn}, and K_e for gas phase states were calculated from tabulated and estimated values of the ΔH_f, ΔG_f, and C_{pm}. The ΔH_f values of MTA, DEA, EtOH and water at 25°C were taken from a standard reference database (NIST Chemistry WebBook, 2001) while the values for DEET and ETA were estimated using Joback fragmentation rules (CS Chem Pro v5, 1999). The ΔS_f values of MTA, DEA, ETA and DEET at 25°C were calculated from the equation $\Delta S_f = (\Delta H_f - \Delta G_f)/T$, where the ΔH_f and ΔG_f values were estimated using Joback fragmentation rules (CS Chem Pro v5, 1999), ΔS_f values of water and ethanol were taken from standard references (NIST Chemistry WebBook, 2001; Handbook of Chemistry and

Physics, 54th ed., 1973-1974). C_p values at 25°C except for ethanol and water were estimated using Joback fragmentation rules (CS Chem Pro v5, 1999). Cp values of water were found from NBS/NRC Steam Tables (1984). C_p values of MTA, DEA, ETA and DEET at 227°C and 327°C were estimated from equation (3-3) (Perry et al., 1997). Table 3.1 gives a1 to a5 values at 227°C and 327°C. C_p values at other temperatures between 227°C and 327°C were calculated from equation (3-4). Cp values of ethanol at 227°C and 327°C were found from a standard reference (NIST Chemistry WebBook, 2001) while Cp values at other temperatures were estimated using equation (3-4). $C_{pm,i}$ values were calculated by averaging. Comparisons were made between some of the values calculated using the CS Chem3D Pro software (1999) and some of the values obtained from standard references to determine the accuracy of the calculations. It was found that for the calculated values there was less than 5% error except ΔH_f of DEA where the error was 28% (Table 3.2).

Table 3.1. Values of Constants for Eq. (3-3)

Temperature, °C	A1	a2	a3	a4	a5
227	-1.85	15.5	8.89	15.7	16
327	-4.61	17.5	10.5	17.5	17.3

$$C_{Pi,T} = a1 + a2C + a3H + a4O + a5N \qquad (3-3)$$

Where
T, 227°C or 327°C;
C, the number of carbon atoms in the molecule;
H, the number of hydrogen atoms in the molecule;
O, the number of oxygen atoms in the molecule;
N , the number of oxygen atoms in the molecule.

$$C_{pi,T} = C_{pi,227C} + (C_{pi,327C} - C_{pi,227C}) \times (\frac{T - 227}{100}) \qquad (3-4)$$

T in °C.

The ΔH_{rxn} at 25°C was calculated from the heats of formation at 25°C:

$$\Delta H_{rxn} = \sum_i \nu_i \times \Delta H_{f,i} \qquad (3-5)$$

The K_e^0 value at 25°C was calculated from the following equations (Smith and Ness, 1987):

$$K_e{}^0 = \frac{P_{DEET} P_{H_2O}}{P_{MTA} P_{DEA}} = \exp\left(-\Delta G^0{}_{rxn} \Big/ RT\right) \qquad (3-6)$$

The K_e values at other temperatures were calculated by integrating the van't Hoff equation from 25°C to the desired temperature T (K):

$$\frac{d(\ln(K_e))}{dT} = \frac{\Delta H_{rxn}}{RT^2} \qquad (3-7)$$

After integration, the above equation can be expressed as:

$$\ln(\frac{K_e}{K_e{}^0}) = \frac{1}{R}\left\{\sum_i \nu_i \Delta H^0{}_{f,i}(\frac{1}{T_0} - \frac{1}{T}) + \sum_i \nu_i C_{pm,i} \ln(\frac{T}{T_0}) - \sum_i \nu_i C_{pm,i}(1 - \frac{T_0}{T})\right\} \qquad (3-8)$$

Table 3.2 gives the values at 25°C used in these calculations. The C_{pi} values at other temperatures are summarized in Table 3.3.

Table 3.2. Thermodynamic Data for the Main and Side Reaction in DEET Synthesis (298 K, 0.1013 MPa)

Chemicals	$\Delta H^0{}_f$, kJ/mol	$\Delta G^0{}_f$, kJ/mol	$\Delta S^0{}_f$, J/mol/K	$C^0{}_p$, J/mol/K	$\Delta H^0{}_f$, kJ/mol	Error of $\Delta H^0{}_f$, %
DEA	-99.8[1]	44.9[2]	-485[3]	115[3]	-72.4[3]	-28
MTA	-328[1]	-236[2]	-309[3]	145[3]	-317[3]	-4
m-DEET	111[3]	135[2]	-825[3]	241[3]		
H_2O	-241.8[1]	-298.1[2]	188.8[1]	13.6[4]	-247.7[3]	-1
ETA	-137[3]	77[2]	-825[3]	190[3]		
EtOH	-235[1]	-319[2]	282[5]	65[1]	-237[3]	2
1=NIST databank, 2= Calculated from $\Delta H^0{}_f$ and $\Delta S^0{}_f$, 3=Joback calculation, 4=Perry's Chemical Engineers Handbook (7th edition), 5=Handbook of Chemistry and Physics, 54th ed..						

All gas phase data.

$C_p{}^0$ of EtOH from Joback calculation, 64.6J/mol/K, error%=-1%.

Table 3.3. C_p (J/mol/K) at Different Temperatures

T, ^oC	245	250	260	300	320
MTA	230	232	234	246	252
DEA	178	180	182	192	196
DEET	376	379	384	405	415
H_2O	35.82[1]	35.9[1]	35.9[1]	36.3[1]	36.5[1]
ETA	308	310.0	314	331	339
EtOH	98.0[2]	98.7[2]	99.9[2]	105[2]	107[2]
1= NBS/NRC Steam Tables; 2=NIST databank; other data from equation (3-3) and (3-4) calculation					

The equilibrium constants at different temperatures were calculated by equation (3-8). The equilibrium constants of the main reaction (3-1) at different temperatures can also be calculated from the empirical equation K_e = exp(8.81-3019.25/T) (T = 273.15+T(^oC), 260-320 ^oC) using $HClO_4$ as catalyst (de Vekki and Mozzhukhina, 1997). K_e values can also be estimated from the best MTA conversions of de Vekki and Mozzhukhina (1997) according to equation (3-9).

$$K_e = \frac{(\alpha + x)x}{(1 - x)(\beta - x)} \qquad (3-9)$$

$$\alpha = {}^{[DEET]}\!/\!_{[MTA]}\, molar \quad ratio \quad in \quad feed$$

$$\beta = {}^{[DEA]}\!/\!_{[MTA]}\, molar \quad ratio \quad in \quad feed$$

$$x, MTA \quad conversion$$

The equilibrium constants K_e calculated by data from Table 3.2 and Table 3.3 at different temperatures are summarized in Table 3.4 and compared with those calculated from the empirical equation and those estimated from the best data of de Vekki and Mozzhukhina (1997).

Using the K_e values, the equilibrium MTA conversions for the main reaction (3-1) at different temperatures and feeds were calculated from equation (3-9) and summarized in Table 3.5.

Table 3.4. Comparison of Equilibrium Constants at Different Temperatures

T (^oC)	Reaction (3-1)			Reaction (3-2), from thermodynamic data
	From best conversions of de Vekki and Mozzhukhina (1997)	From Ke=exp(8.81-3019.25/T)	Estimated from thermodynamic data	
245	-	-	4.57	2.5×10^{10}
250	-	-	5.39	3.0×10^{10}
260	1.98	23.2	7.43	4.2×10^{10}
300	2.56	34.5	23.9	1.5×10^{11}
320	4.46	41.2	40.3	2.7×10^{11}

Table 3.5. MTA Equilibrium Conversions for Reaction (3-1)

T (^oC)	MTA Conv.%[2]			MTA Conv.%[3]			MTA Conv.%[4]		
	Feed A[1]	Feed B	Feed C	Feed A	Feed B	Feed C	Feed A	Feed B	Feed C
245	58.6	62.5	68.1	-	-	-	-	-	-
250	60.8	64.6	69.9	-	-	-	-	-	-
260	65.0	68.4	73.2	77.4	79.7	82.8	43.4	48.3	55.8
300	77.7	80.0	83.0	80.9	82.8	85.5	50.5	55.1	61.7
320	82.1	83.9	86.4	82.3	84.1	86.5	58.3	62.2	67.9

[1] Feed A, DEA/MTA/DEET = 1/1/0.75; Feed B, DEA/MTA/DEET = 1/1/0.4; Feed C, DEA/MTA = 1/1, no DEET.
[2] K_e, estimated from data of Table 3.2 and Table 3.3.
[3] Ke, calculated from equation $K_e = \exp(8.81-3019.25/T)$.
[4] Ke, estimated from the best MTA conversions of de Vekki and Mozzhukhina (1997).

From Table 3.4, it is seen that the equilibrium constants of reaction (3-2) are very large. From Table 3.5, it is seen that it is impossible to obtain very high MTA conversion at the above temperatures. The MTA conversions and K_e values estimated from the best MTA conversions of de Vekki and Mozzhukhina are much lower than those estimated from thermodynamic data, which shows that the reaction never approached equilibrium in their experiments. Conversions of slightly >80% with >90% selectivity, could be obtained in a batch reactor at 235-255^{o}C with 1.0 wt% solid Tyzor TE/Al_2O_3 catalysts in ~ 4-8 h (Dooley, 2000b), when the product water was removed continuously.

From Table 3.5, it is also seen that the predicted conversions from thermodynamic data at 300°C and 320°C are close to those obtained from the empirical equation K_e = exp(8.81-3019.25/T), which suggests that the estimation of K_e from thermodynamic data is pretty good.

3.1.2 Catalyst Characterization

Catalysts for DEET synthesis were tested by the BET method to determine the surface area. Table 3.6 gives the results. TGA was used to determine catalyst stability and metal loadings for some catalysts. TGA results for supported Tyzor TE and hydroxyapatite (HEA) catalysts are shown in Table 3.7.

Table 3.6. Surface Areas of Catalysts

Catalysts (fresh)	Surface Area (m^2/g)
TiO_2 support	120
Al_2O_3 support	190
MCM-41 (1st batch)	575
MCM-41 (2nd batch)	1080
4.6 atom% Tyzor TE/TiO_2	46
11.4 atom% Tyzor TE/Al_2O_3	72
HEA00 (hydroxyapatite, Ca^{2+}/H^+ = 7.9)	79
HEA01 (hydroxyapatite, Ca^{2+}/H^+ = 6.3)	36
40 wt.% HPA /Silica gel (YJ01)	150
40 wt.% CsHPA/MCM-41 (1st batch) (YJ03, Cs^+/H^+ = 2.5/0.5)	150
50 wt.% CsHPA/MCM-41 (2nd batch) (YJ10, Cs^+/H^+ = 1/2)	290

Table 3.7. TGA results for catalysts

Catalyst	Atmosphere	1st peak, T_{loss} (°C)	wt loss (%)	2nd peak, T_{loss} (°C)	wt loss (%)
4.6 atom% Tyzor TE/TiO_2 (fresh)	Air	250	1.7	450	2.5
4.6 atom% Tyzor TE/TiO_2 (used)	Air	250	0.1	450	3.4
11.4 atom%Tyzor TE/Al_2O_3 (fresh)	Air	250	5.6	450	12.6
HEA00 (fresh)	He	500-900	1.07	-	-
HEA01 (fresh)	He	500-900	1.32	-	-

In air at high temperatures, the oxidation reaction (3-10) should go to completion for supported Tyzor TE catalysts. From this reaction and the above weight loss, the Tyzor TE content of the catalyst can be estimated. From this equation, it is seen that the molecular weight loss is (376-114) = 262 per mole supported Ti complex. Therefore by this method, the supported Tyzor complex composition can be calculated by the equation (3-11) and (3-12).

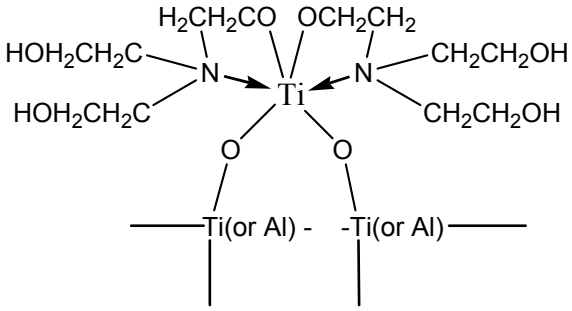

$$\xrightarrow{O_2} (OH)_2TiO_2 \qquad (3\text{-}10)$$

$$mmol\ \ TyzorTE/\ \ g\ \ catalyst = \frac{wt\%_{lost}}{262*100}*1000, \qquad mmol/\ \ g \qquad (3-11)$$

$$atom\% = \frac{mmol\ \ TyzorTE/\ \ g\ \ catalyst}{mmol\ \ TyzorTE/\ \ g\ \ catalyst + mmol\ \ \sup port/\ \ g\ \ catalyst}*100\% \qquad (3-12)$$

For a new 4.6 atom% Tyzor TE/TiO_2 catalyst, the calculated Tyzor atom% is 1.4 mol%. For the used Tyzor TE/TiO_2 catalyst, it is 1.1 mol%. For the fresh 11.4 atom% Tyzor TE catalyst, it is 7.9 mol%.

These weight losses were recorded after extensive treatment (vacuum and overnight) in inert gas at 250ºC, so the samples were dry, and any condensation reaction of the isopropyloxy ligands would have been complete. The theoretical weight losses if all the complexes reacted as in (3-10) would have been far higher for these loadings. Therefore it is clear that for the most part this reaction (3-9) takes place at 250ºC even in

inert gas, and it will complete upon multiple high temperature air treatments (NOTE: surface reactions always take place more efficiently in a TGA than in an actual catalytic reactor, because the small sample is efficiently contacted by a comparatively infinite gas volume, and because the Pt pan often contributes to adsorbing certain components, which then "spillover" to the other solid).

This result is consistent with stability analyses of Tyzor TE in air and in inert gas. The decomposition temperature of Tyzor TE is about 160-300ºC according to estimates of ligand stability (Cotton and Wilkinson, 1980; Jacek, 1988), and the decomposition temperatures of the similar Ti complexes ($(Pr^{i}O)_3Ti(OCH_2CH_2NM_e)$, $(EtO)_3Ti(OCH_2CH_2NM_e)$, Tetrakis(dimethyamido) titanium and Tetrakis(diethyamido) titanium (Alyea and Merrell, 1973; Yun et al., 1999). Tyzor TE is more unstable in air than in inert gas (Wilkinson, etal, 1978; Cotton and Wilkinson, 1980). Therefore, each Ti atom (from the original Tyzor TE) only has 0.55 triethanolaminato ligand (4.6 atom% catalyst) or 1.6 ligands (11.4 atom% catalyst) after extensive treatment in inert gas at 250ºC. The Tyzor TE attached to the Al_2O_3 support is obviously more stable in inert gas than that attached to the TiO_2. It is not suitable to use air to regenerate supported Tyzor TE catalysts.

A used Tyzor TE/TiO_2 (TiO_2, 85 wt% TiO_2/15 wt% Al_2O_3, LeRoche Chemical Company) catalyst lost only 0.1 wt% at 250ºC and 3.4 wt% at 450ºC in high temperature air. This shows that during use whatever changes take place in the structure of attached Tyzor TE at 250ºC are completed within the reactor. The small difference in weight loss at 450ºC for the used vs. the new catalyst suggests that coking was not a problem.

For hydroxyapatites, assuming the following reaction (3-13) occurs at 500-900ºC (Bett et al., 1967) in He atmosphere, the proton content can be calculated from equation (3-14):

$$Ca_{10-n}(PO_4)_{6-2n}(HPO_4)_{2n}(OH)_2 \longrightarrow Ca_{10-n}(PO_4)_{6-2n}(P_2O_7)_n(OH)_2 + nH_2O \qquad (3\text{-}13)$$

$$\text{Proton content } (mmol/g) = \left(\frac{2 \times wt\%_{lost}}{Mw_{water} \times wt\%_{500^\circ C}}\right) \times 1000 \quad mmol/mol \qquad (3-14)$$

The proton contents for HEA00 and HEA01 are 1.19 mmol/g and 1.47 mmol/g, respectively. A higher proton content or smaller Ca^{2+}/H^+ ratio suggests weaker acidity for the hydroxyapatite. The value of n can be calculated by equation (3-15), and then the Ca^{2+}/H^+ ratio. For HEA00, n is 0.595 and Ca^{2+}/H^+=7.9. For HEA01, n is 0.731 and Ca^{2+}/H^+=6.3.

$$\text{Proton content } (mmol/g) = \frac{2n * 1000}{40 \times (10-n) + 95 \times (6-2n) + 96 \times 2n + 34} \qquad (3-15)$$

The adsorptions and desorptions of 1-propanamine (1-PA) for Davison 57 silica Gel, HEA01, YJ01 and YJ10 catalysts were also measured by TGA to estimate the total strong acid and strong Brønsted acid contents of these catalysts (Dooley et al., 1995). Figs. 3.1-3.4 are the desorption TGA curves of 1-PA for these catalysts.

From these figures, it is seen that the total amount adsorbed was proportional to the surface areas of the fresh catalysts (YJ10 > YJ01 > HEA01). The greatest adsorption occurred on 50 wt% Cs-heteropolyacid with Cs^+/H^+=1/2 which had the greatest surface area.

The strong acid contents of the catalysts were estimated by equation (3-16) and the strong Brønsted acid contents were estimated by equation (3-17) using the highest temperature peak (Dooley et al., 1995). These values are summarized in Table 3.8.

Table 3.8. Estimated Strong Acid and Brønsted Acid Contents

Catalysts	Davison 57 silica gel		HEA01		YJ01		YJ10	
	fresh	used	fresh	used	fresh	used	fresh	Used
Strong acid (mmol/g)	0.2	0	7.3	15.1	9.8	5.4	18.9	5.8
Strong Brønsted acid (mmol/g)	no	no	no	no	3.2	no	5.9	No

$$strong\,acid\,(mmol/g) = \frac{\left(\frac{wt\%_{300^{\circ}C} - wt\%_{final}}{100}\right)\left(\frac{1000}{Mw_{1-PA}}\right)}{Dry\quad Weight\quad of\quad Catalyst} \qquad (3-16)$$

$$Strong\,Bronsted\quad acid\quad content\quad (mmol/g) = \left(\frac{\int_{T_{beinning}}^{T_{end}} \frac{dwt\%}{dt}\,dt}{100 \times dry\quad weight\quad of\quad catalyst}\right) \times \left(\frac{1000}{Mw_{1-PA}}\right) \qquad (3-17)$$

From the results for 1-PA thermal analysis, it is seen that the strong acid contents above 300℃ of fresh catalysts are in the order of YJ10 > YJ01 > HEA01 > SiO_2. One reason that YJ01 has the highest strong acid contents may be its high surface area. The used HEA01 catalyst had more acid sites than fresh HEA01. The weight percent of the used HEA01 decreased rapidly after 400 ℃. This is because the structure of this catalyst has changed (losing structural water) during the reaction to form more strong acid sites. Only fresh YJ10 and YJ01 have a small strong Brønsted acid peak (386-501ºC for YJ10 and 391-484ºC for YJ01). It is obvious that there is not a clear deconvolution of this peak in these catalysts, unlike zeolites. Therefore, it is the total strong acid site contents that are the relevant values. Although Brønsted acid sites are the main sites for the proton transfer and are probably responsible for much of the activity of acid catalysts,

there is still considerable uncertainty over their role relative to that of Lewis acids sites in various acid-catalyzed reactions (Satterfield, 1980).

The coke contents of some used catalysts (HEA01 and YJ01) were investigated by oxidation in the TGA. Fig. 3.5 and Fig. 3.6 are the results. The coke content in HEA01 is about 0.82 mg/g catalyst, which may one of the reasons for the deactivation of the catalyst. The coke content in the YJ01 catalysts is almost zero, and the YJ01 catalyst did not deactivate.

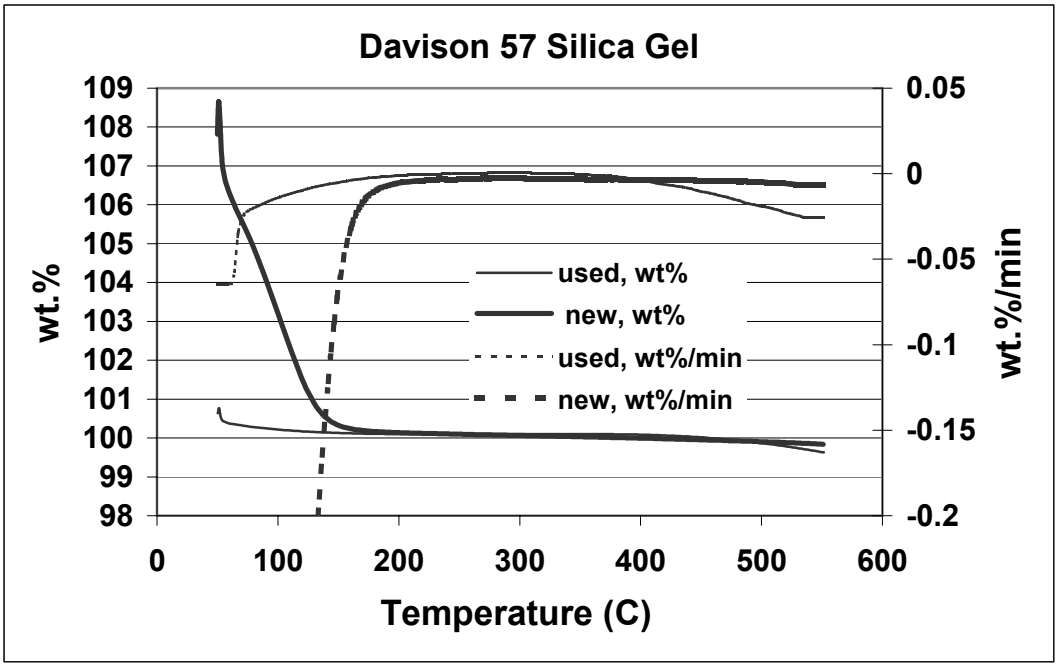

Fig. 3.1. Thermal analysis (TGA) of 1-PA for Davison 57 Silica Gel

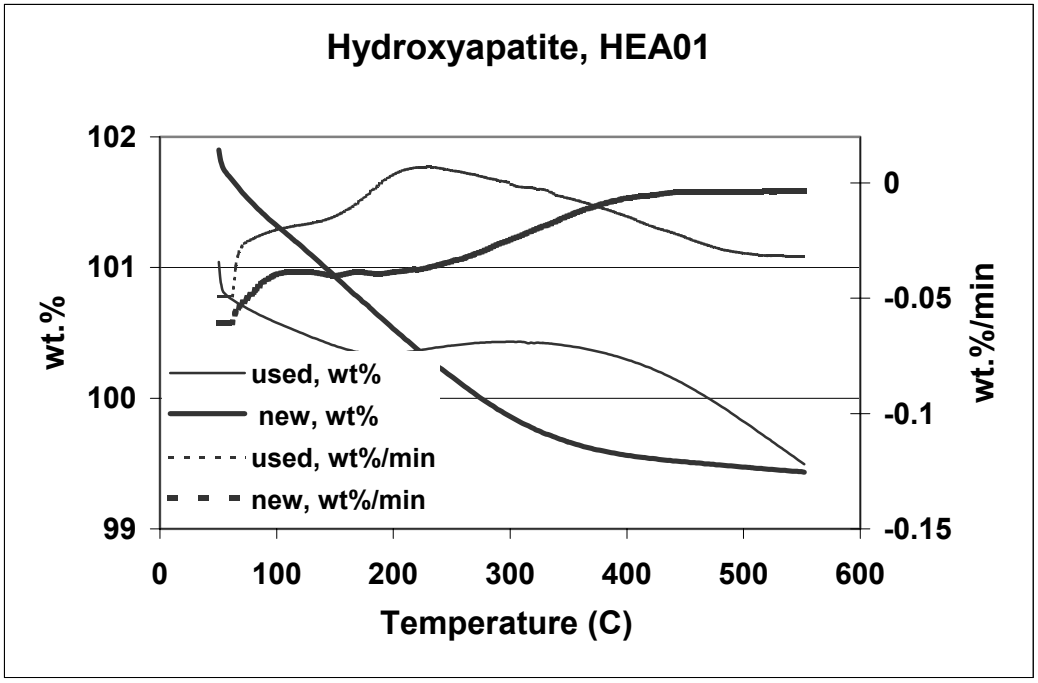

Fig. 3.2. Thermal analysis (TGA) of 1-PA for HEA01

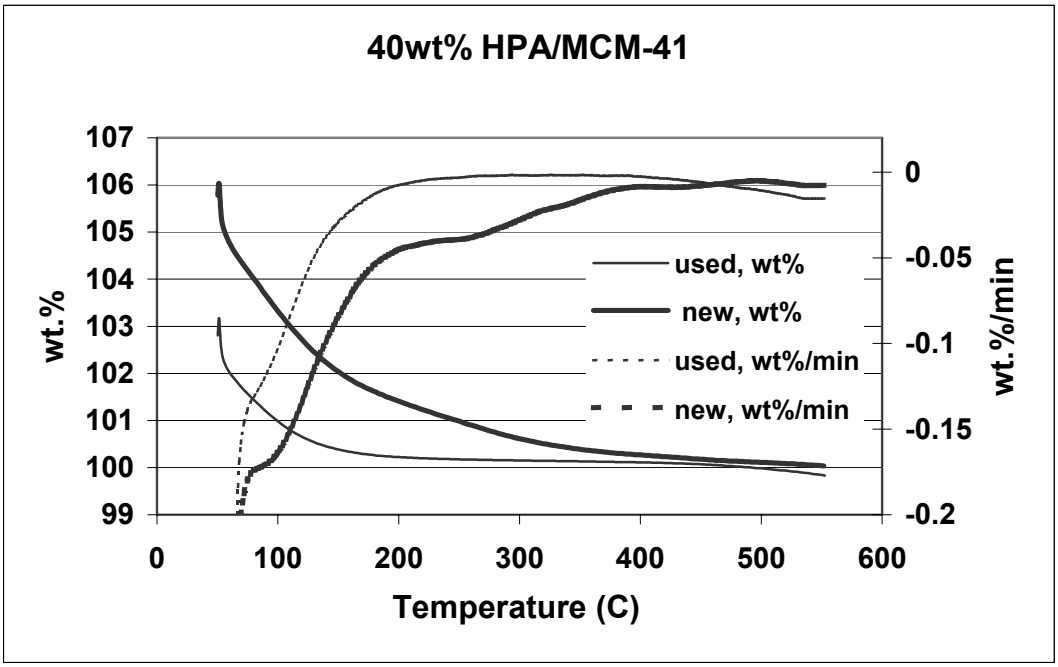

Fig. 3.3. Thermal analysis (TGA) of 1-PA for YJ01

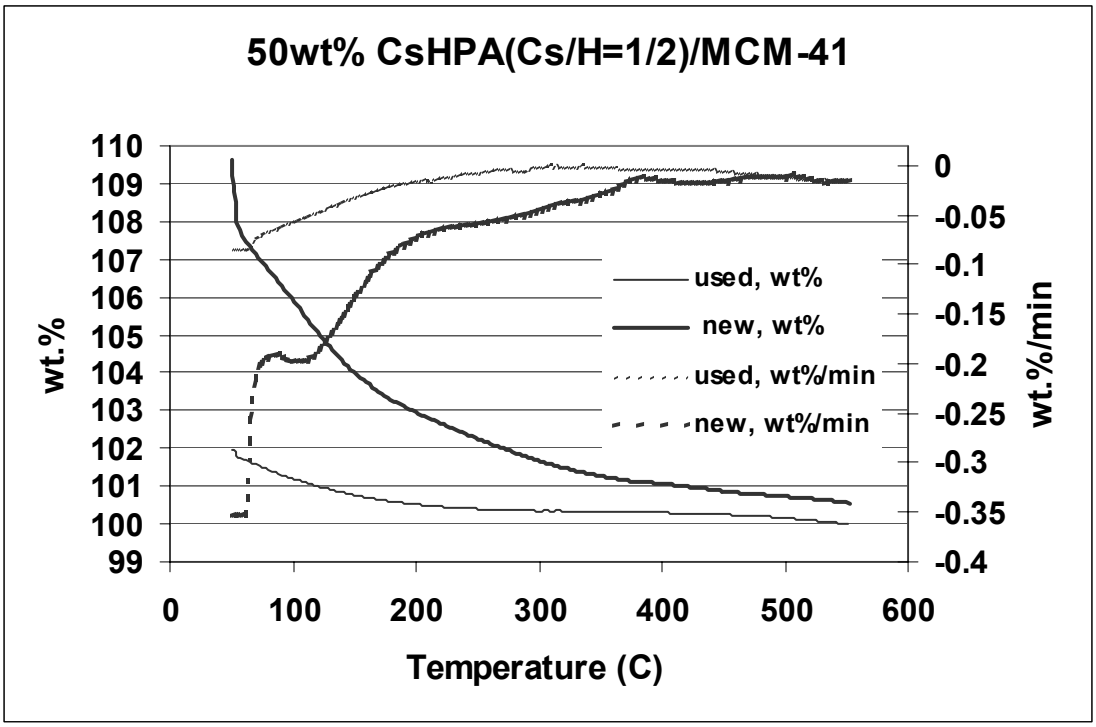

Fig. 3.4. Thermal analysis (TGA) of 1-PA for YJ10

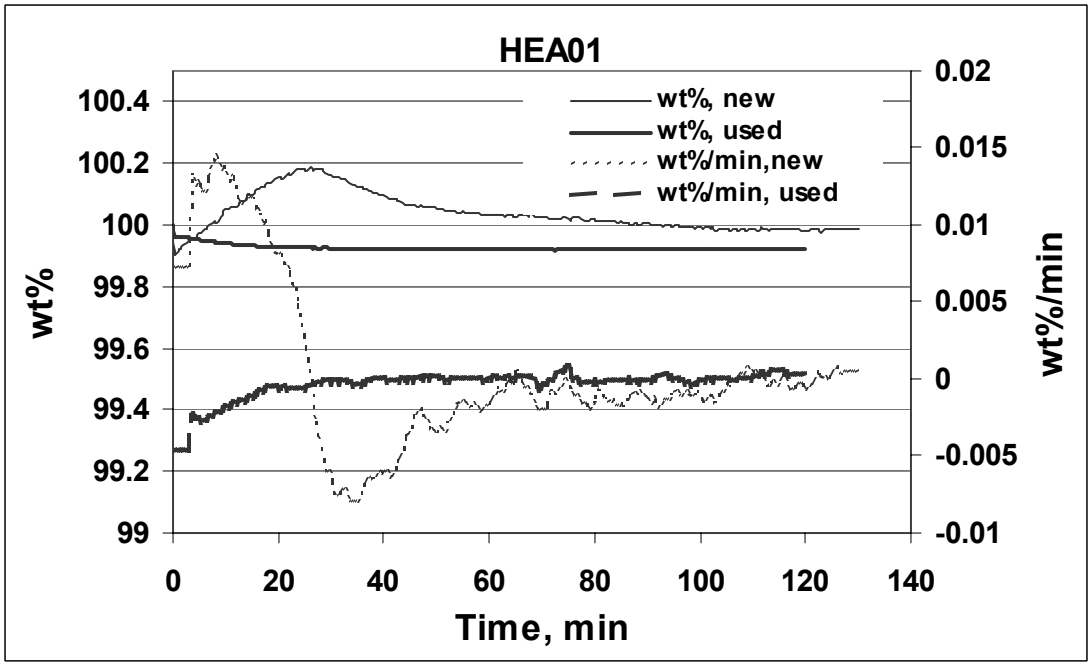

Fig. 3.5. Coke content measurement for HEA01 by TGA

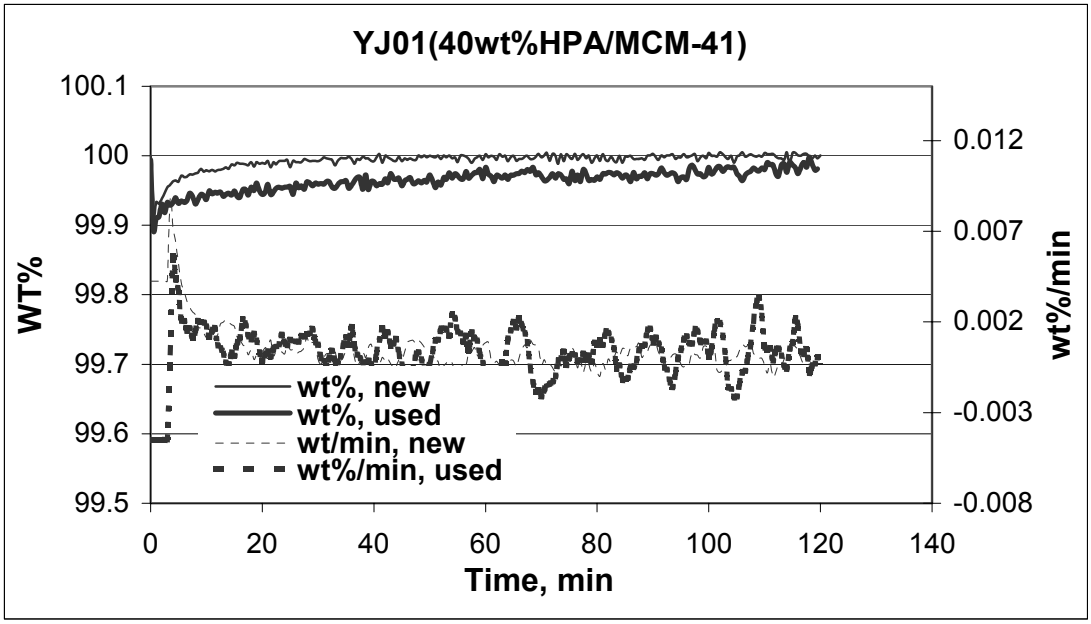

Fig. 3.6. Coke content measurement for YJ01 by TGA

3.1.3 Results and Discussion on the Effect of Different Catalysts

The complete records of the product analyses for DEET kinetics experiments are given in Appendix B. The terminology used to describe the results here and in these spreadsheets is as follows. The products made from MTA include 3-methylbenzonitrile (MTN), ethyl-m-methyl benzoate (EMB), N,N-diethylbenzamide (DBA), ETA, o-DEET, m-DEET, p-DEET, trimethylbiphenyl (TMB), N-butyl, N-ethyltoluamide (BETA) and other heavies. The products not made from MTA are triethanolamine (TEA) and 1-butanamine (1-BA).

% MTA conversion = (moles MTA reacted)/(moles MTA fed)

Raw wt% DEET Selectivity = (weight of DEET)/(∑weight of all compounds in samples)

Adjusted wt% DEET selectivity in Products (real selectivity) = (weight of DEET produced)/(∑weight of products made from MTA)

Weight Hourly Space Velocity (WHSV) = (weight of feed)/(weight of Catalyst)/time.

In all runs except where noted, the mol ratio of Feed A was MTA/DEA/DEET = 1/1/0.75 and that of Feed B was MTA/DEA/DEET = 1/1/0.4.

♦ Control Reactor Experiments

When a 1/1/0.75 = DEA/MTA/DEET feed passes through a blank reactor at 245ºC, 1.97MPa and volume hourly space velocity (VHSV) = 1.6 hr^{-1}, an MTA conversion of about 2.2% with 97.3 wt.% selectivity to DEET was obtained at steady state conditions. When compared with the results below, this clearly indicates that catalysts are responsible for most of the observed activity in the amidation reaction.

It is well known that both strong acids and strong bases can catalyze amidation reactions. Amorphous silica gel is a weak solid acid and can be used as a support for other catalysts. Davison 57 silica gel (W. R. Grace, Grade 57, 8 mesh) was investigated for DEET synthesis. Figs. 3.7 give the results.

From Fig. 3.7, it is seen that a MTA conversion of 47±4% with 82±5% DEET selectivity can be obtained when the reaction was performed at 250ºC, 0.1 MPa and WHSV 6-12 h^{-1}. The MTA conversion and DEET selectivity are almost the same as the best past work (45±9% MTA conversion and 84±3% DEET selectivity) at Louisiana State University for a continuous flow reactor (Dooley, 2000b), performed at 255ºC and 2.14 MPa using a 15 wt% Tyzor TE/SiO_2 catalyst at WHSV = 3.0 h^{-1}. It is also seen that a MTA conversion of 55±2% with 80±5% DEET selectivity can be obtained when the reaction was performed at 300ºC, 0.1 MPa and at WHSV 6-11 h^{-1}. The MTA conversions are far higher than those of the control reactor experiment, and are the same as the best reported result (55.1%) that was obtained in a continuous flow reactor at

300ºC and WHSV = 0.3 h^{-1} using a solid catalyst (de Vekki and Mozzhukhina, 1997). However, MTA conversions at both 250ºC and 300ºC are lower than those predicted by the van't Hoff equation using estimated thermodynamic data (64.5% at 250ºC and 80.0% at 300ºC). Side reactions are partly the reason, because the selectivity to DEET is only about 80% at 300ºC.

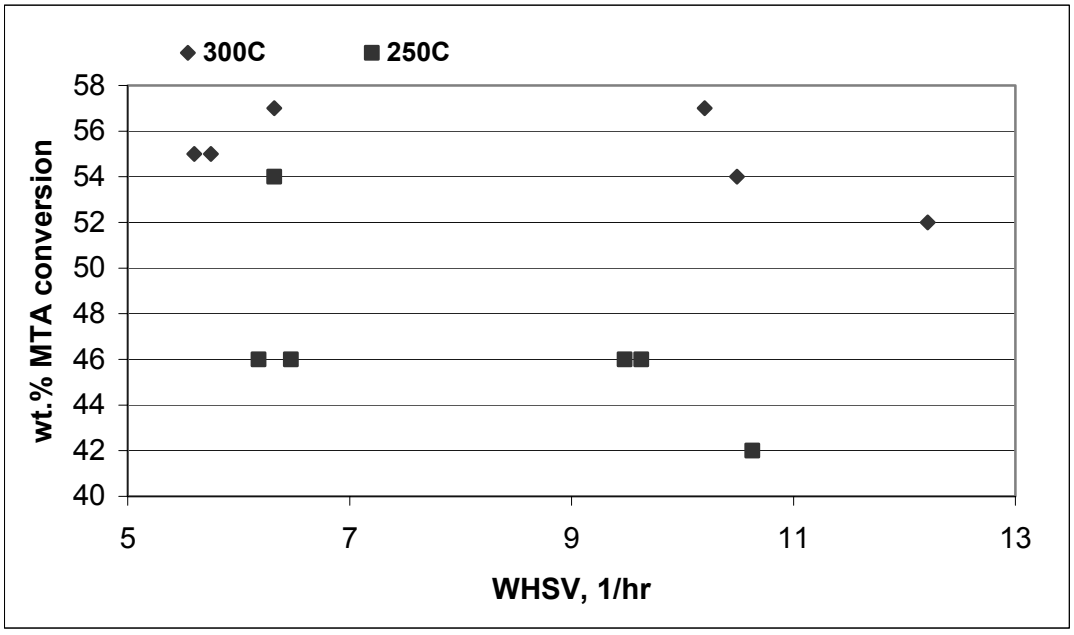

Fig. 3.7A. MTA conversion, Davison 57 Silica Gel, Feed B, 0.1MPa.

Although the fresh Davison 57 Silica Gel adsorbs 1-PA, the total strong acid contents in both the fresh and the used silica are almost zero (Fig. 3.1). This suggests that strong acid sites are not necessary to catalyze the amidation reaction at high temperatures.

The catalyst stability was determined by measuring the change in the conversion and selectivity with time on-stream. Fig. 3.7C shows the stability of the catalyst, which appears fair.

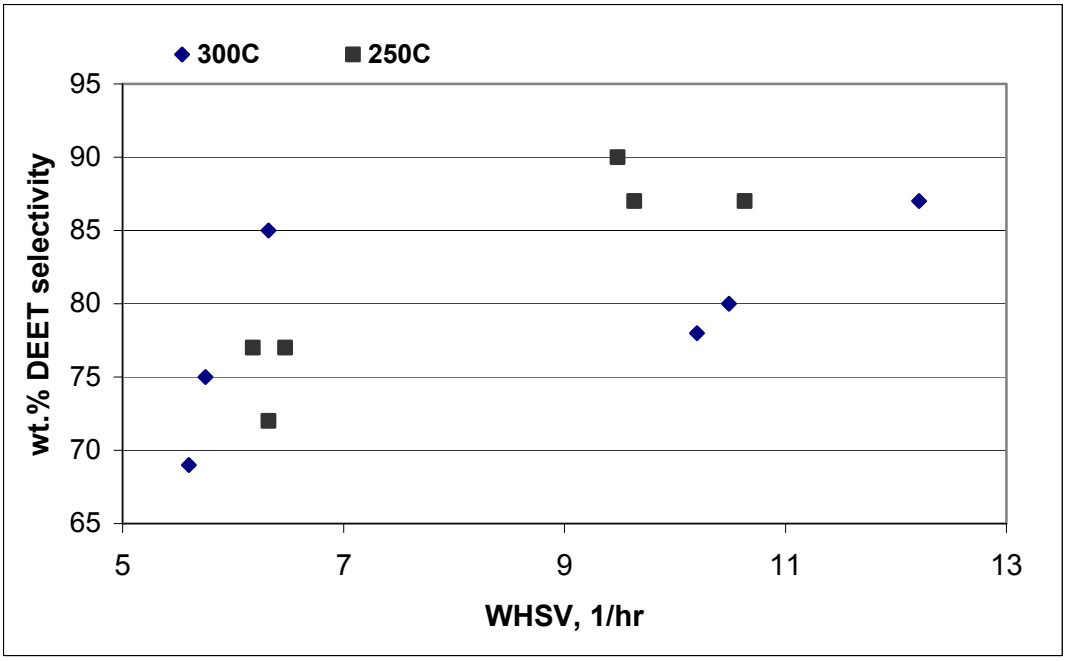

Fig. 3.7B. DEET Selectivity, Davison 57 Silica Gel, Feed B, 0.1MPa.

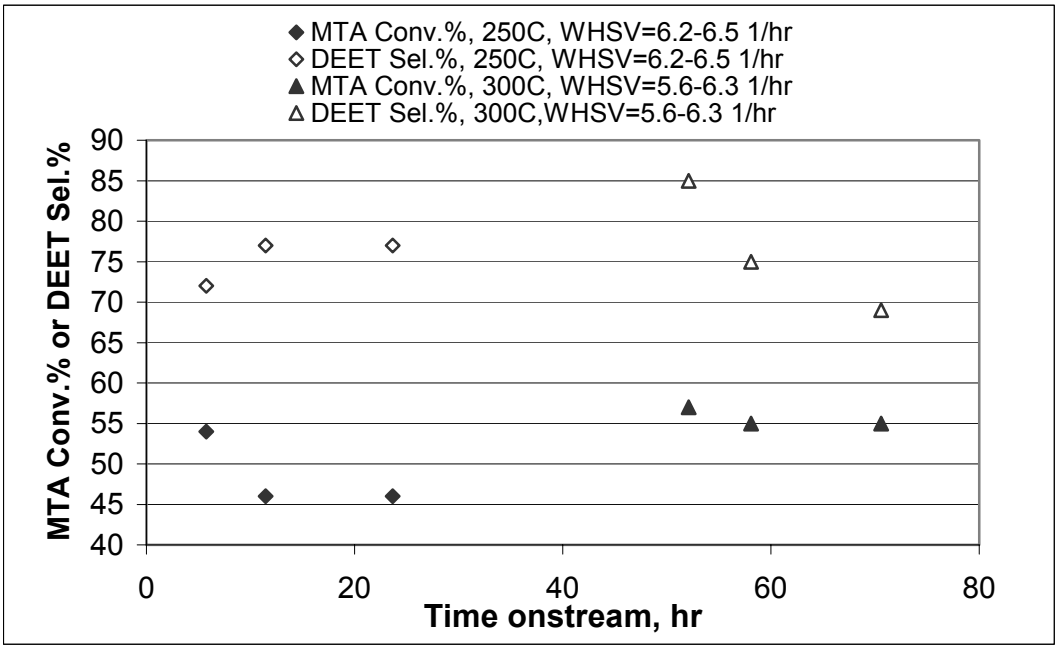

Fig. 3.7C. Catalyst Stability, Davison 57 Silica Gel, 0.1MPa, Feed B

Table 3.9. Run with THN/DEA feed[1], Davison 57 Silica Gel Catalyst. 300ºC, 0.1MPa, WHSV = 11.2 hr^{-1}.

Compounds	Raw Wt % Sel.	
	Feed	Product sample
Diethylamine (DEA)	24.8	23.6
Triethylamine (TEA)	0	0
Toluene (TOL)	0	0
N,N-Diethyl, 1-Butanamine (1-BA)	0.2	0.2
3-methylbenzonitrile (MTN)	0.6	0.9
Tetrehedronaphathalene (THN)	74.0	72.4
m-Toluic acid (MTA)	0.4	0.8
Ethyl-m-methyl benzoate (EMB)	0	0
N,N-diethyl benzamide (DEA)	0	0
N-ethyl, m-toluamide (ETA)	0	0
o-DEET	0	0
m-DEET	0	1.7
p-DEET	0	0
Trimethylbiphenyl (TMB)	0	0.3
N-butyl, N-ethyl toluamide (BETA)	0	0
Heavies (C)	0	0

[1] DEA wt% is the same as that in the usual Feed B, 25.6%.

ETA is the primary side product in DEET synthesis from MTA and DEA (for detail see section 2.1.3 and Dooley, 1998). The typical ETA selectivity is about 16 wt% (300ºC, Feed B) when using Davison Silica Gel 57 as catalyst. In the continuous reactor run, enough DEET must be added to the feed in order to get a single liquid phase. Therefore, ETA can be made either by the decomposition of DEET or by the amidation of MTA with the disproportionation compounds of diethylamine (monoethylamine and triethylamine). A run with a feed of only tetrehydronaphthalene (THN) solvent and DEA was conducted to determine whether DEA disproportionation could take place at the temperatures of the DEET reaction. In this run, THN was a very stable solvent and did not react with any compounds in the feed. If little TEA is produced, then it is likely that ETA is being produced mostly from the decomposition of DEET. Table 3.9 shows the product distribution in the feed and the product sample. The result shows that no TEA

was produced and little DEA reacted. It was judged from the results that ETA was formed by decomposition of DEET.

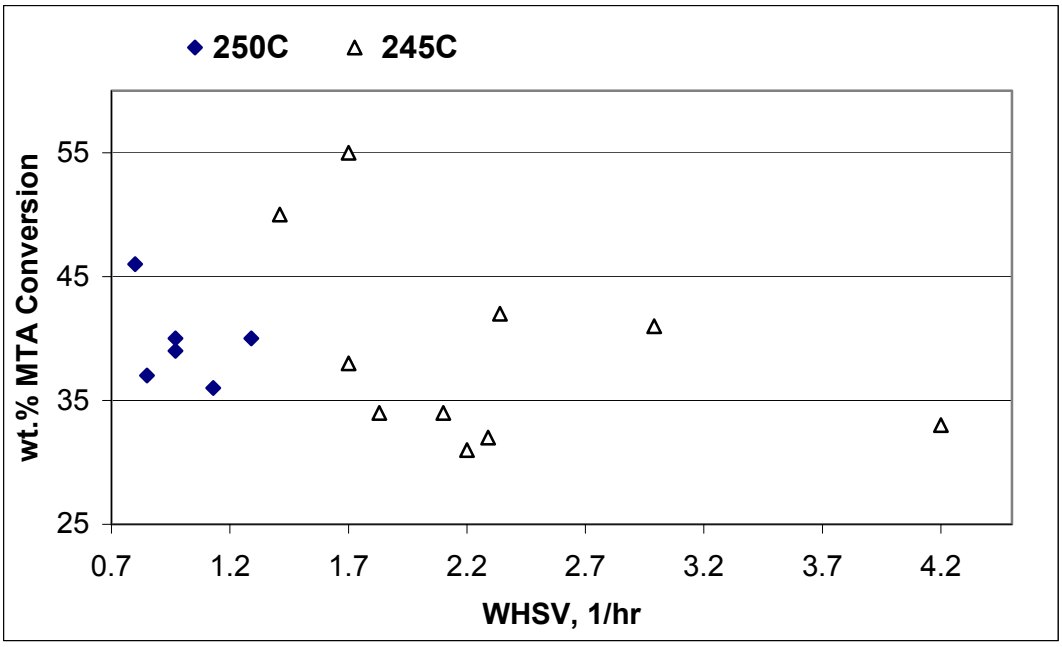

Fig. 3.8A. MTA Conversion, 4.6 mol% Tyzor TE/TiO_2, 2.14MPa, Feed A

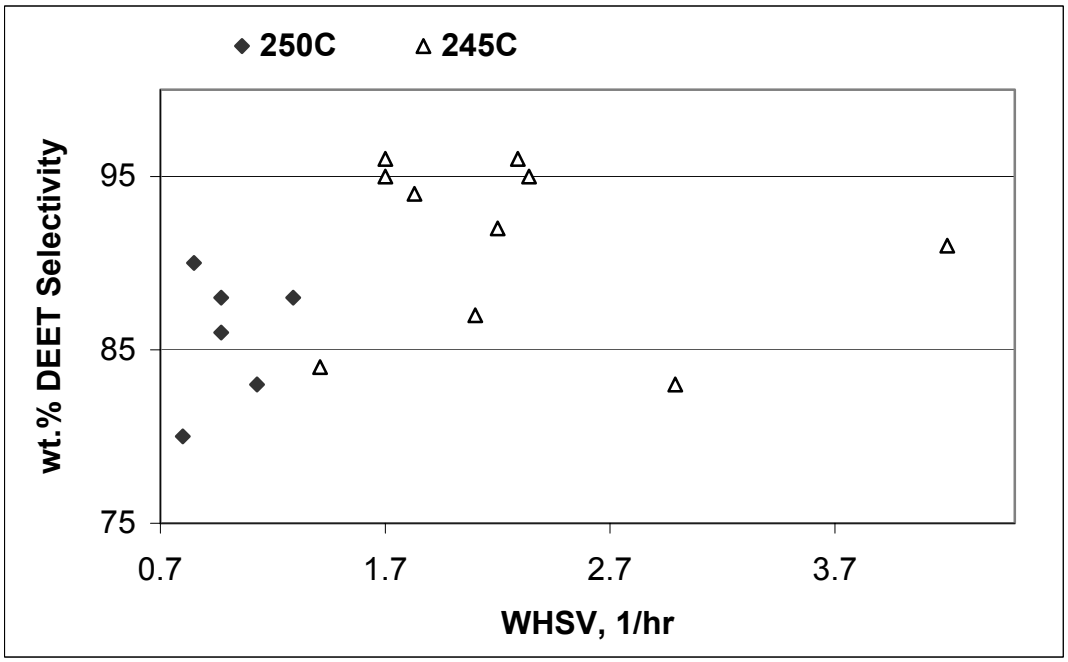

Fig. 3.8B. DEET Selectivity, 4.6 mol% Tyzor TE/TiO_2, 2.14MPa, Feed A

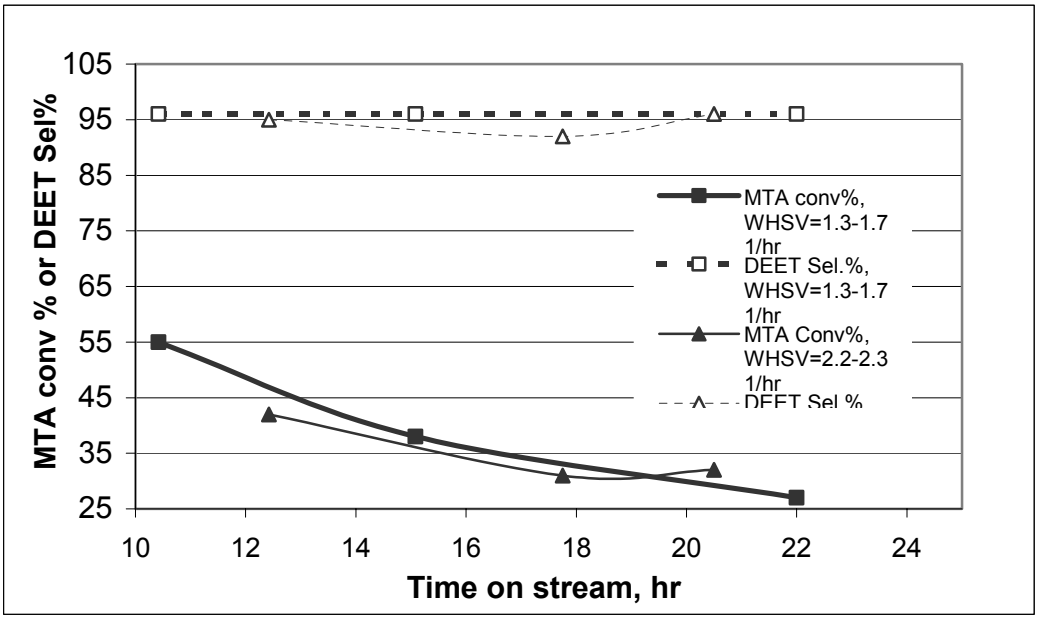

Fig. 3.8C. Stability of 4.6 mol% Tyzor TE/TiO_2, 245ºC, 2.14MPa, Feed A

♦ Reactor Experiments using 4.6 mol% Tyzor TE/TiO_2 Catalysts

Tyzor TE, a weakly basic organometallic complex, is the best homogeneous catalyst (Hull, 1979). Tyzor TE can be mounted onto the almost neutral oxide supports TiO_2 or Al_2O_3 to form heterogeneous catalysts. Fig 3.8 gives the results using TiO_2 as the support at 245ºC and 250ºC, here mol% = (mols of Tyzor TE)/(mols of Tyzor TE + mols of support)×100%. The precisions for conversion and selectivity in this run are ±3% (absolute STDEV). From Fig. 3.8A, it is obvious that the conversion data at 245ºC can be divided into two areas. From Fig. 3.8C, it is seen that this catalyst deactivates very fast with time on-stream (the conversion decreased almost 30% in 24 hours). It is found that points with lower conversions appeared at longer times on-stream when the catalyst

had deactivated. Therefore, regeneration is needed for this catalyst. The run at 250ºC was performed using fresh Tyzor TE/TiO_2, typically with regeneration by N_2 at 250ºC overnight. The stability appears better. Contact with N_2 does have a positive benefit, probably resulting from a stripping of residual heavies from the catalyst. The presence of trimethylbiphenyls and other heavies in the product stream suggests that heavies do build up on the catalysts during a run. That the Tyzor TE/TiO_2 catalyst has more wt% loss at 450ºC than the fresh Tyzor TE/Al_2O_3 catalyst supports this conclusion (Table 3.7).

According to the predicted thermodynamic data (Table 3.5), the conversion at 250ºC should be slightly higher than that at 245ºC. However, from experimental results this is not the case. From Fig. 3.8B, it is also seen that the selectivity at 250ºC is lower than at 245ºC. In this run, most of the reactants are liquid phase because the reaction pressure is 2.14 MPa, much higher than the estimated saturation vapor pressure of Feed A at 250ºC (1.1 MPa), so these phenomena are not related to phase equilibria. From Fig 3.8A, it is easy to see that deactivation of the catalyst occurred at both 250ºC and 245ºC, and the data at 250ºC were obtained at low WHSV while the data at 245ºC were obtained at high WHSV. The deactivation of the catalyst occurred more rapidly at 250ºC and low WHSV than at 245ºC and high WHSV. The average conversions at 245ºC and 250ºC are 45% and 38% before catalyst deactivation, respectively, which are near the equilibrium conversions (Table 3.5). For any positive order kinetics, a reversible reaction near equilibrium will change less with respect to WHSV than an irreversible reaction, especially when the irreversible reaction is at low conversion. Therefore the secondary reaction (3-2) will increase greatly as WHSV decreases (reaction (3-2) is irreversible, see Table 3.4). It is also clear that the difference in WHSV is far more important than the

5ºC temperature difference. That is why both MTA conversion and DEET selectivity are lower at 250ºC than at 245ºC.

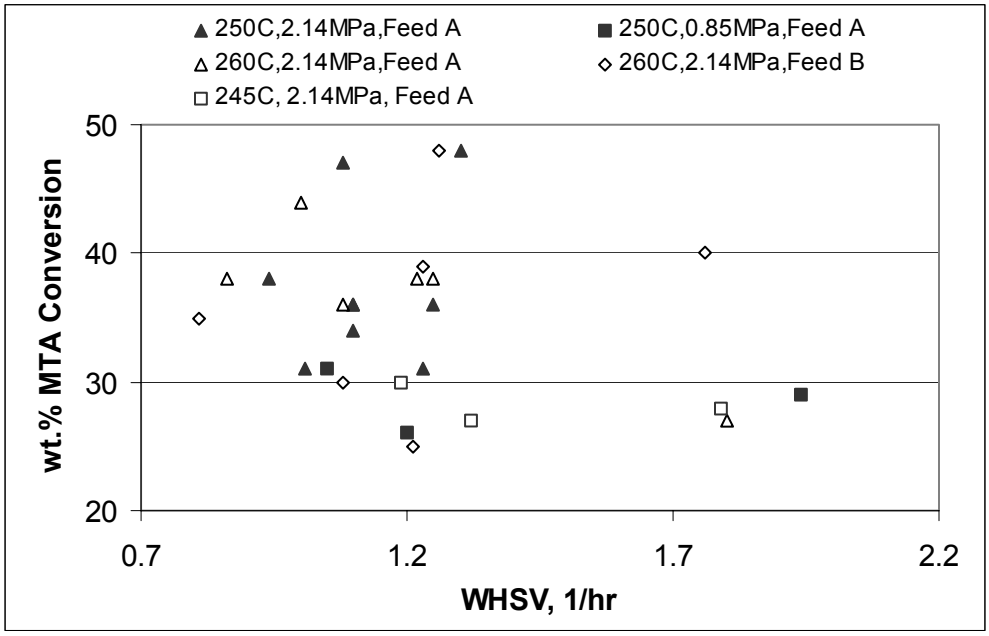

Fig. 3.9A. MTA Conversion, 11.4mol Tyzor TE/Al_2O_3

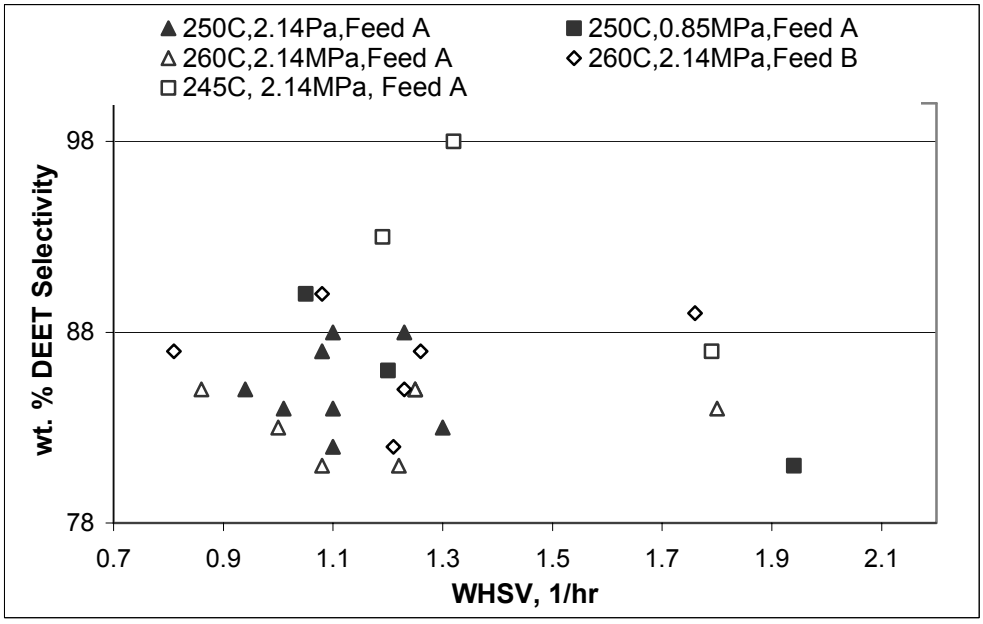

Fig. 3.9B. DEET Selectivity, 11.4mol Tyzor TE/Al_2O_3

♦ Reactor Experiments Using 11.4 Mol% Tyzor TE/Al_2O_3 Catalysts

In order to determine the effect of support on the activity and selectivity of Tyzor TE catalysts, an 11.4 mol% Tyzor TE/Al_2O_3 catalyst was also investigated (Fig. 3.9). A high loading was used with Al_2O_3 because the original surface area of Al_2O_3 is higher than that of TiO_2. Both the conversion and selectivity precisions in this run are ±3% (absolute STDEV). From Fig. 3.8A-B and Fig. 3.9A-B, it is seen that both the activity and selectivity of Tyzor TE/Al_2O_3 are lower than those of Tyzor TE/TiO_2 at 245ºC and 250ºC. Al_2O_3 is not as good a support as TiO_2.

It is seen that at 2.14 MPa the conversion at 250ºC is almost the same as that at 260ºC while the selectivity is higher at 250ºC than at 260ºC. The saturation vapor pressure at 260ºC was estimated as 1.2 MPa for Feed A (App. D). Therefore, the feed was primarily liquid phase at 2.14 MPa. Still, more DEA will enter into the gas phase than DEET because reaction temperatures are higher than the T_c of DEA (225ºC) but lower than that of DEET (493ºC), while the reaction pressure is near the P_c of DEET (2.52 MPa) but far lower than that of DEA (3.76 MPa). Therefore, the DEET/DEA ratio in the liquid phase probably increases with temperature. This will tend to promote side reactions such as DEET decomposition.

From Fig. 3.9A, it is seen that the spread in conversion at 250ºC and 260ºC and high pressures is large at constant WHSV but not the spread in selectivity. This shows that catalyst deactivation took place at both 250ºC and 260ºC. However, the conversion before deactivation at high reaction pressure (2.14 MPa) is > 10% higher than at low reaction pressure (0.85 MPa), with almost the same selectivity. The calculated saturation vapor pressure at 250ºC is 1.1 MPa for Feed A. Therefore, the feed was primarily gas

phase at 0.85 MPa while the feed was mostly liquid phase at 2.14 MPa. It is obvious that the initial conversion increase at high pressure results from an increase in concentration of MTA and DEA in the reactor. However, in the long run, the conversions are almost same at high pressure and low pressure after catalyst deactivation. The high pressure improved the conversion at short times, but not at long times.

The effects of varying the DEET composition of the feed were also investigated using Tyzor TE catalysts. It is found that the selectivity increases but the conversion does not change when the DEET content in the feed decreases. This is consistent with the results of the control experiment, which indicated that ETA is formed from the decomposition of DEET (for Feed A, 260ºC, 2.14 MPa, ETA selectivity = 16%; for Feed B, ETA selectivity = 11%,).

The stability of Tyzor TE/Al_2O_3 and its regeneration were investigated by the change in the conversion and selectivity with time on stream. Fig. 3.9C gives the results. From Fig 3.9C, it is seen that a nitrogen purge at 250ºC or 260ºC is effective in regenerating the activity of Tyzor TE/Al_2O_3 catalysts. However, this catalyst still deactivates rapidly with the time on stream. High temperature air was also used to regenerate this catalyst (500ºC, 10 hrs). The results appeared very bad. MTA conversion was only 28% while DEET selectivity was still 87%, which is the same catalytic behavior as TiO_2 (Dooley, 2000b). This suggests that most of the Tyzor TE was oxidized to TiO_2. This result is consistent with the results obtained by TGA, that the Tyzor TE series catalysts are decomposed in air. High temperature air regeneration is not possible because triethanolaminato ligands are slowly oxidized in air when the temperature is greater than 280ºC (Cullis and Waddington, 1958).

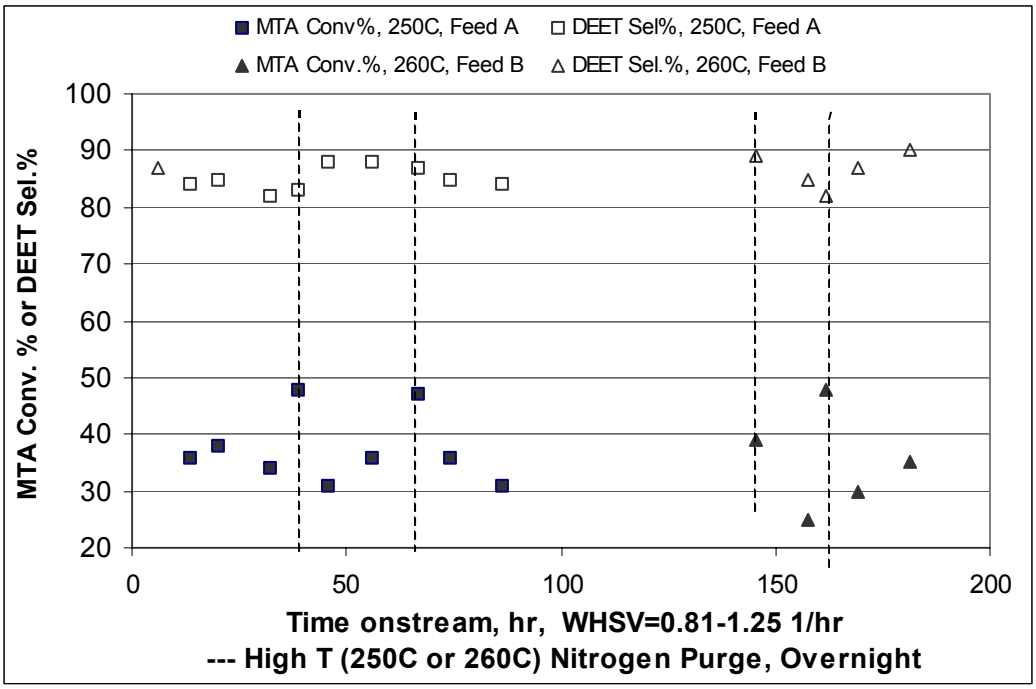

Fig. 3.9C. Stability of 11.4 mol% Tyzor TE/Al_2O_3 catalysts, 2.14MPa

Generally, the selectivity using Tyzor TE/TiO_2 catalysts can be 95%, which is the same as that obtained using the homogeneous Tyzor TE catalysts (Hull, 1979). The MTA conversion using Tyzor TE/TiO_2 is 45±3% at 245ºC, which is far less than the reported homogeneous MTA conversion of 93% (Hull, 1979) but close to the equilibrium conversion (58.6%) estimated from thermodynamic data. However, this conversion using homogeneous catalysts was obtained by removing a product (water) continuously, and the reaction time was about 24 h at 225-235ºC. In past work at Louisiana State University, a MTA conversion of slightly > 80% with > 95% maximum selectivity was also obtained using the homogeneous catalyst Tyzor TE (0.01 gcat/g MTA) in the range of ~4-8 h in a batch reactor at 235-255ºC when some water was removed (Dooley, 2000b).

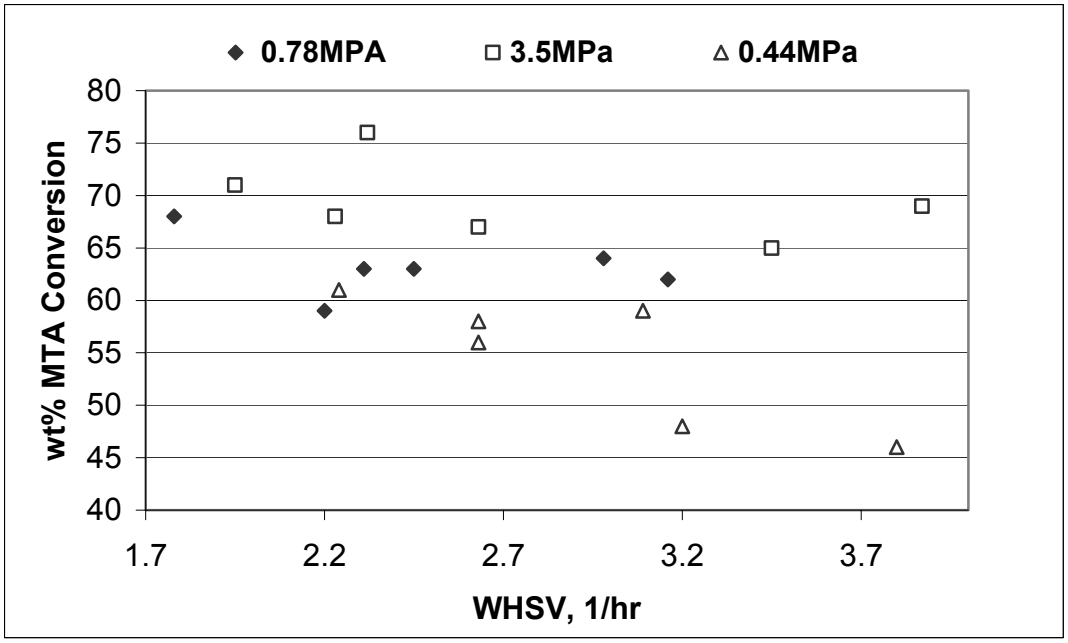

Fig. 3.10A. MTA conversion, effect of pressure for HEA00, Ca^{2+}/H^{+}=7.9, 300ºC, feed B

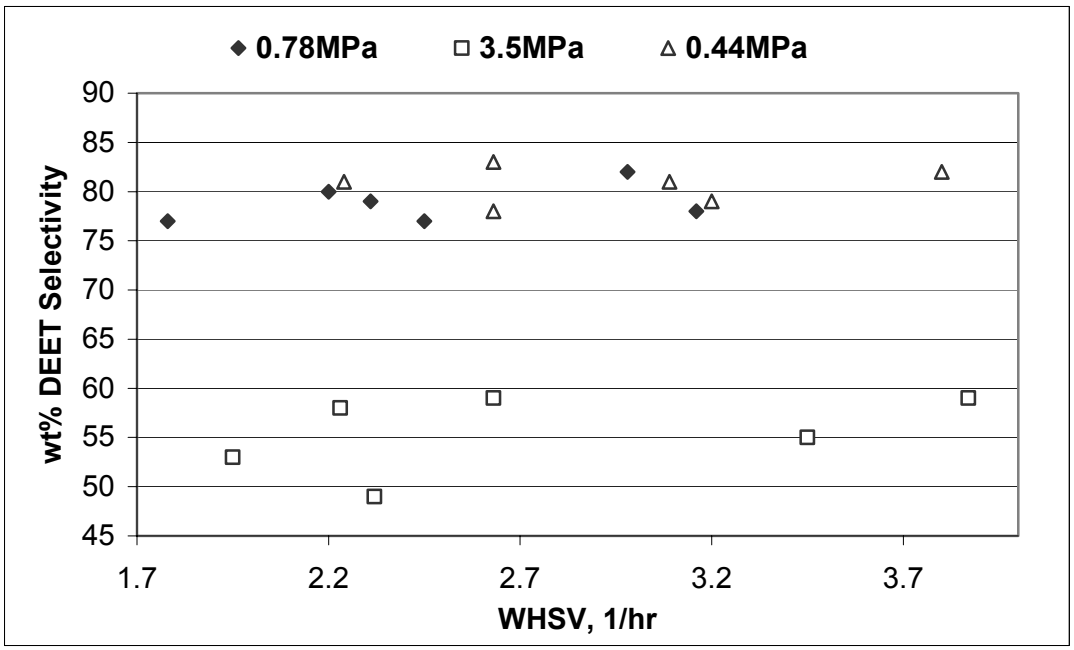

Fig. 3.10B. DEET selectivity, effect of pressure for HEA00, Ca^{2+}/H^{+}=7.9, 300ºC, feed B

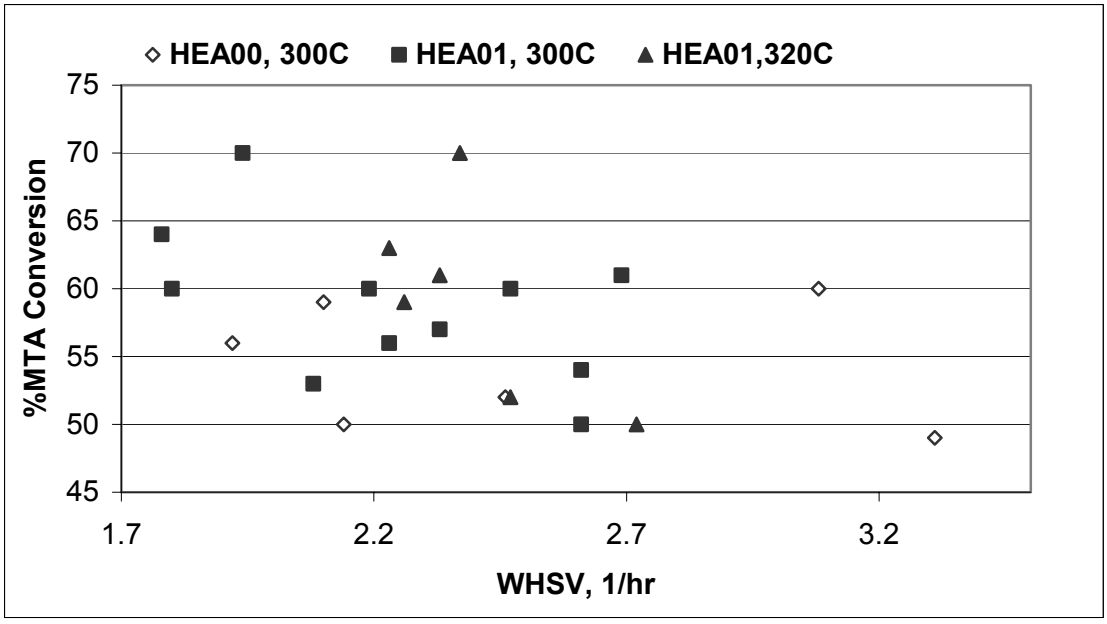

Fig. 3.11A. MTA conversion, temperature and Ca^{2+}/H^{+} effects for HEA00, Ca^{2+}/H^{+} =7.9, HEA01, Ca^{2+}/H^{+} =6.3, 0.1MPa, Feed B.

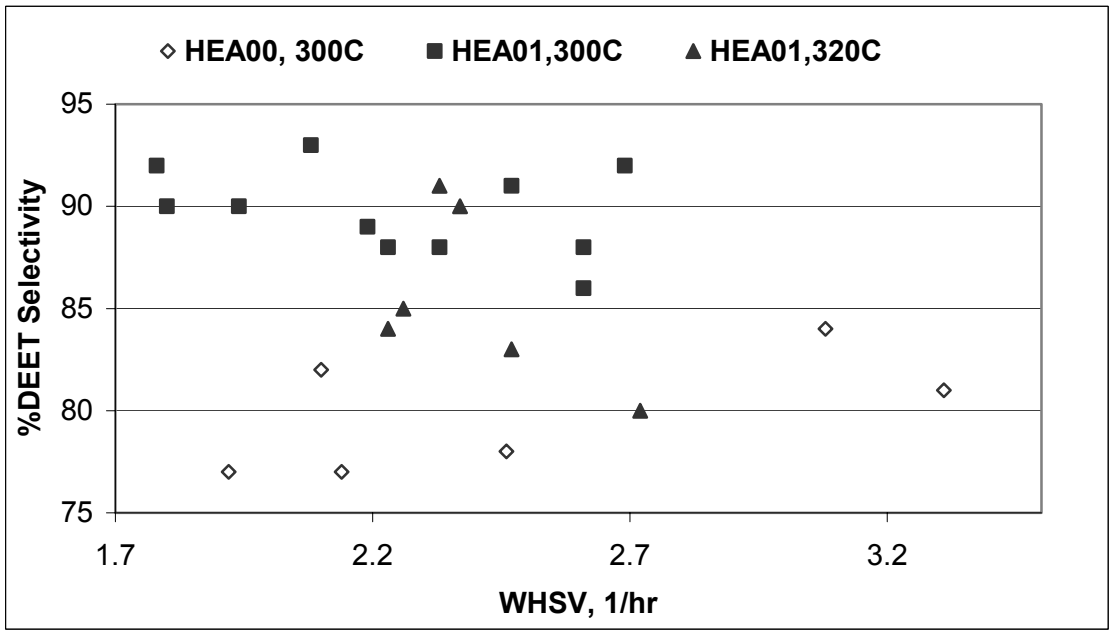

Fig. 3.11B. DEET selectivity, temperature and Ca^{2+}/H^{+} Effects for HEA00, Ca^{2+}/H^{+} =7.9, HEA01, Ca^{2+}/H^{+} =6.3, 0.1 MPa, Feed B.

♦ **Continuous Reactor Experiments - Hydroxyapatite Catalysts**

de Vekki and Mozzhukhina (1997) investigated the catalysis of the DEET reaction using a series of catalysts from weak bases to strong acids. It was found that orthophosphoric acid was the optimum catalyst. However, the strength of phosphoric acid is not uniform when supported. It was also found that calcium hydroxyapatite, a solid acid phosphate, gives an average acid strength similar to phosphoric acid, but with more uniform acid strength.

A series of runs were performed using different Ca^{2+}/H^{+} hydroxyapatites (for Ca^{2+}/H^{+} calculation, see section 3.1.2); pressure effects were investigated (Figs. 3.10A-B). In these experiments, the conversion precision is ±4% (absolute STDEV) and the selectivity precision is ±2% (absolute STDEV). The estimated saturation vapor pressure of Feed B at 300ºC is 1.87 MPa (Appendix D), which suggests that the feed was mostly gas phase at 0.44 and 0.78 MPa but mostly liquid phase at 3.5 MPa. Hydroxyapatites have acidic sites that can easily coordinate DEA or DEET while MTA can bond to hydroxyapatites through the oxygens of the hydroxyl groups or by the electrophilic aromatic ring bonding to PO_4^{2-}. DEA is a stronger base than DEET (amine vs. amide). At low pressure, where both are probably gas phase, DEA would preferably be adsorbed. An increase in pressure increases the reactant concentrations but should not affect the adsorbate distribution on the active sites of hydroxyapatites unless multiple phases form. Therefore the selectivity will not change with respect to pressure. At high pressure, unless temperature is much lower than T_c of DEA, there would still be DEA in the gas phase. In this run, the pressure is lower than P_c of DEA (3.76 MPa) but higher than P_c of DEET (2.5 MPa). The temperature (300ºC) is higher than T_c of DEA (225ºC) but lower

than T_c of DEET (493ºC). Therefore, assuming the liquid phase wets the catalyst more efficiently, the DEET/DEA molar ratio would increase on the catalyst, the decomposition of DEET would increase, and the DEET selectivity would decrease. This is what happened here.

The Ca^{2+}/H^+ ratio and temperature effects were also investigated for hydroxyapatites. In these experiments, the conversion precision is ±4% (absolute) and the selectivity precision is ±2% (absolute). From Figs. 3.11A-B, it is seen that hydroxyapatite with low Ca^{2+}/H^+ ratio (HEA01) is more selective than that with high Ca^{2+}/H^+ ratio (HEA00), although HEA01 has lower surface area (Table 3.6). That may be because HEA01 has more Brønsted acid sites than HEA00, which probably adsorb DEA in preference to DEET. From Fig. 3.11, it is seen that greater deactivation occurred at 320ºC than at 300ºC. Side reactions such as DEET decomposition also increased during deactivation. This may be a reason why higher temperature did not result in an increased conversion when the temperature is greater than 300ºC, although the conversion should increase according to the thermodynamic calculations. The best temperature for hydroxyapatite catalysts is ~300ºC.

The stabilities of HEA00 and HEA01 were also investigated. Figs. 3.12A-B give the results. From these figures, it is seen that the activities of the hydroxyapatite catalysts decrease with the time on-stream like the other catalysts, but the stabilities of the hydroxyapatite catalysts are better than the supported Tyzor TE catalysts. Unlike the Tyzor TE/Al_2O_3 catalyst, high temperature (300ºC) N_2 cannot regenerate the HEA01 catalyst while high temperature (500ºC) air does somewhat. From the coke analyses, it is seen that a little coke formed on the hydroxyapatite catalysts. Also, desorption and

thermal analyses (TGA) of 1-PA for HEA01 suggest that the used catalyst has more strong acid sites than the fresh catalyst (Table 3.8). That is because there is more structural water in the fresh catalyst, and high temperature air can remove some structural water from the HEA01 catalyst to produce more strong acid sites. These results show that high temperature air regeneration is necessary for this kind catalyst to recover active sites.

Generally, the best results (about 60-65% MTA conversion, 85-93% DEET selectivity could be obtained when the amidation reaction was conducted using the HEA01 catalyst at 300ºC, 0.1MPa and at WHSV of 2-2.7 hr^{-1}.

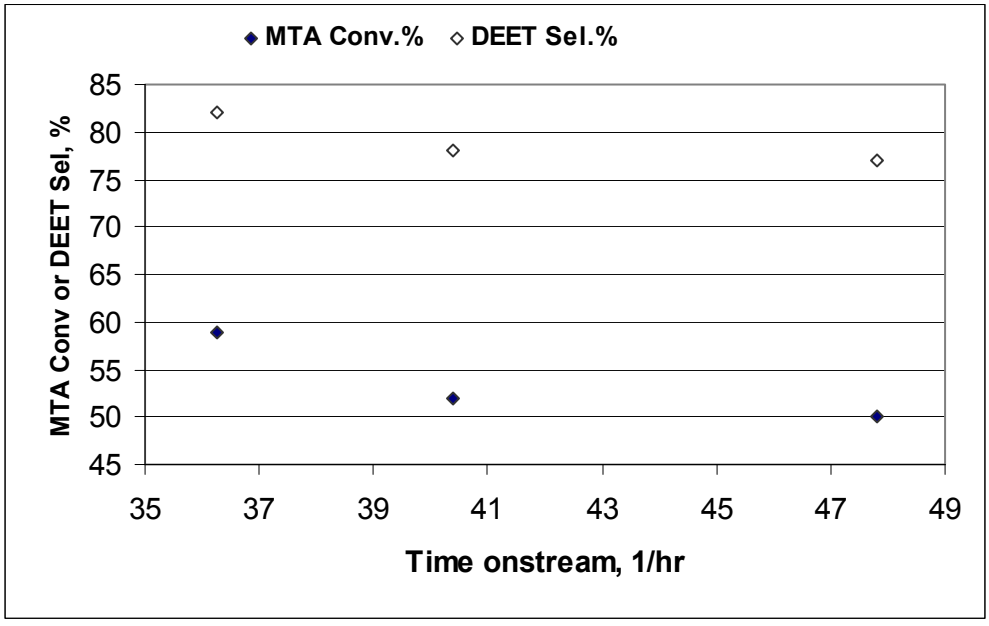

Fig. 3.12A. Stability of HEA00, Ca^{2+}/H^{+}=7.9, 300ºC, 0.1 MPa, feed B, WHSV=2.1-2.3hr^{-1}

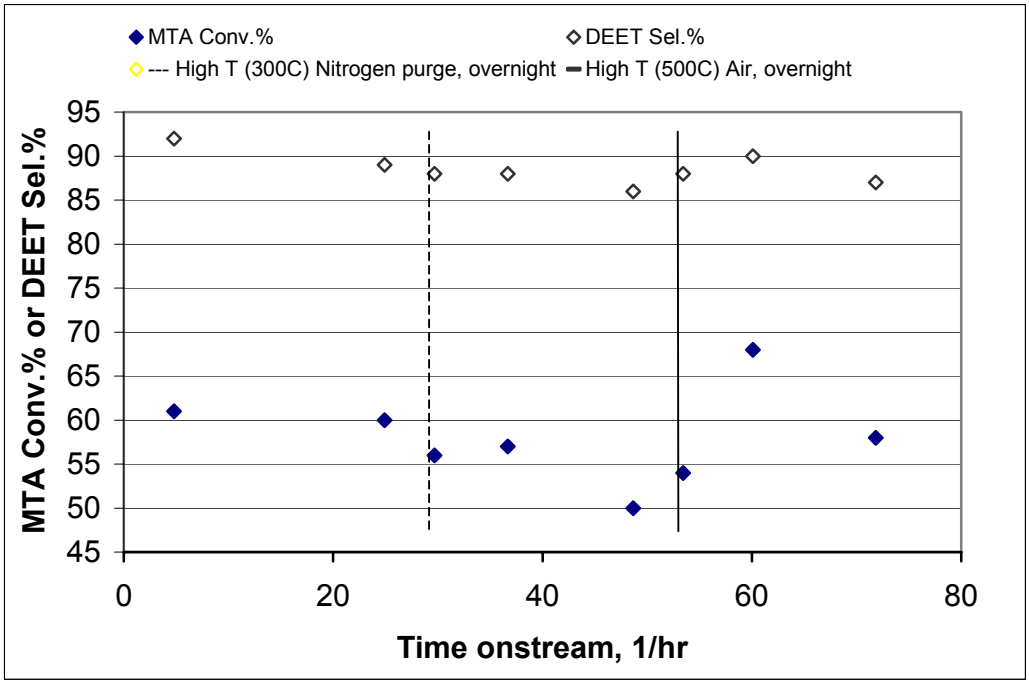

Fig. 3.12 B. Stability of HEA01, Ca^{2+}/H^{+}=6.3, 300ºC, 0.1 MPa, feed B, WHSV=2.0-2.7hr^{-1}

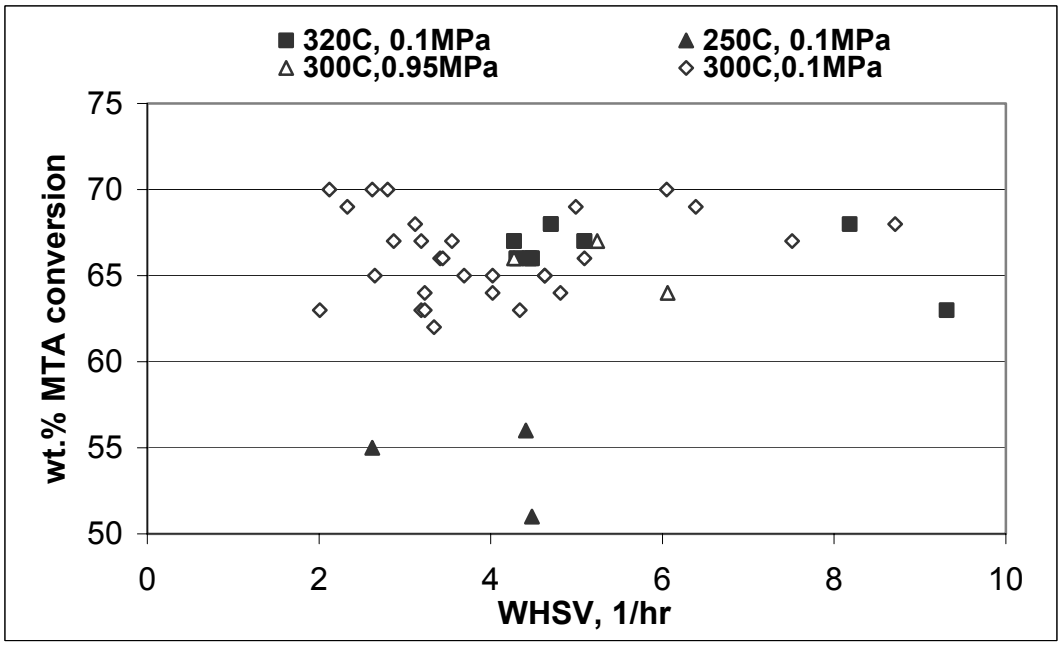

Fig. 3.13A. MTA conversion, 40 wt.% HPA/Silica gel (YJ01), feed B

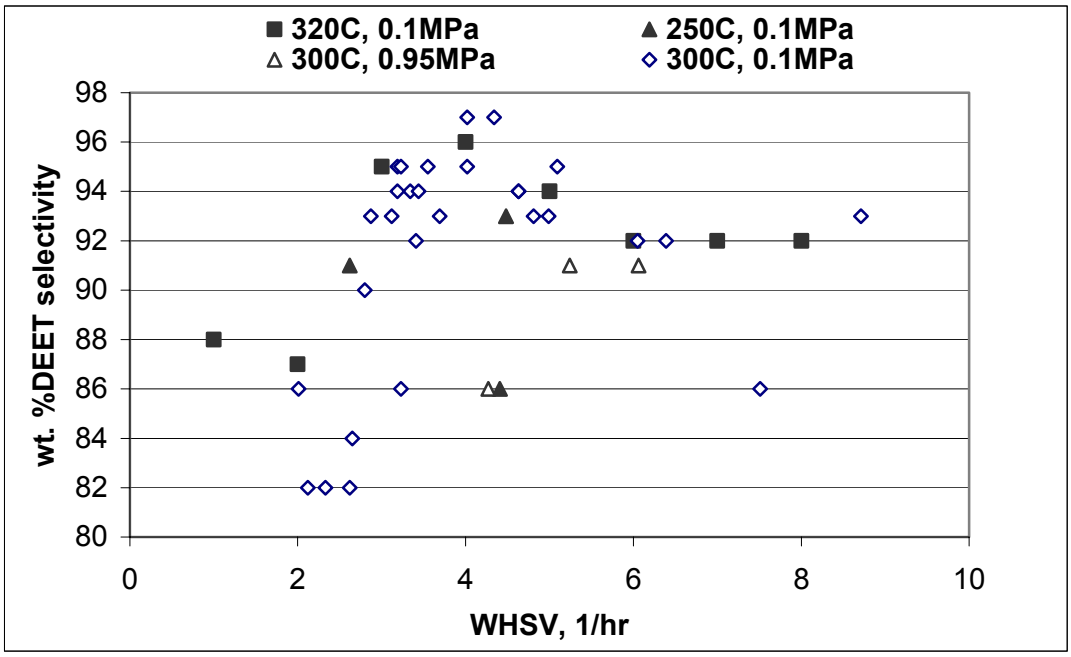

Fig. 3.13B. DEET Selectivity, 40 wt.% HPA/Silica gel (YJ01), feed B

♦ **Continuous Reactor Experiments – Heteropolyacid Catalysts**

The success of the hydroxyapatites led us to explore other supported acids that are known to be relatively uniform in acid strength. A candidate material is tungsten heteropolyacid ($H_3PW_{12}O_{40}$, sometimes known as a "Keggin ion"); the P-atom is on the inside and the protons on the outside of the structure, bonded to both bridging and terminal oxygens in the solid state (Kozhevnikov, 1995). Heteropolyacids (HPAs) are highly uniform acids useful for both acid-catalyzed and redox reactions. Their stability in the solid state is good, up to 450-500ºC (Kozhevnikov, 1995). This means that HPAs can be regenerated with air, if necessary, at temperatures where coke could be decomposed (~500ºC). The YJ series of catalysts were prepared from HPA supported on either silica gel or on MCM-41 mesoporous silica with monodimensional pores of 50 Å (Beck et al.,

1992; Kresge et al., 1992). According to the 1-PA desorption data (Table 3.8), the fresh YJ catalysts have more strong acid sites than HEA01.

YJ01 is 40 wt.% HPA mounted on silica gel. The best results (about 66±4% MTA and 94±3% DEET selectivity) were obtained when the amidation reaction was conducted at 300ºC, 0.1-0.95 MPa and with WHSV 3-9 hr^{-1} using Feed B (Figs. 3.13A-B). Temperature, pressure and WHSV effects were investigated for YJ01. Unlike the supported Tyzor TE catalysts and hydroxyapatite catalysts, the selectivity showed almost no change when the reaction temperature was increased from 250ºC to 320ºC. When the reaction temperature was increased from 250ºC to 300ºC, the MTA conversion increased by about 15%. The conversion and selectivity showed almost no change when the temperature changed from 300ºC to 320ºC. At 300-320ºC, the conversion is 66±4%, close to the predicted equilibrium conversions (300ºC, 80.0%; 320ºC, 83.9%). When the pressure increased from 0.1 MPa to 0.95 MPa at 300ºC, the conversion remained almost the same while the selectivity decreased. This is probably because of the higher concentration of DEET in contact with the catalyst at 0.95 MPa, increasing the rate of the secondary reaction.

From Fig 3.13, it is also seen that the conversion and selectivity show almost no change when the WHSV increases from 3 to 9 h^{-1} at 300ºC and 0.1 MPa. As the WHSV is decreased to 1-3 h^{-1}, instead of an increase in conversion, as expected, there is a decrease in selectivity. That is because the conversion in a reversible reaction near equilibrium will change less with respect to contact time (or WHSV). But excessive contact time will make secondary reactions such as DEET decomposition more important.

The stability of the YJ01 catalyst was determined by examining conversion and selectivity changes with time on stream (Fig. 3.13C). AlthoughYJ01 catalysts deactivated somewhat, they can last at least 24 h without regeneration. The MTA conversion was not helped by high temperature (300ºC) nitrogen treatment. From the coke analysis, it is clear that there is almost no permanent coke on YJ01. Desorption and thermal analysis (TGA) of 1-PA showed that the estimated strong acid content in the used YJ01 was less than that in the fresh YJ01, and the strong Brønsted acid peak disappeared in the used YJ01. This suggests that deactivation is from loss of the active sites, and high temperature nitrogen cannot recover them. However, high temperature (450ºC) air treatment can recover the active sites efficiently. The catalyst showed no sign of apparent deactivation in 11 days of operation if there were periodic overnight air treatments at 450ºC.

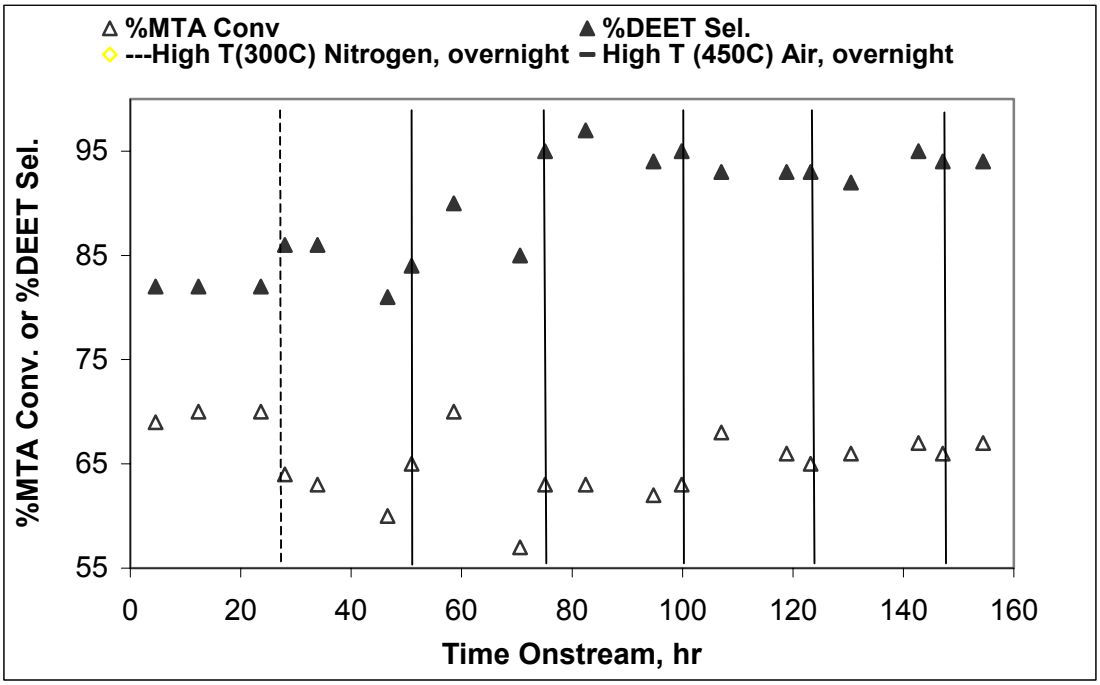

Fig. 3.13C. Stability of YJ01 (40 wt% HPA/SiO_2) catalysts, 300ºC, Feed B, WHSV = 2-3 h^{-1} before the first air regeneration, WHSV = 2.8-4.0 h^{-1} after the first air regeneration.

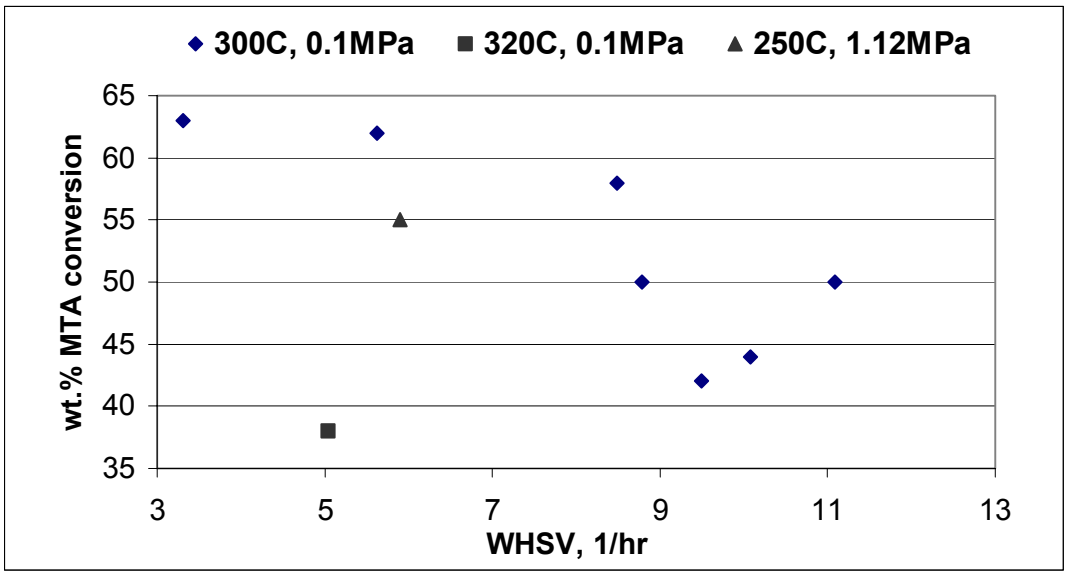

Fig. 3.14A. MTA conversion of YJ03 (40 wt.% CsHPA/MCM-41, $Cs^+/H^+ = 2.5/0.5$), feed B.

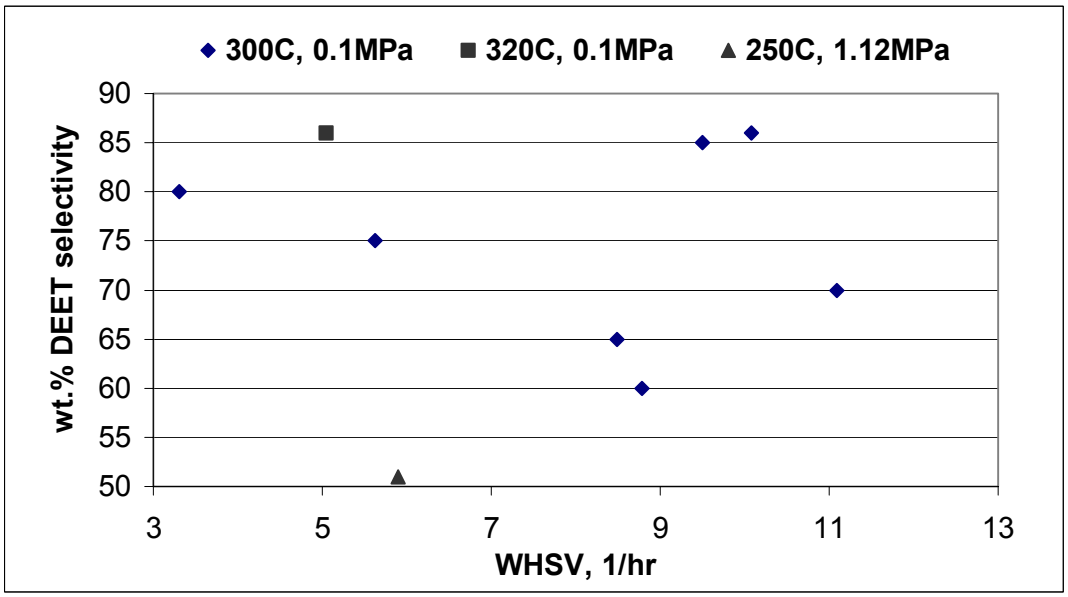

Fig. 3.14B. DEET selectivity of YJ03 (40 wt.% CsHPA/MCM-41, $Cs^+/H^+=2.5/0.5$), feed B

In order to check the cation substitution effect on the catalytic behavior of HPA catalysts, Cs substituted heteropolyacid catalysts were prepared and investigated. YJ03 is a 40 wt% Cs substituted heteropolyacid catalysts supported on MCM-41 mesoporous silica. The results are shown in Fig. 3.14. Cs^+/H^+ is the molar ratio of Cs ions to protons in this catalyst. In this run, the precision of MTA conversion is ±4% (absolute) and the precision of DEET selectivity is ±5% (absolute). Only about 55% MTA conversion with 80% DEET selectivity can be obtained using YJ03 at 300ºC and 0.1MPa, which are both less than those obtained using YJ01. The result shows that the protons (Brønsted acid sites) in YJ01 catalysts may be mainly responsible for the activity and selectivity of this kind acid catalyst.

In order to further check the effects of loading and proton content, a 50 wt% Cs substituted HPA/MCM-41 catalysts (Cs^+/H^+=1/2) was investigated (Fig 3.15). In this run, the precision of MTA conversion is ±4% (absolute) and the precision of DEET selectivity is ±3% (absolute). The results show that the selectivity (about 94%, the highest about 97%) using YJ10 is higher than that YJ03 but about the same as YJ01. The conversion (about 50%, the highest 52%) using YJ10 is almost the same as YJ03 except at low WHSV. A comparison of YJ01, YJ03 and YJ10 shows that the HPA protons are indeed mainly responsible for the activity of the solid acid catalysts and the DEET reaction does not require the very strong acid sites produced by Cs exchange.

YJ03 and YJ10 were prepared using the same method (a two-step impregnation method). The only difference was that the HPA was dissolved in water for preparing YJ03 while the HPA was dissolved in 1-butanol for preparing YJ10. It is said that using 1-butanol can reduce pore plugging and leads to a good diffusivity of the TPA during

impregnation and so a more uniform pore structures (Wang et al., 2001). If so, YJ10 should be more active than YJ03. However, the results did not show this. This may be because that Cs-HPA cannot disperse in MCM-41 as well as in large-pore silica gel. This may also be a reason why both YJ03 and YJ10 have lower conversions than YJ01.

According to the above investigations on different catalysts and operation conditions, it is seen that the best catalyst is YJ01 (tungsten HPA/silica gel) and the best reaction conditions are at 300ºC and low pressure. The best results (about 65-70% MTA conversion and 93-97% DEET selectivity) can be obtained at WHSV of 3-9 h^{-1} using Feed B, mole ratio DEA/MTA/DEET=1/1/0.4. The highest MTA conversion is close to the predicted value of 80% estimated using thermodynamic calculations. This conversion is higher than the best-reported equivalent MTA conversion of 55% (de Vekki and Mozzhukhina, 1997) using a heterogeneous catalyst. The selectivity is also higher than the best reported value of 93% (de Vekki and Mozzhukhina, 1997). However, the WHSVs of de Vekki and Mozzhukhina were very low, about 0.3 h^{-1}. When the WHSV was increased, the MTA conversion decreased rapidly, to only about 40% at 0.9 h^{-1}, 39% at 1.3 h^{-1} (de Vekki and Mozzhukhina, 1997). The selectivities obtained in this work are almost the same as those obtained using homogeneous catalysts (Hull, 1979). However, the conversions were lower than the reported value of 91% at 225-245ºC, which was obtained by removing the product water continuously and using a reaction time of about 24 h (Hull, 1979). It is true that MTA conversions slightly > 80% with > 90% DEET selectivity were obtained with supported Tyzor catalysts in batch reactor trials (Dooley, 1998). However, this was only possible with reaction times in the range of ~4-8 h and

with water removal. The residence times in this reactor were ~10 min at the highest space velocities used.

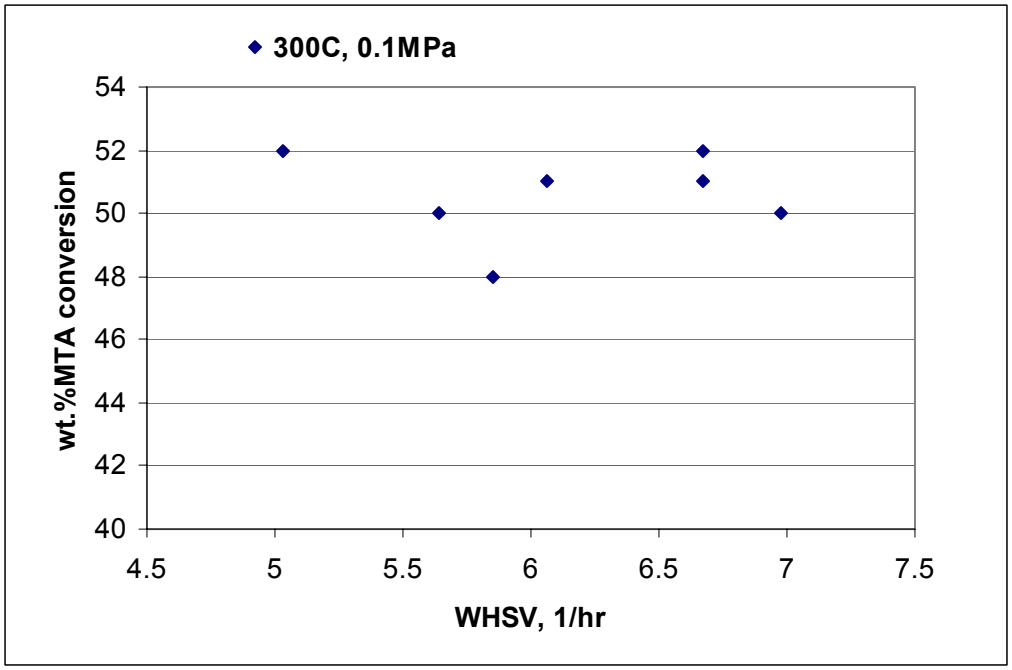

Fig. 3.15A. MTA conversion, YJ10 (50 wt.% CsHPA/MCM-41, Cs^+/H^+=1/2), feed B

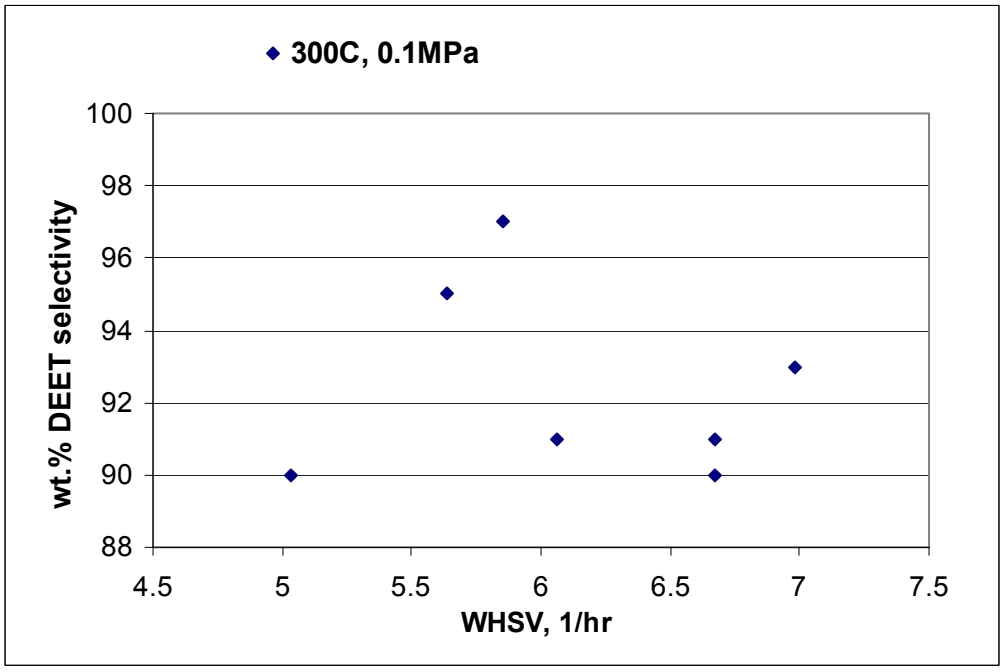

Fig. 3.15B. DEET selectivity, YJ10 (50 wt.% CsHPA/MCM-41, Cs^+/H^+=1/2), feed B

3.1.4 Product distributions

The typical product distributions for different catalysts are summarized in Table 3.10. The raw wt.% gives the actual amounts in the product stream. The adjusted wt.% selectivity gives the amounts after adjustment for the feed composition. They have also been adjusted to be on an MTA-product (only) basis. In other words, only the selectivities of the products resulting from MTA were accounted for. This makes little difference because this accounted for almost the entire product slate anyway. From Table 3.12, it was seen that every catalyst could produce a certain amount of N,N-diethyl,1-butanamine and N,N-diethylbenzamide, and N-ethyl, m-toluamide (ETA) is always the most important side product. The next most important by-product was different for different catalysts. It was triethyamine, N,N'-diethyl,1-butanamines, triethylamine, N,N'-diethyl,1-butanamines and 3-methylbenzonitrile, for Tyzor TE/Al_2O_3, HEA01, SiO_2, YJ01 and YJ10 catalysts, respectively. It is also seen that YJ01 and YJ10 produce the least ETA. The route of formation to side-products is complicated except for the principal side product (ETA), TEA from the disproportionation of DEA, and o-DEET and p-DEET formed from the reaction of the isomers of MTA. 1-BA was probably formed by the disproportionation of DEA. MTN was probably formed by removing water from DEET, with cracking. DBA was likely the product of DEA with benzoic acid formed from MTA by cracking. EMB was likely formed from the esterification of MTA with ethanol, a product of ETA formation. TMB was probably the product of several reactions, such as MTA decomposition and oligomerization. BETA was likely formed from the further reaction of ETA with 1-BA. Other heavies all resulted from the further reactions of MTA or DEET. Scheme 3.1 gives the structures of these side products.

Table 3.10. Products Distribution of Different Catalysts using Feed B

Catalysts / Compounds	Tyzor TE/Al_2O_3, 260°C , 2.14MPa		HEA01, 300°C , 0.1MPa		SiO_2, 300 °C, 0.1MPa		YJ01,300 °C, 0.1MPa		YJ10,300 °C, 0.1MPa	
	Raw Wt % Sel.	Adj Wt % Sel.	Raw Wt % Sel.	Adj Wt % Sel.	Raw Wt % Sel.	Adj Wt % Sel.	Raw Wt % Sel.	Adj Wt % Sel.	Raw Wt % Sel.	Adj Wt % Sel.
Diethylamine (DEA)	13.4		10.8		21.2		11.1		13.6	
Triethylamine (TEA)	1.0		0.2		1.5		0.5		0.1	
Toluene	0		0		0		0		0	
N,N-Diethyl, 1-Butanamine (1-BA)	0.6		1.0		0.5		1.2		0.2	
3-methylbenzonitrile (MTN)	0	0	0	0	0.2	0.4	0.0	0	0.5	0.7
m-Toluic acid (MTA)	28.0		19.8		17.0		16.7		23.5	
Ethyl-m-methyl benzoate (EMB)	0	0	0	0	0	0	0	0	0	0
N,N-diethyl benzamide (DBA)	0.2	0.1	0.2	0.3	0.3	0.6	0.2	0.3	0.2	0.2
N-ethyl, m-toluamide (ETA)	4.0	11.5	4.4	10.1	5.4	16.0	3.6	5.2	1.2	3.6
o-DEET	0	0	0	0	0	0	0.0	0	0	0.1
m-DEET	51	85.0	63.2	89.4	53.8	83.0	66.2	93.8	60.6	95.1
p-DEET	0.0	0	0.0	0.0	0	0.1	0.0	0.1	0	0
Trimethylbiphenyl (TMB)	0.5	1.2	0	0.0	0.03	0.03	0.2	0.3	0.2	0.3
N-butyl, N-ethyl toluamide (BETA)	0.5	1.2	0.4	0.2	0.04	0.04	0.1	0.2	0	0
Other unnamed heavy compounds (C)	0.8	2.0	0	0.0	0.03	0.03	0.2	0.2	0	0
Total	100	100	100	100	100	100	100	100	100	100

Scheme 3.1 Structures of side products

TEA

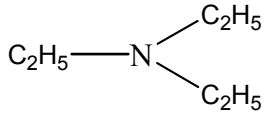

1-BA

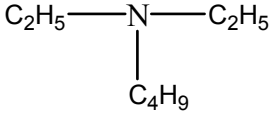

MTN

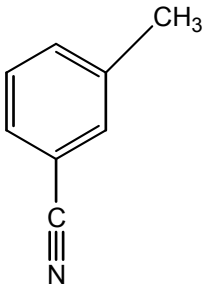

EMB

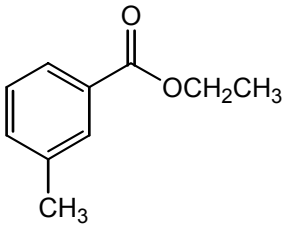

DBA

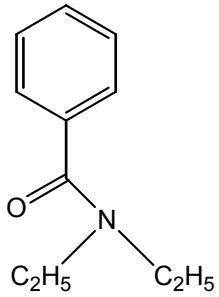

ETA

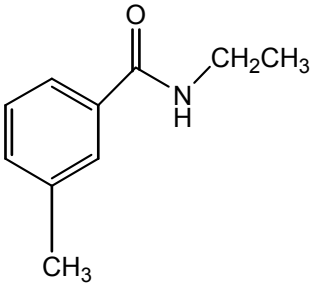

o-DEET

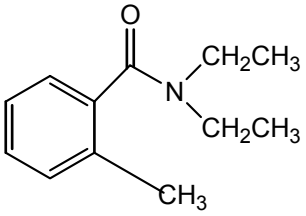

p-DEET

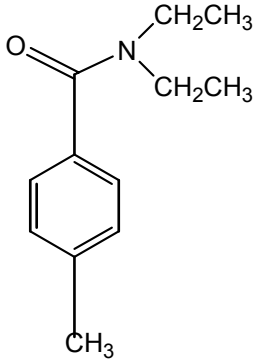

BETA

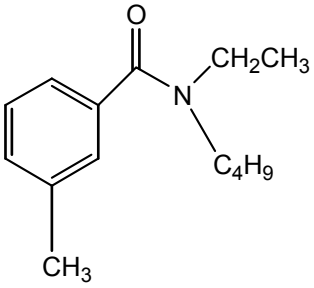

TMB

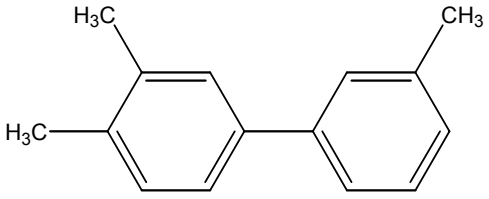

3.2 M-Toluic Acid Synthesis by Catalytic Oxidation

3.2.1 Kinetics of m-Xylene Catalytic Oxidation

There are no papers on the kinetics of m-xylene catalytic oxidation, but the kinetics of p-xylene catalytic oxidation have been studied intensively. Since the oxidation products and catalysts are similar, it is reasonable to assume that the p-xylene kinetics are relevant to m-xylene oxidation.

The classical catalytic mechanism for alkylaromatic oxidation involves initiation, propagation and termination steps that are quite complex. By taking into account only the reactions leading to the most important intermediate and final products according to previous experimental evidence (Cao and Servida, 1994), the following lumped kinetic scheme for MX to MTA can be proposed:

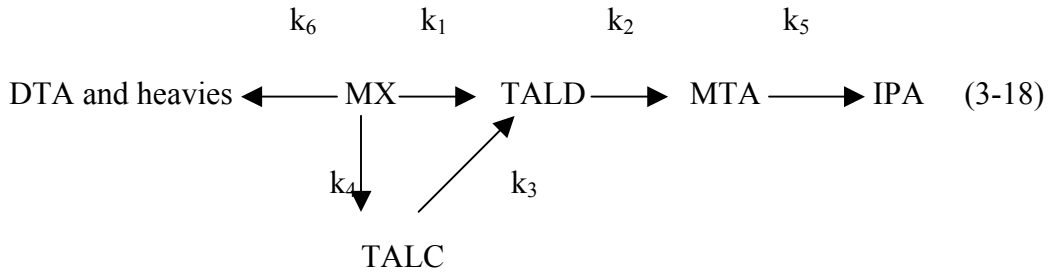

In this scheme $(r_1+r_4+r_6)$ is the total reaction rate of m-xylene (MX) oxidation producing tolualdehyde (TALD), methybenzylalcohols (TALC), m-toluic acid (MTA), isophthalic acid (IPA), ditolylalkanes (DTA) and heavies. The term (r_1+r_4) is the reaction rate of MX oxidation producing the desired products (TALD, TALC and MTA). As discussed in Chapter 1, the kinetics of each of the lumped reactions above are typically zeroth order with respect to oxygen and first-order with respect to the liquid reactant, as long as the oxygen supply is enough to sustain the maximum rate of oxygen consumption in the liquid bulk.

The oxidation can be either kinetics-limited or mass-transfer-limited in the liquid phase. The chemical kinetics control the overall process at sufficiently high P_{O2}, while mass-transfer may be the controlling process at low P_{O2} (Cao and Servida, 1994).

In these experiments, the total reaction rate constant is given by equation (3-19), assuming first-order reactions of m-xylene.

$$k = [\ln(1 - x_1) - \ln(1 - x_2)] / (t_2 - t_1) \qquad (3-19)$$

x_1 and x_2, MTA conversion at the first point and the second point, respectively;

t_1 and t_2, reaction time at the first point and the second point (min);

$k = k_1 + k_4 + k_6$.

The term (k_1+k_4) can be calculated from the yields of TALD (Y_{TALD}), TALC (Y_{TALC}), MTA (Y_{MTA}), and IPA (Y_{IPA}) (3-20).

$$(k_1 + k_4) = k\left(\frac{Y_{TALD} + Y_{TALC} + Y_{MTA} + Y_{IPA}}{x}\right) \qquad (3-20)$$

In order to compare with the kinetics data for p-xylene oxidation (Cao and Servida, 1994), (k_1+k_4) was adjusted to a temperature that Cao and Servida used (120ºC) (3-21), then it was adjusted again to the catalyst concentration that Cao and Servida used (3-22), assuming first-order kinetics in catalyst concentration.

$$(k_1 + k_4)_{adj,T} = (k_1 + k_4)\exp\left[\frac{-E_a}{R}\left(\frac{1}{T_{adj}} - \frac{1}{T}\right)\right] \qquad (3-21)$$

T in K, T_{adj} = 393K (120ºC). The activation energy E_a was calculated from data of Cao and Servida (1994) (see Appendix F).

$$(k_1 + k_4)_{adj} = (k_1 + k_4)_{adj,T}\left(\frac{C_{base}}{C_{cat.}}\right) \qquad (3-22)$$

Here, C_{base} is the catalyst concentration that Cao and Servida used (0.19 mmol/mol xylene). C_{cat} is the catalyst concentration in our experiments (mmol/mol m-xylene). The term $(k_1 + k_4)_{adj}$ can be used to compare our experimental rate constants to the rate constants for p-xylene oxidation (0.022 min^{-1}), using 0.19 mmol metal/mole xylene at 120ºC (Cao and Servida, 1994).

3.2.2 Catalyst Characterization

The supported Co(salen) catalyst was tested by the BET method to determine the surface area, which was 423 m^2/g. TGA was used to determine the Co content in Co(salen), which was 0.51 mmol Co/g catalyst. This is near the expected stoichiometric Co content of 0.52 mmol Co/g catalyst, assuming the imidization reaction of salen with APTMS took place (see Appendix G). The chemical structure of the supported Co(salen) catalyst was analyzed by FT-IR in diffuse reflectance (DRIFTS) mode (Fig 3.16).

From Fig 3.16, a $\nu_{C=N}$ band appeared at 1614. This band was at 1620 cm^{-1} in the work of Murphy et al. (2001). A possible ν_{C-N} band appeared at 805 cm^{-1}. This band was at 802 cm^{-1} in the work of Tsuji et al. (2001). The wavenumbers of these bands are consistent with a prior preparation (Murphy et al., 2001), which suggested that the supported Co(salen) shown in Fig. 2.1 was present.

3.2.3 Results and Discussion, m-Xylene Oxidation

The results for m-xylene oxidation to m-toluic acid and related products are given in Table 3.11 (in this table, all runs before XY85 were done by previous members of Dr. Dooley's group). The terminology used to describe the results here and in the spreadsheets is as follows. All conversions and selectivities were computed on the basis

of moles carbon in the initial feed [mols of m-xylene in feed = (8) x (mols carbon in feed)].

% Xylene conversion = (moles of xylene reacted)/(moles of xylene fed).

% Selectivity of Product j = (moles carbon for product j)/(total moles carbon in all products).

Time is given as the cumulative time of reaction. The moles of air are also given as cumulative amounts. A negative selectivity means that a component already present in the feed was used up rather than produced up to that time; there were no large negative selectivities in any runs. The remaining products not shown in Table 3.11 are primarily benzaldehyde, benzyl alcohol, ditolylalkanes, the heavy acid $C_{16}H_{16}O_2$, and two unidentified heavy acids or aldehydes of similar molecular weight denoted A and C in the spreadsheets (Dooley, 1998). The recycled liquid products were subtracted out from the product analyses; the product amounts reported here represent freshly produced material only. In the experiments, there were two kinds of reactors used, one a 20 mL high surface-area/volume (S/V) reactor and the other a 500 mL autoclave.

The computation of the rate constants from the experimental results is also given in Table 3.11. The units on the rate constant are min^{-1}. The adjustment of these rate constants to base conditions of 120ºC and 0.19 mmol catalyst/mol xylene is also in the Table. The base rate constants and estimation energies were computed from the data of Cao and Servida (1994; see Appendix F).

♦ Reactor Control Experiments

Run XY86 was a blank experiment with no catalyst in the reactor. None of the desired products were produced, while almost 3.5% MX was converted to heavy

compounds. This shows that non-catalyzed oxidation of MX is a slow process without selectivity to the desired products.

♦ Reactor Surface/volume (S/V) Effects

Run XY96 was performed in the 20 mL reactor while run XY99 was performed in the 500 mL reactor. Both of them were performed at the same temperature using the same catalyst system, but run XY96 was at a higher P_{O2} (0.56 MPa) than XY99 (0.51 MPa) and a higher O_2/MX mol ratio (8) than XY99 (O_2/MX = 4) in the first 900 min. However, the MX conversion for run XY99 was far higher than XY96, and the adjusted reaction rate constant $(k_1+k_4)_{adj}$ was about 9 times greater than run 96 at 300 min. This suggests that the 500 mL reactor is superior to the 20 mL reactor.

Even when the molar ratio of O_2/MX used in an oxidation was ~12 times higher in the 20 mL reactor (XY84, XY89-90, XY93-94), the MX conversion and MTA selectivity were still lower than those obtained in the 500 mL reactor with a similar catalyst system, the same P_{O2}, and the same temperature (XY80, XY83, XY85, XY87). Comparing the results of XY85 to XY89-90, it is evident that the 500 mL reactor can give a higher MX conversion and MTA selectivity even at a lower temperature and O_2/xylene ratio. Comparing the $(k_1+k_2)_{adj}$ values for the 20 mL reactor (XY84, XY89-90, XY93-94, XY96 and XY98) with those for the 500 mL reactor (XY80, XY83, XY85, XY92, XY95, XY97 and XY99-100), it is seen that the rate constant to desired products for the 500 mL reactor is generally 5-10 times higher than for the 20 mL reactor. However, few heavy compounds were produced in the small reactor, only ~1% selectivity except 14% and 2.4% selectivity to IPA for XY90 and XY93, respectively.

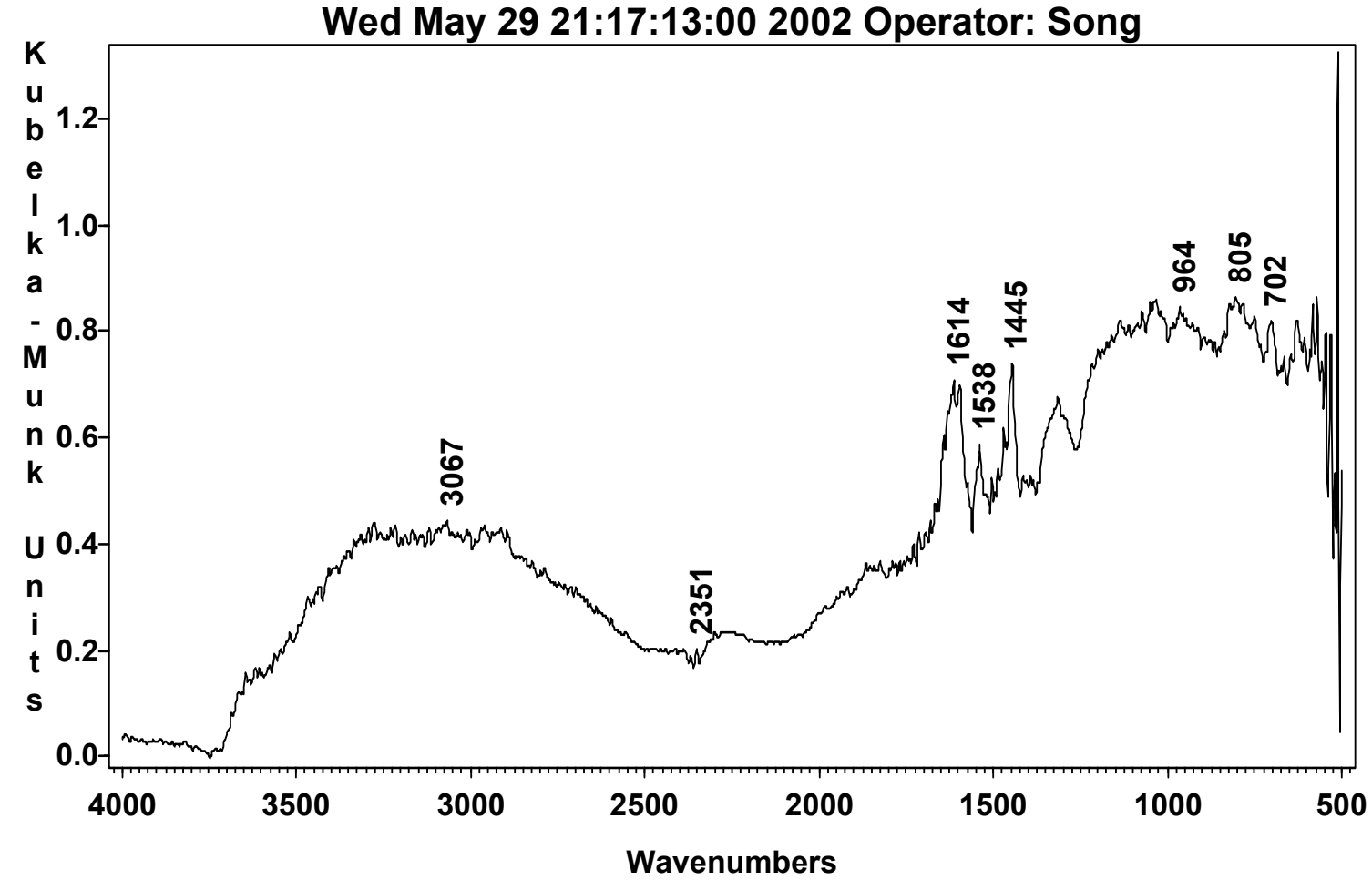

Fig. 3.16. FTIR spectra under vacuum (~7×10^{-7} MPa) of Co(salen), dried in vacuum at 60ºC for 24 h

Table 3.11. - m-Xylene Oxidation, Catalysts, Reaction Conditions and Results

RUN	FEED COMP.	CATALYST	T °C	P MPa	TIME min	AIR mols	CONV. %	Selectivity % to j					Reaction Rate Const.		
								XYL Isomers	MTAld MTAlc	MTA	IPA	CO_2 +CO	k	(k_1+k_4)	$(k_1+k_4)_{adj}$
XY24-1	12 wt.% HAc in 223.8mL MX	CoOct, 350ppm	120	0.78	60	1.52	4.52	4.0	30.6	28.1	0	0	7.71E-4	4.53E-4	1.19E-4
XY29-1	200 mL MX	CoOct, 350ppm	120	0.78	60	1.36	3.17	4.86	66.7	4.17	0	0	5.37E-4	3.80E-4	1.15E-4
XY39-1	10mL MX	1 wt.% CuO/ZrO_2	100	5.54	60	0.14	11	0.74	52	0.67	0	0	1.94E-3	1.02E-3	4.5E-4
XY42-1	6wt.% MTA in 10mL MX	1wt% CuO/ZrO_2	130	2.82	90	0.21	2.97	0.2	73.9	25.3	0	0.06	3.35E-4	3.33E-4	1.9E-4
XY44-1	6 wt.% MTA in	CoOct, 350ppm	130	0.1	20	low	4.4	0	85.4	0	0	0	2.25E-3	1.92E-3	3.2E-4
XY44-3	100 mL MX		130	0.1	1060	air	42.0	0.1	86.2	10.3	0	0	4.16E-4	3.58E-4	5.81E-5
XY44-5			130	0.1	2360	flow	52.9	0.1	69.3	25.0	0	0	6.37E-5	6.00E-5	9.74E-6
XY44-6			130	0.1	3440		57.3	0.1	62.7	28.9	0	0	9.08E-5	8.32E-5	1.35E-5
XY52-1	12 wt.% MTA in	CoOct, 350ppm	130	0.1	1030	low	45.7	0	85.5	8.7	0	0	5.93E-4	5.58E-4	8.43E-5
XY52-2	100 mL MX		135	0.1	2490	air flow	53.8	0	75.7	17.2	0	0	1.11E-4	1.38E-4	1.19E-5
XY65-1	10ml 20 wt% HAc	CuOAc, 1750ppm	155	2.82	1029	2.03	7.82	0.4	65.7	25.9	0	0	7.91E-5	7.43E-5	7.77E-7
XY65-2	in m-xylene		157	2.82	2044	8.55	13.0	0.3	56.4	34.5	0	0	5.70E-5	5.26E-5	4.96E-7
XY65-2			112	2.82	3262	15.0	15.6	0.2	54.6	36.5	0	0	2.49E-5	2.30E-5	2.38E-6
XY66-1	95mL m-xylene	CoOct, 350ppm	129	0.1	1001	2.0	9.2	0.2	73.3	18.5	0	0	9.61E-5	8.94E-5	1.53E-5
XY66-2	w/5wt% recycle		147	0.1	2294	4.6	30.3	0.1	24.3	47.7	0	0	2.05E-4	1.48E-4	9.98E-6
XY66-3			137	0.1	3604	6.3	39.1	0.7	22	50.0	0	0	1.03E-4	7.48E-5	8.36E-6
XY67-1	5 wt% recycle,	CoOct, 350ppm	132	0.1	952	1.9	4.2	0.5	85.6	4.4	0	0	4.18E-5	3.88E-5	5.67E-6
XY67-2	95ml m-xylene	0.5 wt% t-butylproxy benzoate	131	0.1	2264	23.9	9.4	0.3	80.2	6.5	0	0	4.41E-5	3.90E-5	6.0E-6
XY68-1	20wt% HAc in 10	0.0614g CuO/TiO_2	141	2.82	184	no	1.6	2.4	40.9	16.3	0	0	8.66E-5	6.01E-5	
XY68-2	ml m-xylene	(1 wt%)				flow									
			142	2.82	1340	6.16	5.9	0.6	75.6	16.5	0	0	3.74E-5	3.56E-5	
XY70-1	5wt% recycle in	CoOct, 350ppm	140	0.1	91	0.2	1.3	1.5	89.2	0	0	0	1.39E-4	1.36E-4	1.23E-5
XY70-2	95mL m-xylene	Br^-, 350ppm	137	0.1	1144	1.7	8.1	0.2	76.7	13.3	0	0	6.85E-4	6.23E-5	6.58E-6
XY70-3			140	0.1	2432	6.9	22.7	0.1	47.7	34.0	0	0	1.34E-4	1.10E-4	9.11E-6
XY70-4			143	0.1	3672	9.7	36.5	0.03	33.4	45.2	0	0	1.59E-4	1.25E-4	9.66E-6

Table 3.11. cont'd.

RUN	FEED COMP.	CATALYST	T °C	P MPa	TIME min	AIR mols	CONV. %	Selectivity % to j					Reaction Rate Const.		
								XYL Isomers	MTAld MTAlc	MTA	IPA	CO_2 +CO	k	(k_1+k_4)	$(k_1+k_4)_{adj}$
XY71-1	10 mL 20	CoOct, 1750ppm	141	2.82	52	0.83	6.88	3.29	55.3	10.4	0	0	1.37E-3	9.46E-4	1.46E-5
XY71-2	wt%Hac/MX		151	2.82	1074	1.66	11.1	1.64	59.6	30.4	0	0	4.32E-5	3.96E-5	3.70E-7
XY71-3			120	2.82	1214	3.32	18.7	1.0	46.2	45.4	0	0	7.36E-5	3.29E-5	3.29E-6
XY72-2	20wt% recycle in	CoOct, 350ppm	131	0.1	361	0.7	2.2	3.3	81.5	8.2	0	0	2.54E-5	2.36E-5	3.09E-6
XY72-3	80mL MX		133	0.1	722	1.4	3.6	2.4	81	10.7	0	0	4.02E-5	3.79E-5	4.44E-6
XY72-4			133	0.1	2026	4.1	8.2	1.6	73.1	23.2	0	0	3.72E-5	3.64E-5	4.27E-6
XY73-1	5 wt% recycle in	CoOct, 1750ppm	133	0.1	78	0.2	5.8	3.4	76	3.0	0	0	7.66E-4	6.31E-4	1.76E-5
XY73-2	95mL MX		132	0.1	373	0.8	8.5	2.0	71.8	12.9	0	0	9.97E-5	8.64E-5	2.54E-6
XY73-3			134	0.1	742	1.8	10.2	1.4	68.9	16.4	0	0	4.99E-5	4.33E-5	1.14E-6
XY74-2	10mL 20wt%	CoOct, 1750ppm	120	2.82	275	3.01	11.4	1.88	73.6	15.1	0	0	6.13E-4	5.55E-4	2.68E-5
XY74-3	Acetic acid/MX		118	2.82	1283	3.86	20.3	1.05	46.9	45.0	0	0	8.25E-5	7.66E-5	4.14E-6
XY75-1	6 wt% MTA in 100	CoOct, 1750ppm,	135	0.1	63	0.1	4.3	1.4	82.3	0	0	0	6.98E-4	5.84E-4	1.53E-5
XY75-2	mL MX	Br^-, 1750ppm	135	0.1	318	0.6	10.0	0.7	80.1	0.8	0	0	2.41E-4	1.97E-4	5.14E-6
XY75-3			128	0.1	1728	3.5	30.6	0	64.7	22	0	0	1.84E-4	1.60E-4	6.09E-6
XY77-2	10wt% HAc in	CoOct, 1750ppm	123	0.1	307	1.23	6.44	3.87	71.5	6.23	0	0	2.17E-4	1.17E-4	7.94E-6
XY77-3	9.15mL MX		122	0.1	1027	1.39	14.6	1.53	63.7	25.5	0	0	1.27E-4	1.15E-4	5.46E-6
XY77-4			120	0.1	2167	1.89	21	0.95	47.8	42.7	0	0	6.83E-5	6.25E-5	3.32E-6
XY78-2	20wt% HAc in	CoOct, 1750ppm	82	0.1	360	2.31	4.98	4.63	68.1	9.7	0	0	1.42E-4	1.77E-4	6.23E-5
XY78-3	8.30 mL MX		82	0.1	1740	21.6	8.67	2.59	73.9	12.5	0	0	2.87E-5	2.55E-5	1.36E-5
XY78-4			81	0.1	3300	51.4	12.6	1.55	63.2	26.6	0	0	2.82E-5	2.58E-5	1.47E-5
XY80-1	5wt% recycle in 380mL MX	CoOct, 350ppm	140	2.82	331	13.54	17.6	0.49	65.8	25.2	0	0	5.85E-4	5.35E-4	4.85E-5

Table 3.11. cont'd.

RUN	FEED COMP.	CATALYST	T °C	P MPa	TIME min	AIR mols	CONV. %	Selectivity % to j					Reaction Rate Const		
								XYL Isomers	MTAld MTAlc	MTA	IPA	CO_2 +CO	k	(k_1+k_4)	$(k_1+k_4)_{adj}$
XY83-1	5wt% recycle in 380mL MX	CoOct, 50ppm $Mn(OAc)_2$, 300ppm	140	2.82	360	2.94	16.1	0.27	71	22.9	0	0	4.88E-4	4.59E-4	4.16E-5
XY84-1	5wt% recycle in	CoOct, 750ppm	142	2.82	63	0.83	0.65	25.2	54.9	6.4	0	0	1.15E-3	9.96E-4	2.06E-5
XY84-2	10mL MX	$Mn(OAc)_2$, 750ppm	140	2.82	376	4.96	7	2.4	84.3	11	0	0	2.11E-4	2.06E-4	4.72E-6
XY85-1	5 wt.% recycle in 380mL MX	CoOct, 50ppm $Mn(Oac)_2$, 300ppm	140	2.82	390	6.0	19.0	0.43	65.4	26.5	0	0	5.4E-4	4.99E-4	4.30E-5
XY86-1	400 mL m-xylene	None	160	2.82	300	14.4	3.5	-0.3	0	0	0	0	1.17E-4	0	0
XY87-1	285 mL m-xylene	$Mn(OAc)_2$, 300ppm	163	2.82	300	14.4	19.2	-0.5	35.4	65.6	0	0.044	7.11E-4	7.11E-4	2.09E-5
XY87-2	5wt% recycle	CoOct, 50ppm	160	2.82	900	42.4	30.7	-0.3	15.1	74.9	0	0.028	2.56E-4	2.30E-4	7.79E-6
XY87-3		NaBr, 350 ppm	160	2.82	1500	71.8	38.2	-0.3	13.3	71.3	0	0.22	1.90E-4	1.61E-4	5.43E-6
XY88-1		$Mn(OAc)_2$, 300 ppm	160	2.82	300	14.1	26.7	-0.3	26.9	61.8	0	2.71	1.04E-3	9.20E-4	1.32E-5
XY88-2	274 mL xylene 5wt% recycle	CoOct, 500 ppm NaBr, 1200 ppm	160	2.82	595	32.7	31.2	-0.3	19.3	54.8	0	3.31	2.13E-4	1.58E-4	2.26E-6
XY89-1	9.06mL xylene	$Mn(OAc)_2$, 300ppm	160	2.82	300	5.65	8.2	-0.2	80.5	19.5	0	0	2.87E-4	2.87E-4	9.19E-6
XY89-2	5 wt% recycle	CoOct, 50ppm	160	2.82	900	16.9	13.0	-0.2	78.2	22.8	0	0	8.94E-4	8.94E-4	2.87E-6
XY89-3	5 wt% H2O														
XY90-1	9.34 mL xylene	$Mn(OAc)_2$, 250ppm	160	2.82	300	4.6	4.3	-0.1	85.9	14.1	0	0	1.45E-4	1.45E-4	1.01E-6
XY90-2	5 wt% recycle	CoOct, 1500ppm	160	2.82	900	16.9	12.4	-0.2	71.1	15.2	13.7	0	1.49E-4	1.48E-4	1.03E-6
XY90-3			160	2.82	1500	28.2	23.2	0.4	61.3	24.5	13.7	0	2.18E-4	2.17E-4	1.50E-6
XY91-1	9.98 mL xylene	1wt% H_3PW_{40}/SiO_2	160	2.82	300	5.65	1.3	-0.4	84.0	6.0	0	0	4.36E-5	3.92E-5	2.60E-6
XY91-2		CoOct, 200ppm	160	2.82	900	16.9	6.1	-0.6	79.0	12.8	0	0	8.37E-5	7.69E-5	5.09E-6
XY91-3			160	2.82	300	28.2	12.4	0.0	46.4	31.3	0	0	1.15E-5	8.95E-5	5.93E-6
XY92-1	135 mL xylene	300ppm Co(Acac)	160	2.82	300	7.00	30.7	-0.3	17.5	71.6	5.8	1.8	1.22E-3	1.16E-3	1.19E-5
XY92-2	5wt% recycle 5wt% water	800ppm $Mn(OAc)_2$ 1500ppm NaBr	160	2.82	765	17.1	62.8	-0.3	13.6	73.5	7.5	1.06	1.34E-3	1.27E-3	1.29E-5
XY93-1	9.38 mL xylene	1500ppm Co(Acac)	160	2.82	300	5.65	2.2	-1.0	76.9	23.1	0	0	7.30E-5	7.30E-5	5.15E-7
XY93-2	5wt% recycle	250ppm $Mn(Oac)_2$	160	2.82	900	16.9	7.7	-0.3	69.4	30.6	3.6	0	9.74E-5	9.74E-5	6.87E-7
XY93-3			160	2.82	1500	28.2	24.0	-0.3	58.1	38.3	2.4	0	3.24E-4	3.20E-4	2.25E-6
XY94-1	9.34 mL xylene	$Mn(OAc)_2$, 250ppm	160	2.82	300	1.47	2.5	-4.1	54.4	45.6	0	0	8.40E-5	8.40E-5	5.92E-7
XY94-2	5wt% recycle	CoOct, 1500ppm	160	2.82	900	3.24	5.1	-1.8	80.2	19.8	0	0	4.40E-5	4.40E-5	3.13E-7
XY94-3			160	2.82	1500	5.01	12.3	-0.8	70.8	29.2	0	0	1.31E-4	1.31E-4	9.26E-7

Table 3.11. cont'd.

RUN	FEED COMP.	CATALYST	T °C	P MPa	TIME min	AIR mols	CONV. %	Selectivity % to j					Reaction Rate		
								XYL Isomers	MTAld MTAlc	MTA	IPA	CO_2 +CO	k	k_1+k_4	$(k_1+k_4)_{adj}$
XY95-1	170.9 mL xylene 5wt% recycle	$Mn(OAc)_2$, 300ppm CoOct, 50ppm $Ce(OAc)_3$, 100ppm	170	3.16	300	8.68	25.0	-0.5	53.3	40.8	8.8	1.94	9.58E-4	9.02E-4	1.93E-5
XY96-1	9.49 mL xylene 5wt% recycle	$Mn(OAc)_2$, 300ppm CoOct, 50ppm $Ce(OAc)_3$, 100ppm	150	2.82	300	0.20	2.2	-1.5	88.3	11.6	0	0.09	7.53E-5	7.53E-5	4.12E-6
XY96-2			150	2.82	900	3.13	2.4	-0.9	86.1	13.8	0	0.08	3.04E-6	3.04E-6	1.66E-7
XY97-1	162.9 mL xylene 5wt% recycle 5wt% water	$Mn(OAc)_2$, 300ppm CoOct, 50ppm $Ce(OAc)_3$, 100ppm	170	3.16	300	8.59	36.0	-0.4	35.3	47.8	8.2	3.43	1.49E-3	1.36E-3	2.75E-5
XY97-2			170	3.16	900	13.8	62.8	-0.3	18.6	55.9	17.4	1.96	9.04E-4	8.31E-4	1.68E-5
XY98-1	9.05 mL xylene 5wt% recycle 5wt% water	$Mn(OAc)_2$, 300ppm CoOct, 50ppm $Ce(OAc)_3$, 100ppm	150	2.82	300	0.83	3.4	0.0	80.6	18.5	0	0.91	1.15E-4	1.14E-4	5.91E-6
XY98-2			150	2.82	900	3.94	10.5	-0.3	74.8	24.9	0	0.30	1.27E-4	1.26E-4	6.56E-6
				Po_2		O_2									
XY99-1	170.9mL xylene 5% recycle	$Mn(OAc)_2$, 300ppm CoOct, 50ppm $Ce(Oac)_3$ 100ppm	150	0.51	335	2.06	22.8	-0.5	35.9	56.8	4.1	1.33	7.73E-4	7.48E-4	3.88E-5
XY99-2			150	0.51	910	5.59	35.6	-0.4	23.1	67.9	4.9	0.85	3.16E-4	3.03E-4	1.57E-5
XY99-3			150	0.51	1820	7.03	44.1	-0.3	17.8	68.4	9.2	0.69	1.55E-4	1.48E-4	7.65E-6
XY100-1	170.9mL xylene 5% recycle	$Mn(OAc)_2$, 300ppm CoOct, 50ppm $Ce(Oac)_3$ 100ppm	170	0.51	300	1.86	32.3	-0.6	23.7	64.1	5.6	2.55	1.30E-3	1.21E-3	2.46E-5
XY100-2			170	0.51	900	5.54	68.1	-0.3	12.3	76.1	6.1	1.21	1.26E-3	1.19E-3	2.40E-5
				P_{total}		O_2									
XY101	0.82ml xylene in SC CO_2	Co(salen), 1500ppm	140	19.7	900	0.014	1.3	-6.3	47.1	18	0	0	1.45E-5	9.46E-6	2.22E-7
XY102	0.78mL xylene with 5 wt% recycle in SC CO_2	Co(salen), 1500ppm	140	19.7	900	0.014	1.1	-8.4	39	16.3	0	0	1.23E-5	7.01E-6	1.64E-7

Comparing the efficiency of oxygen usage in the reactors can also reveal the differences between the two reactors. The efficiency of oxygen usage at a particular reaction time can be defined as (3-23).

$$\eta_{O_2} = \frac{moles \quad of\ net \quad O_2 \quad consumed \quad in\ the \quad reactions}{total\ moles \quad of \quad O_2 \quad fed} \qquad (3-23)$$

The mols of net oxygen consumed were calculated according to the product distribution assuming one mol oxygen per mol MTAld and benzaldehyde, 1.5 mol O_2 per mol MTA, 0.5 mol O_2 per mol MTAlc and cresol, and 2 mols oxygen to produce all heavies.

Table 3.12. Oxygen efficiency for different reactors

Run time, min	300 or 335	900 or 910	O_2 supply rate, $mol \cdot (mol\ MX)^{-1} \cdot min^{-1}$
20 mL reactor, XY96	4.5%	0.3%	0.0090
500 mL reactor, XY99	19%	11%	0.0044

Table 3.12 gives the results for two runs. Here the O_2 supply rate is defined as moles oxygen/mol MX per unit time. Runs XY96 and XY99 were performed at the same temperatures, the same catalyst, the same feed and almost the same P_{O2}. From Table 3.14, it is seen that the oxygen efficiency of the 500 mL reactor is about 3-30 times higher than that of the 20 mL reactor. According to the catalyzed free radical chain mechanism (Parshall, 1980), the concentration of free radicals in the reaction mixture affects the oxidation rate directly. Radicals can terminate by collision with the walls of the reactor and thereby slow down the reaction. The S/V of the 20 mL reactor is about 2.7 cm^{-1} while that of the 500 mL reactor is only 1.1 cm^{-1}. It is obvious that the terminations of radicals with the reactor walls slowed down MX oxidation in the 20 mL reactor. This inhibition of activity argues against development of a continuous catalytic process in a tubular-type reactor; any continuous process would have to be run in a stirred

vessel similar to the large autoclave reactor. Another possibility is that the higher air supply rates affected reactant/catalyst contact by vaporizing too much of the m-xylene (note: the amount of vapor space in the small reactor is a much higher fraction of the total system volume than in the large reactor). For the rest of this discussion, only data from the same reactor will be compared.

♦ Acid Solvent and MTA Addition Effects

Comparing the results of XY24 and XY29, it is seen that acetic acid (HAc) added to the reaction mixture can increase the oxidation rate and selectivity to MTA. One reason for this result is that carboxymethyl radicals ($^{\bullet}CH_2COOH$) can be obtained from decomposition of heavy metal acetates; these can abstract protons from MX initiating the desired oxidation or can also add on to aromatic rings or methyl benzyl radicals (Heiba, et al, 1969). Another reason is that electron transfer between MTA and Co(II) acetate can occur easily in acid solution to keep a high Co(III) concentration and MTA formation rate (Kashima and Kamiya, 1974). In addition, adding HAc allows the use of more metal catalyst because this is more soluble in HAc than either xylene, tolualdehyde, or MTA. An acidic solution can prevent precipitation of the metal catalyst to insoluble hydroxy derivatives (Hronec et al, 1985).

However, at high catalyst concentrations, HAc can slow down the electron transfer between MTA and Co(II) acetate by tight coordination of the metal center. Comparing the selectivities to MTA at different HAc concentrations, they have almost identical selectivity at equivalent conversion of 13-15% (XY77 and XY78). This is pretty remarkable considering the difference in temperatures and mols of air used. It suggests almost no effect of using a higher HAc amount.

The $(k_1+ k_4)_{adj,\ T}$ for XY39 was 4.5×10^{-4} min^{-1} while that for XY42 was 1.9×10^{-4} min^{-1}. Therefore, adding MTA to the feed has little effect on activity although the selectivity to MTA increased. When using CoOct as catalyst, MTA addition increased activity slightly but only at the early stage of the reaction ($(k_1+k_2)_{adj}$ of XY44-1 is twice that of XY29), but did not promote conversion of aldehyde to MTA. When MTA concentration in the feed was higher, there was little effect, possibly even a negative effect; compare the selectivities at constant MX conversion for XY44 and XY52. The reason may be because low MTA concentration can promote the electron transfer between Co(II) and MTA, but using even more MTA will further tie up the metal center to slow down the further oxidation of aldehyde.

♦ Effects of Oxygen Supply Rate

Increasing the oxygen supply rate to the reactor could increase the oxygen diffusion rate into the bulk liquid. The effect of oxygen supply rate is different for the 500 mL and the 20 mL reactors due to reactor wall and agitation effects. The stoichiometric ratio for MTA formation is 1.5 mol O_2 per mol MX. In runs XY83 and XY85, the total O_2 supply reached this ratio at 3000 min and 1500 min, respectively. In runs XY86, XY87, XY92, XY95, XY99 and XY100, the times were all ~300 min. In runs XY90 and XY94 in the small reactor, the times to reach this ratio were 38 min and 120 min, respectively.

Table 3.13 shows the effects of supply rate on the uptake rate of oxygen and on the product distribution in the two reactors at 300-400 min. XY90 and XY94 were conducted in the 20 mL reactor using the same feed, catalyst, temperature and O_2 pressure. XY83 and XY85 were performed in the 500 mL reactor using the same feed, catalyst, temperature and O_2 pressure. XY96 was performed in the 20 mL reactor while

XY99 was in the 500 mL reactor, both using the same catalyst, feed, temperature and O_2 pressure. The catalysts of XY96 and XY99 were different from those of XY83, XY85, XY90 and XY94. The uptake rate of oxygen was calculated by equation (3-24).

$$R_{O_2} = \frac{moles\ \ of\ \ net\ \ O_2\ \ consumed}{(moles\ of\ \ MX\ \ used\ \ in\ \ this\ \ run) \times time(\min)} \qquad (3-24)$$

Table 3.13. Effects of oxygen rate for the two reactors

Reactor type	O_2 supply rate mol · (molMX)$^{-1}$ · min^{-1}	R_{O2}^{*} mol · (molMX)$^{-1}$ · min^{-1}	Selectivity to the desired products, %
20 mL	0.013 (XY94)	8.1×10^{-5}	100
	0.040 (XY90)	1.3×10^{-4}	86
	0.0090 (XY96)	2.8×10^{-5}	100
500 mL	0.00053 (XY83)	3.6×10^{-4}	94
	0.00099 (XY85)	3.9×10^{-4}	93
	0.0044 (XY99)	4.7×10^{-4}	96

* Averaged over 300-400 min for runs XY83, XY85, XY90 and XY94; averaged over 900-910 min for runs XY96 and XY99.

It is clear that the uptake of oxygen increased when the air supply rate increased in the 20 mL reactor while it was essentially independent of air supply rate for the 500 mL reactor. Comparing XY96 and XY99, it is seen that the uptake rate of oxygen in the 500 mL reactor was far higher than that in the 20 mL reactor although the oxygen supply rate was far lower than that in 20 mL reactor. Comparing the $(k_1 + k_4)_{adj}$ values (adjusted to the same base temperature and catalyst concentration), it increased by ~4% for the large reactor when the air supply rate was doubled (XY83 and XY85). But it increased by 71% for the small reactor when the air supply rate was tripled (XY90 and XY94). That suggests that the reaction in the small reactor may have been mass-transfer-limited while the reaction in the large reactor was not. There is only an upper agitator in the 20 mL reactor near the surface of the liquid, while the stirring rate for the standard propeller agitator in the 500 mL reactor was about 720 rpm. With the differences in agitation, it is

possible that there were O_2 concentration gradients in the smaller reactor, even though the rates were lower.

Further oxidation of MTA, MTAld and MTAlc to heavier compounds was inhibited either by a reactor wall effect or due to an O_2 concentration gradient in the 20 mL reactor, except in run 90. Here, lots of IPA was produced, but at very high oxygen supply rate. The high O_2 supply rate would result in better mixing, so less resistance to mass transfer.

Assuming that the reaction rate is 1st order with respect to oxygen concentration in the liquid, and the reaction is diffusion controlled in the 20 mL reactor, the reaction rate based on oxygen consumption can be expressed as (3-25) according to a steady-state film model (Carra and Morbidelli, 1987).

$$N_{O_2} = \beta k_{L,O_2} C_{O_2,i} \qquad (3-25)$$

Here, $k_{L,O2}$ is liquid-film mass transfer coefficient; $C_{O2,i}$, the interface concentration of oxygen; β, the enhancement factor by reaction. For runs XY90 and XY94 with similar pressure and temperature, $k_{L,O2}$ and $C_{O2,i}$ are approximately the same. The enhancement factor ratio for the two reactions in the 20 mL reactor can be calculated by the R_{O2} ratio of runs XY90 and XY94 (Table 3.13). Therefore, the enhancement factor ratio for these runs was 1.6. This suggests that a high O_2 supply rate increased the rate of oxygen diffusion into the bulk liquid in the 20 mL reactor.

The above results also suggest that the reaction in the 500 mL reactor was kinetically controlled. In order to further check these results, the maximum oxygen uptake and first order reaction rate constant obtained at 170ºC and P_{O2} = 0.65 MPa using the 500 mL reactor (run XY97) were calculated and compared with values for p-xylene

oxidation at 120ºC and P_{O2} = 0.1 MPa using a similar reactor and almost the same stirring rate (800 rpm) (Cao and Servida, 1994). Table 3.14 gives the results.

Table 3.14. Oxygen uptake rate and reaction rate constant for p-xylene and m-xylene

	R_{O2}, mol·(molMX)$^{-1}$min^{-1}	Reaction rate constant, min^{-1}
p-xylene	0.0017	0.0022
m-xylene	0.0013	0.0015

The oxidation of p-xylene at the above conditions is kinetics-limited and zeroth-order with respect to oxygen concentration (Cao and Servida, 1994). However, both the reaction rate constant and oxygen uptake rate for m-xylene, which were the highest values obtained in our experiments, were lower than those of p-xylene. Therefore, the oxidation of m-xylene in the 500 mL reactor at high pressure is kinetics-limited and zeroth-order with respect to oxygen concentration. Reactions in the 500 mL reactor at lower pressure must also be kinetics-limited, because their rates are even lower.

♦ Pressure Effects

Runs XY66 and XY80 were performed at similar temperature, with the same feed and catalyst. XY80 was performed at 2.82 MPa and XY66 at 0.1 MPa. Comparing the data from these runs, it is seen that high O_2 pressure can increase both the MX conversion and MTA selectivity. The m-xylene oxidation in a standard agitated vessel is therefore a typical "slow" gas-liquid reaction. When the P_{O2} is lower than a certain value, the reaction is kinetically controlled but not zeroth-order with respect to oxygen partial pressure. With the increase of P_{O2}, the concentration of oxygen in the liquid increases according to Henry's law ($P_{O2} = H_{O2} \cdot C_{O2}$). When the partial pressure of O_2 is increased above a certain value, the solution is O_2 – saturated and so the reaction rate will no longer change with P_{O2}. That is why the reaction rate constants at low pressure were usually 2-5 times less than those at high pressures (> 2 MPa air or 0.4 MPa O_2).

Comparing run XY100 with XY95, it is clear that both MX conversion and MTA selectivity were somewhat higher when using pure oxygen as an oxidizing agent. That is probably because using pure oxygen increased the oxygen solubility in the bulk liquid at a given temperature.

♦ Effects of Water in the Feed

It has been suggested that low concentrations of water can help form the complex [$RCH_2^{\bullet}\cdots H_2O$], which increases the overall reaction rate (Zaikov and Maizus, 1968; Czytko and Bub, 1981). Therefore, 5 wt% water was added to the feed in a few experiments. Comparing the results of runs XY88 vs. XY92, XY95 vs. XY97 and XY96 vs. XY98, with the same temperatures, pressures, and oxygen supply rates and similar catalyst systems, it is seen that a small concentration of water in the feed not only increases the reaction rate in the early stages of the reaction, but also increases MTA selectivity. However, the amount of CO_2 and heavies produced in the reactions with water present were slightly higher.

♦ Effects of Reaction Temperature

Both MX conversion and MTA selectivity increased when the reaction temperature was increased if using a selective catalyst (comparing runs XY99 and XY100). MTA yield increased by 8% for the first 300 minutes and about 28% for the first 900 minutes, for a temperature increase of 20ºC. However, more CO_2 and heavy compounds can be produced when the reaction temperature was increased for certain catalysts. In order to keep CO_2 to <3% selectivity and minimize formation of heavy compounds, but obtain high MX conversion and MTA selectivity, the suggested reaction temperature should typically be between 160-170ºC.

♦ **Catalyst System**

Several catalysts were tested for m-xylene oxidation in previous work at Louisiana State University, including the solid CuO/ZrO_2, CuO wires, CuO/TiO_2, supported CoO, and soluble Cu- and Co- catalysts (Dooley, 2000c; Dooley, 2001). It was clear that MTA could not be made selectively by any of the Cu-catalysts when using a purely MX solution (Dooley, 2000c). Even when MTA was added to the feed and the reaction was performed at high temperature (160ºC) and high pressure (2.9 MPa), the selectivity to MTA was still <10% in 120 h using CuO/ZrO_2. In run XY68, the conversion was very low although the selectivity was 16.5% (1340 min) when using CuO/TiO_2. The best results using supported Co-catalysts (1wt.%) also were not promising, only about 13% conversion and 22% MTA selectivity in 4000 min. Although 28% selectivity to MTA could be obtained using soluble Cu acetate (557 ppm), the selectivity to MTA was only 7% in 4900 min. Going to higher catalyst amounts (1750 ppm) did not accelerate MTA formation, only that of xylene isomers. Adding Br^- as an electron-transfer promoter did not help.

Based on the above results and references on p-xylene catalytic oxidation (Raghavendrachar and Ramachandran, 1992), it was clear soluble Co-based catalysts might work. It was then found that MTA could be made slowly from MTALd and MTAlc with some MTA present in the feed using soluble Co salts (runs XY44, XY52, XY75). At 0.1 MPa, close to 30% selectivity to MTA with more than 90% selectivity to the desired products could be obtained at >50% conversion. But the conversion of the aldehyde to the acid was still slow, a matter of days. Most soluble Co-catalysts require some acid for dissolution anyway; it was found that CoOct did not require MTA to

dissolve at the 350 ppm level (a typical amount), but the acetate, $Co(OAc)_2$ did. It was clear that CoOct is better for forming MTA than $Co(OAc)_2$ from the previous results.

Mn salts are also typical catalysts used in p-xylene oxidation (Raghavendrachar and Ramachandran, 1992); a series of tests on a combination of an Mn salt ($Mn(OAc)_2$) and CoOct were made. The results (XY80 vs. XY83 and XY85, and XY84 vs. XY90) showed that Mn salts improved the general reaction rate while Co salts were better for MTA selectivity. However, the differences in either case are not great.

Electron-transfer promoters are also very important in xylene oxidation using metal salts. These can combine with Co(III)/Mn(III) in the production of free radicals by oxidation, and also in re-oxidizing Co(II)/Mn(II). Some work had also been done using such promoters at Louisiana State University (Dooley, 2000c; Dooley, 2001). Peroxide, paraldehyde, acetic acid, MTA and bromide were tested. Effects of acetic acid and MTA have been discussed previously. At low concentrations, these can increase the MX conversion and selectivity to MTA, especially in the early stage of the reaction. From runs XY67 and XY66, it is seen that t-butylperoxy benzoate addition hurt both MTA formation and the overall reaction rate. Combining CoOct with Br^- had no significant effect on MX conversion but decreased the selectivity to MTA at low pressure (XY66 vs. XY70). Combining MTA with Br^- was also ineffective at low pressure (XY75). The recycle solution containing most of the tolualdehyde and methyl benzyl alcohol can also be used as a promoter. It is obvious that good results can be obtained using the recycle solution at high pressure (XY80, XY83, XY85). It is also seen that too much recycle addition (eg., 20 wt%) and too much catalyst were not conductive to MTA formation, comparing the (k_1+k_4) values of XY66 with XY72-73.

$Co(Acac)_2$ is a more soluble Co-salt that has been used previously as a catalyst in MX oxidation (Grane, 1974). In order to test the combined effects of $Co(Acac)_2$, an Mn salt, and Br^- at high pressure and temperature, further experiments were conducted (XY87-88, XY92). The air rate here was ~1.5 mol O_2/mol xylene (stoichiometric requirement) fed in 360 min. When using CoOct/$Mn(OAc)_2$/Br^{-1} as catalyst, 31% conversion was obtained with 75% selectivity to MTA (XY87). Too much Co-salt and Br-salt were not conducive to MTA formation - compare runs XY87 and XY88. But highly soluble Co-salt ($Co(Acac)_2$) at high pressure is beneficial in forming MTA (compare runs XY88 and XY92), which is consistent with the previous work of Grane (1974). A 63% conversion with 73% selectivity to MTA can be obtained in 765 min using 300ppm/800ppm/1500 ppm of $Co(Acac)_2$ /$Mn(OAc)_2$/NaBr at 160ºC and P_{O2} = 0.56 MPa.

Redox systems other than Co and Mn salts with Br^- promoters have also been found beneficial in previous work (Kozhevnikov, 1995). A few such "redox" additives were examined here. The results from run XY91 proved that the solid tungsten heteropolyacid (H_3PW_{40}/SiO_2) was not conducive to forming MTA when used in combination with a typical Co salt. However, rare earth addition (Ce^{3+}/Ce^{4+}) (Masashi et al., 1999) can give even better results than bromide salts. Comparing the results for the first 300 min of runs XY87 and XY95, it was found that the reaction rate constant k for XY95 (100 ppm Ce salt) was higher than for XY87 (350 ppm Br salt), but the MTA selectivity was less. The adjusted reaction rate constants $(k_1+k_4)_{adj}$ in runs XY95, XY97, XY99-100 were generally greater than in runs XY70, XY75, XY87, XY88 and XY92, which means that the Mn/Co/Ce catalyst is a more active oxidation catalyst than either Co/Br or Mn/Co/Br. The apparent activation energy for (k_1+k_4) in m-xylene oxidation

using the Co/Mn/Ce catalyst and pure O_2 could be calculated from the data of XY99 and XY100, and it was 56 kJ/mol. That is slightly lower than the smallest reported value (63 kJ/mol) for p-xylene oxidation (Cao and Servida, 1994). The oxygen uptake rate and the overall xylene reaction rate using the Co/Mn/Ce catalyst for m-xylene oxidation are near to the reported values for p-xylene oxidation using a $Co(NA)_2$ catalyst (Table 3.15, Cao and Servida, 1994).

♦ Reaction in Supercritical (SC) CO_2 Solution

The oxidation of MX was also conducted in SC CO_2 solution (XY101 and XY102) using the 20 mL reactor in batch mode. Here the O_2/MX ratio is 1.6 (stoichiometric requirement for MTA is 1.5 mol O_2). The MX conversion and MTA selectivity in 900 min were very much lower than in previous experiments conducted under liquid-phase conditions, whether or not the recycle liquid was added to the feed. Comparing with results for 2,6-di-tert-butylphenol (DTBP) oxidation to 2,6-di-tert-butyl-1,4-benzoquinone (DTBQ) in SC-CO_2, the conversion and selectivity are also very low (for DTBP to DTBQ, the yield is about 81% in 1260 min, Musie et al, 2000). This may be due to the reactor wall effect but more likely because O_2/MX was far lower than O_2/DTBP in DTBP oxidation (75/1). These results are also not good considering p-xylene oxidation using a Cr(salen) (Cr^{3+}/PX = 0.037 mmol/mol, or ~182 ppm) conducted in liquid phase at 138ºC (yield to PTA of 29% in 1440 min, Chisem et al, 1998).

3.2.4 Product Distribution

Typical detailed product distributions for m-xylene oxidation are summarized in Table 3.15. From this Table, it was seen that isophthalic acid (IPA) was the biggest by-product for runs without acetic acid (about 6~17 wt%). Other side-products were $C_{16}H_{16}O_2$, CO_x, A (Mw = 166, $C_9H_{10}O_3$, likely an isophthalic acid isomer),

benzaldehyde, benzoic acid methyl ester (methyl benzoate), m-cresol, xylene isomers and C (Mw ≈ 240, probably also $C_{16}H_{16}O_2$), in rough order of importance. Comparing the product distributions at different reaction times for the same runs, it was found that more tolualdehyde and methylbenzylalcohol were converted to m-toluic acid with increasing time, proving that MTA was produced in series with MTald and MTalc as intermediates.

The product distribution also varied somewhat with feed composition, catalyst type, reaction temperature and reactor type. When the reaction was conducted in acetic acid feed, the most important side-product was benzaldehyde. Other side-products were A, xylene isomers, m-cresol, C, and ditolylmethanes, in rough order of importance. When a high concentration of MTA was used in the feed, more heavies were produced. When the Co-salts were increased by about 1500 ppm in the 20 mL reactor, and the air rate increased substantially, much IPA was produced. When the temperature was increased, more IPA and CO_x were produced. When Co/Mn/Br was used as the catalyst system, more coupling (heavies other than IPA) products were produced, whether the reaction was conducted in the 20 mL reactor, the 500 mL reactor, at low pressure, or at high pressure (for XY75, low pressure, 15% selectivity to heavies; for XY88 and XY87, high pressure, 22% and 16%, selectivity to heavies). When Co/Mn/Ce was used as the catalyst system, more IPA (rather than coupling products) was produced. When 1 wt% $H_3PW_{12}O_{48}/SiO_2$ was used as catalyst combined with CoOct, about 22% coupling products were produced.

It is obvious that more CO_x appears as the MX conversion increases. Generally, there was minimal CO_x production in any of these runs, except ~3% selectivity in XY88, XY97 and XY100, ~2% in XY92 and XY95, and ~1% in XY98 and XY99. Therefore, in this respect both the Br^-- and Ce^{4+}- promoted systems are almost equivalent.

Table 3.15. Typical Final Product Distributions of m-Xylene Catalytic Oxidation

Compounds (wt%)	XY74-2	XY74-3	XY92-1	XY92-2	XY97-1	XY97-2	XY100-1	XY100-2
Xylene isomers	1.9	1.0	-0.3[1]	-0.3	-0.4	-0.3	-0.6	-0.3
Benzaldehyde	6.3	3.4	0.4	0.2	0.2	0.3	0.2	0.5
Tolualdehyde	48.0	37.1	14.8	13.5	35.6	18.5	24.3	12.6
m-cresol	1.3	0.6	0	0	0	0.1	0.1	0
Methylbenzyl alcohols	25.6	9.8	2.3	-0.2	-0.5	-0.2	-0.5	-0.3
methyl benzoate	0	0.0	0.7	0.4	0	0.4	0.1	0.3
isophthalic acid	0	0.0	5.7	8.3	8.2	17.3	5.6	6.1
m-toluic acid	15.1	45.0	71.6	73.5	47.8	55.9	64.1	76.1
ditolylmethanes	0.0	0.1	0.1	0	0	0.0	0.0	0.0
A (Mw=166)	1.2	2.7	0	0.3	1.9	0.0	1.2	1.2
$C_{16}H_{16}O_2$	0.0	0.1	4.0	3.8	4.7	6.6	4.0	3.1
C (Mw≈240)	0.6	0.2	-1.1	-0.6	-0.9	-0.6	-1.0	-0.5
$CO+CO_2$	0.0	0.0	1.8	1.1	3.4	2.0	2.5	1.2
Total	100.0	100.0	100.0	100.0	100.0	100.0	100.0	100.0

[1] A negative selectivity means that a component already present in the feed was used up rather than produced up to that time.

Chapter 4 Conclusions

4.1 DEET Synthesis

1. Thermodynamic analyses show that DEET synthesis from MTA and DEA is an endothermic reversible reaction with equilibrium constant less than 41 when the reaction temperature is lower than 320ºC. The equilibrium constants at 300ºC and 320ºC estimated from thermodynamic data are close to those determined empirically (de Vekki and Mozzhukhina, 1997). The estimated equilibrium constants for the primary side reaction to produce ETA from MTA and DEA show that this reaction is an endothermic irreversible reaction from 245-320ºC.

2. It is impossible to obtain a high MTA conversion (>80% at 300ºC) when using a stoichiometric MTA/DEA (1/1 molar ratio) feed in a continuous reactor. Both the main reaction and the primary side reaction are very slow without a catalyst at normal operating conditions. With a suitable catalyst, the primary side reaction has a much lower rate than the main reaction. The ETA is produced mostly by DEET decomposition.

3. A kinetics study on catalysts ranging from supported weakly basic organometallic complexes (Tyzor TE series) to solid acid heterogeneous catalysts (hydroxyapatites, supported tungsten heteropolyacids and supported cesium tungsten heteropolyacids) showed that the acidic catalysts were more active, more stable in the presence of a gas phase, and, unlike previous heterogeneous catalysts examined for this reaction, could be used with near stoichiometric feeds. However, both supported acid and weak base catalysts can selectively catalyze the amidation reaction. The protons (Brønsted acid

4. sites) in the solid acid catalysts appear mainly responsible for the activity of these catalysts.

5. The best results (about 65-70% MTA conversion and 93-97% DEET selectivity) were obtained using supported tungsten heteropolyacids at a WHSV of 3-9 hr^{-1} using a feed of molar ratio DEA/MTA/DEET = 1/1/0.4 at 300ºC and low pressure. This conversion is higher than the best-reported MTA conversion of 55% (de Vekki and Mozzhukhina, 1997) using a heterogeneous catalyst. The selectivity obtained in this work is the same as those obtained using homogeneous catalysts (Hull, 1979). This catalyst can last at least 24 h without regeneration and showed no sign of apparent deactivation in 11 days of operation if there were periodic overnight air treatments at 450ºC. High temperature (450-500ºC) air treatments activated hydroxyapatite and heteropolyacid catalysts in their early stage of operation.

6. Both the main and secondary reaction rates (DEET decomposition) increased with temperature. Space velocity had no significant effect on MTA conversion when the reversible reaction to produce DEET was near the equilibrium state. However, long contact times (low WHSV) at high temperatures decrease DEET selectivity without much increase in MTA conversion.

7. Supported Tyzor TE catalysts deactivated more rapidly with respect to time on-stream than the solid acid catalysts. A nitrogen purge at 260ºC can effectively regenerate supported Tyzor TE catalysts; high temperature air deactivates them by oxidizing the triethanolaminato ligands.

4.2 MTA Synthesis

1. Soluble Co, Co/Mn, Co/Mn/Br, and Co/Mn/Ce catalysts are effective for MX oxidation to MTA. When the oxidation was performed in a 500 mL autoclave at P_{O2} =

0.51 MPa and 170ºC, using Co/Mn/Ce as the catalyst and in the presence of a recycle aldehyde/alcohol mixture, 68% MX conversion, 76% MTA selectivity, <2% CO_x selectivity and 4% selectivity to heavy products can be obtained in 900 min. A Ce-salt promoter can effectively substitute for corrosive bromide salts, and recycle alcohol/aldehyde mixture can substitute for an acetic acid solvent. The oxygen uptake rate and reaction rate constants to the desired products are near reported values for p-xylene oxidation at 120ºC. The apparent activation energy for m-xylene oxidation using a Co/Mn/Ce catalyst is ~56 kJ/mol, which is slightly less than the smallest reported value (63 kJ/mol) for p-xylene oxidation (Cao and Sevida, 1994).

2. The type of reactor affects the oxidation rate to desired products both by a wall effect and by affecting the mass transfer rate of oxygen in the liquid phase. The reaction at high pressure and >120ºC appeared to be mass-transfer-limited in a 20 mL reactor with poor agitation, while it was not in a 500 mL reactor with fast agitation. The ratio of enhancement factors for the small reactor was found to be ~1.6 (P_{O2} = 0.56 MPa, 160ºC) when comparing data at high and low air feed rates. Therefore a high air or oxygen supply rate can increase the oxygen uptake rate in a reactor limited by mass transfer. The supply rate had no effect on the MX conversion in the large reactor, because it was not mass-transfer limited. These limitations on activity in the small reactor argue against development of a continuous catalytic process in a tubular-type reactor.

3. Xylene oxidation was relatively slow and non-selective when the reaction was performed in supercritical-CO_2 solution using supported Co(salen) as a catalyst in the 20 mL reactor.

4. Acidic solvents such as acetic acid increase both the reaction rate and MTA selectivity. Adding a small amount of MTA to the feed increased the MX conversion but not the MTA selectivity, at low MX conversions. A high concentration of MTA added to the feed will decrease MTA selectivity. Low water content in the feed increased both the oxidation rate and MTA selectivity for the catalyst systems of this work.

5. Both MX conversion and MTA selectivity increased with temperature, but so did the selectivities to heavier products and CO_x. The optimum temperature was ~160-170ºC. Both the MX conversion and MTA selectivity also increased with the partial pressure of oxygen. A P_{O2} of about 0.5-0.6 MPa appears necessary in this work.

6. When MX oxidation was conducted with acetic acid in the feed, the most important side-product was benzaldehyde. Isophthalic acid (IPA) was usually the most important side-product without acetic acid. A high concentration of metal or Br^--salt can produce more IPA, especially at high oxygen supply rates. Both Br^- salts and certain acidic promoters can increase the selectivity to the coupling products.

References

G. Alberti, S. Cavalaglio, F. Marmottini, K. Matusek, J. Megyeri, L. Szirtes, Appl. Catal. A: General 218, 219-228 (2001).

E. C. Alyea and P. H. Merrell, Inorg. Nucl. Chem. Lett., 9, 69 (1973).

R. J. Angelici, Acc. Chem. Res., 5, 335(1972).

J. C. Bailar, J. R. Urbana, H. J. Emeleus, F. R. S. Cambridge, Comprehensive Inorg. Chem. SIR Ronald Nyholm F R S London. 1st Ed., Pergamon Press Ltd. Compendium Publishers. New York, 10523, USA (1973).

J. S. Beck, J. C. Vartuli, W. J. Roth, M. E. Leonowiez, C. T. Kresge, J. Am. Chem. Soc., 114, 10834-43 (1992).

M. R. Benjaram, G. Ibram and C. Biswajit, Chemistry Letters, 1145-1146 (1997).

J. A. S. Bett, L. G. Christner, and W. Keith Hall, J. Am. Chem. Soc., 89:22, 5535-5541 (1967).

W. F. Brill, Ind. Eng. Chem., 52, 837 (1960).

M. C. Burleigh, A. M. Michael, S. S. Mark, P. Bruce, J. Phys. Chem. B, 105, 9935-9942

(2001).

D. R. Burri, Ki-W. Jun, Y-H. Kim, J. M. Kim, C. E. Park, J. S. Yoo, Chem. Lett., 212-213 (2002).

G. Cao and A. Servida, M. Pisu, M. Morbidelli, Reactors, Kinetics and Catalysis. 40(7), 1156-1166 (1994).

M. W. Jr Chase, *NIST-JANAF Themochemical Tables, Fourth Edition*, J. Phys. Chem. Ref. Data, Monograph 9, 1-1951 (1998).

S. A. Chavan, D. Srinivas, P. Ratnasamy, J. Molec. Catal. A: Chemical, 49, 161 (2000).

S. A. Chavan, D. Srinivas and P. Ratnasamy, Chem. Commun., 1124-1125 (2001).

S-T. Chen, M-K. Jang and K-T. Wang, Synthesis, 858-960 (1993).

I. C. Chisem, J. Rafelt, M. T. Shieh, J. Chisem, J. H. Clark, R. Jachuck, D. Macquarrie, C. Ramshaw, K. Scott, Chem. Commun., 18, 1949-50 (1998).

A. P. Clark. U.S. Patent 3,607,920 (1971).

M. Colomina, P. Jimenez, M. V. Roux, C. Turrion, An. Quim., 82, 126-130 (1986).

F.A. Cotton and G. Wilkinson. Advanced Inorganic Chemistry, 4th Edition. John Wiley & Sons, New York (1980).

J. D. Cox, D. D. Wagman, V A Medvedev, CODATA Key Values for Thermodynamics, Hemisphere Publishing Corp., New York (1984).

B. F. Crowe and O. C. Elmer, U.S. Patent 2,742,502 (1956).

CS Chem Pro v5, Cambridge Soft Corporation (1999).

C. F. Cullis and D.J. Waddington, Proc. Roy. Soc. (London), A244, 110 (1958).

M. P. Czytko and G. K. Bub, Ind. Eng. Chem. Process Des Dev., 20, 481-486 (1981).

J. F. Day. U.S. Patent 5,496,959 (1996).

A. V. de Vekki and T. N. Mozzhukhina. Petrol. Chem., 37(4), 320-331 (1997)

N. G. Digurov, J. A. Dyakonov, N. N. Lebedev, V. V. Suchkov, L. A. Yoshkova, Izv. Vyssh. Uchebn. Zaved. Khim. Tekhnol., 13, 407 (1970).

B. D. Dombek and R. J. Angelici, J. Catal., 48, 433 (1977).

B. D. Durad and C. Lassau. Tet. Lett., 2329(1969).

K. M. Dooley, T. F. Guidry, and G. L. Price, J. Catal., 157, 66-75 (1995).

K. M Dooley, Year-End Report and 1999 Proposal, to MGK Co. (1998).

K. M. Dooley, Year-End Report and 2000 Proposal, to EagleView Technologies (2000a)

K. M. Dooley, DEET Analysis and Old DEET Batch Reaction Data (2000b).

K. M. Dooley, Report – Oxidation of m-Xylene to m-Toluic Acid, to EagleView Technologies (2000c).

K. M. Dooley, Year End Report and 2001 Proposal – Condensation and Oxidation Work, to EagleView Technologies (2001).

G. F. van Stryk, US Patent 3,198,831 (1965).

D. Yadov Ganapati, J. Phys. Chem. A:101, 36-48 (1997).

Z. Gao, Y. Shao, S. Wang, P. Yang, Appl. Catal. A: General 209, 27-32 (2001).

G. T. Musie, M. Wei, B. Subramaniam, D. H. Busch, Inorg. Chem., 40, 3336-3341 (2001).

H. R. Grane, U.S. Patent 3,832,395 (1972).

L. Haar, J. S. Gallagher, G. S. Kell, NBS/NRC Steam Tables, Thermodynamic and Transport Properties and Computer Programs for Vapor and Liquid States of Water in SI Units. Hemisphere Publishing Co., Washington, D.C. 271-276 (1984).

M. Hanotier and M. Hanotier-Bridoux, J. Molec. Catal., 12, 133 (1981).

L. Hans and W. Hans-Jorg, U.S. Patent 4,908,471 (1990).

Hasegaw and Toshiyuki, EP Patent 0,374,938 (1989)

Ch. F. Hendriks, H. C. A. van Beck and P M Heerties, Ind. Eng. Chem. Prod. Res. Dev., 17, 256 (1978).

E. I. Heiba, R. M. Dessau, Jr. W. J. Koehl, J. Am. Chem. Soc., 91, 135 (1969).

I. Hirose, K. Yamamoto and H. Okitsu, U.S. Patent 4,354,037 (1982).

T. Hosokawa, M. Takano, Y. Kuroki and S-I Murahashi, Tetrahedron Letters, 33(44), 6643-6646 (1992).

M. Hronec, J. Ilavsky, Ind. Eng. Chem. Prod. Res. Dev., 21, 455 (1982).

M. Hronec, J. Ilavsky, React. Kinet. Catal. Lett., 33, 299 (1987).

M. Hronec, J. Ilavsky, React. Kinet. Catal. Lett., 33, 323 (1987).

M. Hronec, Z. Cvengrosova and J. Ilavsky, Ind. Eng. Chem. Process Des Dev., 24, 787-794 (1985).

Ezekiel H. Hull, Greensboro N. C., U.S. Patent 4,133,833 (1979).

Y, Ichikawa, G. Yamashita, M. Tokashiki, T. Yamaji, Ind. and Eng. Chem., 62(4), 38-42 (1970).

N. S. Imyanitov and D. M. Rudkvsku, Zu. Pribl. Khim., 39, 2335 (1966).

I. Iovel, M. Shymanska, Synth. Commun., 22(18), 2691-2696 (1992).

K. Ishihara, S. Kondo and H. Yamamoto, Synlett, 9, 1371-1374 (2001).

K. Ishihara, S. Ohara and H. Uamamoto, J. Org. Chem., 61, 4196-4197 (1996).

N. Isogai, T. Okawa and T. Takeda, U.S. Patent 3,981,909 (1976).

Y. Kamiya and M. kashima, J. Catal., 25, 326 (1972).

M. Kashima and Y. Kamiya, Bull. Chem. Soc. Japan, 33, 481 (1974).

I. G. Kolesnik, Zhizhina, E. G., Matveev, K. I., J. of Molec. Catal. A: Chemical, 153(1-2), 147-154 (2000).

I. V. Kozhevnikov, A. Sinnema, R. J. J. Jansen, K. Pamin, H. van Bekkum, Catal. Lett,, 30, 241 (1995).

C. T. Kresge, M. E. Leonowiez, W. J. Roth, J. C. Vartuli and I. S. Beck, Nature, 359, 710 (1992).

J. W. LeFevre. J. Chem. Educ., 67, A278-A279 (1990).

Y. Masashi, O. Hiroshi, O. Atsushi, T. Kazuo, EP 0,896,960 (1999).

E. McEntire, E. Sellstrom and B. Kathy, U.S. Patent 4,613,673 (1986).

S-I Murahashi, Takeshi Naota and Eiichiro Saito. J. Am. Chem. Soc., 108, 7846-7847 (1986).

E. F. Murphy, L. Schmid, T. Burgi, M. Maciejewski, A. Baiker, Chem. Mater., 13, 1296-1304 (2001).

K. Nakaoka, Y. Miyama, S. Matasuhisa, S. Wakamatsu, Ind. Eng. Chem. Prod. Res. Develop., 12(2), 150-155 (1973).

P. P. Nicholas, U.S. Patent 5,312,984 (1984).

P. P. Nicholas, EP 0, 185,350 (1985).

P. P. Nicholas, U.S. Patent 5, 312,984 (1994).

NIST Chemistry WebBook, http://webbook.nist.gov/chemistry/ (2001).

R. Nomura, Takao, Wada, Yamada, Haruo and Matsuda. Chem. Lett., 1901-1904 (1986).

R. Nyholm, 1st Ed., Pergamon Press Ltd. Compendium Publishers. New York, 10523, USA (1973).

Tokura, N., Takefumi, T., Matsumoto, S., Shiokawa, Y., U.S. Patent 5,011,987(1991).

Z. Pan, Polymer Chemistry, Chapter 7, Chemical Industry Publisher, Beijing (1983).

D. K. Parker and G O Schulz, Rubber Chem. Technol., 62(4), 732-49 (1989).

G. W. Parshall, Homogeneous Catalysis, Wiley: New York (1980).

W. Partenheimer, J. Molec. Catal. A: Chemical 174, 29-33 (2001).

W. Partenheimer, In Catalysis of Organic Reactions; D W Blackburn , Ed. Marcel Dekker: New York, p321 (1990).

J. W. Patton and N. F. Seppi, Ind. Eng. Chem. Prod. Res. Dev. 9, 521(1970).

W. Peppe and H. Kroper. Ger. Patent 868,149 (1951).

R. H. Perry, Perry's Chemical Engineers' Handbook, 7th Ed., R. R. Donnelley & Sons Company (1997).

R. J. Perry and B D. Wilson, J. Org. Chem., 61, 7482-7485 (1996).

L. Pizzio, P. Vazquez, C. Caceres, M. Blanco, Catal. Lett., 77(4), 233-240 (2001).

P. Raghavendrachar and S. Ramachandran, Ind. Eng. Chem. Res., 31, 453-462 (1992).

A. A. Ravdel, Thermodynamics of Chemical Reactions. Severno-Zapadnyi Zaochnyi Politekhnicheskii Institut, Leningrad, Russian (1981).

G. L. Rempel, P. legzdins, H. Smith and G. Wilkinson, Inorg. Syth., 13, 90 (1978).

A. Saffer, R. S. Barker, U.S. Patent 2,833,816 (1958).

C. N. Satterfield, Heterogeneous Catalysis in Practice, Chapter 7, p. 152, R. R. Donnelley & Sons Company (1980).

Y. Sasson, Chem Commun., 73-74 (1998).

E. J. Y. Scott, J. Phys. Chem., 74, 1174 (1970).

D. Sehgal and I. K. Vijay, Anal. Biochem., 218, 87-91 (1994).

J. M. Smith and H. C. Van Ness, Introduction to Chemical Engineering Thermodynamics, R. R. Donnelley & Sons Company (1987).

I. V. Spirina, V. P. Maslennikov and Yu A. Aleksandrov, Russian Chemical Reviews, 56(7), 670-681 (1987).

M. H. N. Tabako, T. Kyoko, S. M. N. Tabako. EP 0,239,954 (1987).

Takeda, S., Nanobe, M., Ishida, K., Omoto, Y., Anno, T., U.S. Patent 4,398,037 (1983).

J. T. Tian and J. M. Tian. J. Mater. Sci., 36, 3061-3066 (2001).

T. Toru and T. Kazuo, EP 0,527,642 (1993).

I. Tkatchenko, G. Wilkinson, F. G. A. Stone, and E. W. Abel (Eds.), Comprehensive Organometallic Chemistry, Vol. 8, Pergamon prss, Oxford, p. 173 (1982).

T. Toru, T. Kazuo and A. Teruo, EP0,520,762 (1992).

Y. Tsuji, T. Ohsumi, T. Kondo and Y. Watanabe, J. Organom. Chem., 309, 333-344 (1986).

M. Ueda, A. Kameyama, and K. Hashimoto, Macromolecules, 21(1), 19-24 (1988).

F. J. Waller, U.S. Patent 4,416,801 (1982).

F. J. Waller, U.S. Patent 4,431,839 (1984).

F. J. Waller, U.S. Patent 4,463,103 (1984).

Y. Wang, C. H. E. Peden and S. Choi, Catal. Letts, 75, 169-173 (2001).

R. C. Weast, Handbook of Chemistry and Physics, 54th ed., CRC Press, Cleveland Ohio (1973-1974).

K. O. Xavier, J. Chacko and K. K. Mohammed Yusuff, J. Molec. Catal. A: Chemical 178, 275-281 (2002).

O. Yoshiaki, EP 0,653, 420 (1995).

J-Y Yun, M-Y, Park, S-W Rhee, J. Electrochem. Soc., 146(5) 1804-1808 (1999).

G. E. Zaikov and Z. K. Maizus, Adv. Chem. Ser., 75, 150 (1968).

Appendix A: Gas Chromatography, TGA and FT-IR Details

Table A1: GC Settings for DEET Feeds

Parameter	Setting
Injector Temperature	280°C
Detector Temperature	280°C
Maximum Oven Temperature	350°C
Initial Temperature	35°C
Ramp Rate	10°C/min?
Final Temp	210°C
Initial Time	3 min
Final Time	9.5 min
Purge	On Throughout Run
Column He flow rate	11cc/min
Split Vent He Rate	40 cc/min
Split Ratio	3.63
Purge Vent Flow Rate	3cc/min
Column Head Pressure	15 psig
Hydrogen flow rate	306cc/min
Air flow rate	30cc/min

Table A2: Retention Times for DEET Compounds using GC Varian 3400

Compound	Retention Time (min)	Calibration Slope
Diethylamine	1.1	3.772
Triethylamine	1.7	3.772
Toluene	4.1	0
1-Butanamine, N,N-Diethyl	5.5	3.772
Benzene, 1-isocyano,3-methyl	6.9~9.5	1.89
m-Toluic acid	10.5	1.12
Ethyl-m-methylbenzoate	12.1	1.89
N,N-diethylbenzamide	13	1.89
m-toluamide, N-ethyl	13.3	1.89
o-DEET	13.7	1.89
m-DEET	13.8	1.89
p-DEET	14	1.89
Trimethylbipheny	15.4~15.7	1.89
N-butyl, N-ethyltoluamide	16.1	1.89
C	>17	1.89

Table A3: GC Settings for MTA Feeds (Liquid and Solid)

Parameter	Setting
Injector Temperature	300°C
Detector Temperature	300°C
Maximum Oven Temperature	350°C
Initial Temperature	80°C
Initial Time	15 min
1st Ramp Rate	4°C/min
1st Stage End Temp	120°C
2nd Ramp Rate	20°C/min
End temperature	280°C/min
Final Time	2 min
Purge	ON throughout run
Methane Retention Time	1.0 min
Volumetric Flow through Column	10 cc/min
Split Vent Rate	40cc/min
Split Ratio	4.0
Column Head Pressure	5.3psig

Table A4: Retention Times and Slope for MTA Compounds using GC HP 5890A

Compound	Retention Time (min)	Calibration slope
m-xylene	2.4	0.629
xylene isomers	2.7	0.629
benzaldehyde	5.4	1.95
tolualdehyde	6.6	1.95
m-cresol	8	0.99
methylbenzyl alcohols	10.1	0.99
benzoic acid	13.1	0
methyl benzoate	15.9	1.15
phthalic acid	27	8.33
m-toluic acid	17~21	0.633
di tolylmethanes	23.1	0.0537
A	24~26	8.33
C16H16O2	29.8	0.633
C	31~35	0.633

Table A4: GC Settings for MTA Gas Phase

Parameter	Setting
Injector Temperature	190°C
Detector Temperature	190°C
Maximum Oven Temperature	250°C
Initial Temperature	40°C
Ramp Rate	15°C/min
Final Temp	230°C
Initial Time	8 min
Final Time	3 min
Volumetric Flow through Column	20~30 cc/min

Table A5: Retention Times for MTA Gas Phase Compounds using GC5890A

Compound	Retention Time (min)
Air	0.3
CO_2	1.1
H_2O	6.9
Xylene	10.1

Table A6: TGA Temperature Profile for Catalysts Hydroxypitate (100mL/min He)

Temperature (°C)	Ramp (°C/min)	Time (min)
50	5	0
500	5	120
900		60

Table A7: TGA Temperature Profile for Catalysts Co(Salen) and Co(DMBA) (50mL/min air + 50mL/min He)

Temperature (°C)	Ramp (°C/min)	Time (min)
50	5	0
500		30

Table A8: Drying Temperature Profile before 1-PA Adsorption (100 mL/min He)

Temperature (^{o}C)	Ramp (^{o}C/min)	Time (min)
50	10	0
575	0	10

Table A9: TGA Temperature Profile for 1-PA Adsorption (100 mL/min He)

Temperature (^{o}C)	Ramp (^{o}C/min)	Time (min)
50	0	10

Table A10: TGA Temperature Profile for 1-PA Desorption (100 mL/min He)

Temperature (^{o}C)	Ramp (^{o}C/min)	Time (min)
50	5	0
550		0

Table A11: FT-IR Operation Data for Co(Salen)

Cell type	Detector type	Scan number	Resolution	Vacuum pressure
DRIFTS Collector^{TM} II	MCT (cooled)	1024	4	6.58×10^{-7}Mpa

Appendix B: Calculations for DEET Synthesis and Spreadsheets

Toluene (TOL, MGK, 99.5%) was used as an internal standard. For DEET feeds, 1.0 mL of a 10vol% toluene/methanol solution was added to a 0.1mL product sample before GC analysis.

Let: SL_i=slope of calibration curve of i.

ρ_i=calibration compound density.

A_i=area%.

A_{ref}=area% of internal standard.

V_i=volume%.

V_{ref}=volume% of internal standard.

The calibration slopes of the various compounds were calculated from the formula:

$$SL_i = \frac{V_i/V_{TOL}}{A_i/A_{TOL}},$$

Let

$$Y_i = \frac{A_i}{A_{TOL}}$$

Then,

$$\text{Raw weight of i} = wt_i = (SL_i) * (Y_i) * (\rho_i)$$

$$raw\ wt\%_i = \frac{100 * wt_i}{\sum_j wt_j}$$

Now the feed used in the run must be determined, and the raw weights as shown are used in the equation below.

Let

$$(\text{Wt converted}) = \frac{W_j}{\sum_j W_j} - \frac{W_{i,feed}}{\sum_i W_{i,feed}}$$

where the subscripts i, j represent all compounds.

Then,

$$\%\text{Conversion of MTA} = \frac{100 * \left[\frac{Wt_{MTA,feed}}{\sum_i Wt_{i,feed}} - \frac{Wt_{MTA}}{\sum_j Wt_j} \right]}{\frac{\text{Wt}_{\text{MTA,feed}}}{\sum_i \text{Wt}_{\text{i,feed}}}}$$

$$\%\text{Conversion of DEA} = \frac{100 * \left[\frac{Wt_{DEA,feed}}{\sum_i Wt_{i,feed}} - \frac{Wt_{DEA}}{\sum_j Wt_j} \right]}{\frac{\text{Wt}_{\text{DEA,feed}}}{\sum_i \text{Wt}_{\text{i,feed}}}}$$

Where i represents any compounds in the feed, j any compound in the product stream..

The adjusted weight selectivity to compound j is given by the formula

$$\%\text{ Adjusted Weight Selectivity of j} = \frac{100 * \text{Wt}_\text{j}}{\sum_\text{j} \text{Wt}_\text{j}}$$

Where j are EMB, DBA, ETA, o-DEET, m-DEET, p-DEET, TMB, BETA, Heavies.

These formulae were put into a spreadsheet for the runs performed. Those spreadsheets are presented on the following pages.

Table B1. RUN NAME: D-26 FEED: DEA/MTA/DEET=1/1/0.75 FEED DENSITY 0.9366 g/mL
CATALYST: 4.6 atom% Tyzor TE/TiO_2 CAT. WT. : 2.612 g

Sample	T °C	P MPa	WHSV hr^{-1}	Conv. %	Adjusted wt.% DEET in products	Raw wt. DEET sel.%	ETA+DEET Sel. %	TOS hr	Comment
26A	245	2.21	4.2	33	91	97	98	5.67	
26B	246	2.21	2.1	34	87	96	97	7.42	
26C	245	2.21	1.7	55	96	97	98	10.42	
26D	245	2.21	2.3	42	95	98	97	12.42	
26E	245	2.82	1.7	38	96	98	96	15.09	
26F	245	2.82	2.2	31	92	97	95	17.76	
26G	246	3.01	2.3	32	96	97	98	20.51	
26H	247	2.21	1.3	27	96	98	98	22.01	

Table B2. RUN NAME: D-28 FEED: DEA/MTA/DEET=1/1/0.75 FEED DENSITY 0.9366 g/mL
CATALYST: 4.6 atom% Tyzor TE/TiO_2 CAT. WT. : 5.381 g

Sample	T °C	P MPa	WHSV hr^{-1}	Conv. %	Adjusted wt.% DEET in products	Raw wt. DEET sel.%	ETA+DEET Sel. %	TOS hr	Comment
28A	245	2.21	1.8	34	91	97	98	5.67	
28B	245	2.21	3.0	41	87	96	97	7.42	

Table B3. RUN NAME: D-32 FEED: DEA/MTA/DEET=1/1/0.75 FEED DENSITY 0.9366 g/mL
CATALYST: 4.6 atom% Tyzor TE/TiO_2 CAT. WT. : 7.356 g

Sample	T °C	P MPa	WHSV hr^{-1}	Conv. %	Adjusted wt.% DEET in products	Raw wt. DEET sel.%	ETA+DEET Sel. %	TOS hr	Comment
32A	250	2.14	1.1	36	82	52	98	4.58	
32C	250	2.14	1.3	40	88	64	98	24.41	
32D	250	2.21	0.97	39	88	67	97	31.91	N_2@250C
32E	255	2.21	0.97	40	86	67	99	45.91	
32F	250	2.14	0.85	37	90	61	99	50.49	N_2@250C
32H	265	2.14	0.80	46	80	56	99	69.74	

Table B4. RUN NAME: D-27 FEED: DEA/MTA/DEET=1/1/0.75 FEED DENSITY 0.9366 g/mL
CATALYST: 11.4 atom% Tyzor TE/Al_2O_3 CAT. WT. : 5.907 g

Sample	T °C	P MPa	WHSV hr^{-1}	Conv. %	Adjusted wt.% DEET in products	Raw wt. DEET sel.%	ETA+DEET Sel. %	TOS hr	Comment
27A	245	2.07	1.8	28	87	95	96	6	
27B	245	2.07	1.2	30	93	97	99	10	
27C	245	2.07	1.3	27	98	98	99	16.25	
27D	245	2.07	1.1	19	97	98	88	20	

Table B5. RUN NAME: D-33 A-P FEED: DEA/MTA/DEET=1/1/0.75 FEED DENSITY 0.9366 g/mL
CATALYST: 11.4 atom% Tyzor TE/Al_2O_3 CAT. WT. : 5.555g

Sample	T °C	P MPa	WHSV hr^{-1}	Conv. %	Adjusted wt.% DEET in products	Raw wt. DEET sel.%	ETA+DEET Sel. %	TOS hr	Comment
33A	250	2.14	1.10	36	84	66	99	13.5	
33B	250	2.14	0.94	38	85	64	99	20.08	N_2@250C
33C	250	2.14	1.10	34	82	59	99	32.33	
33D	250	2.14	1.28	48	83	62	99	38.5	N_2@250C
33E	250	2.14	1.23	31	88	59	99	45.5	
33F	250	2.14	1.08	42	90	63	99	46.17	
33G	250	2.14	1.08	47	87	64	99	56.84	N_2@250C
33H	250	2.14	1.25	36	85	54	98	63.92	
33I	250	2.14	1.01	31	84	61	98	76.42	
33J	250	2.14	1.94	29	81	56	96	80.5	N_2@250C
33K	250	2.14	1.05	31	90	54	98	86.97	
33L	250	2.14	1.20	26	86	49	98	99.93	
33M	250	2.14	1.22	38	81	56	99	103.4	N_2@250C
33N	250	2.14	1.25	38	85	58	99	110.40	
33P	250	2.14	0.99	44	83	60	99	123.23	

Table B6. RUN NAME: D-33 Q-ZB FEED: DEA/MTA/DEET=1/1/0.4 FEED DENSITY 0.9236 g/mL
CATALYST: 11.4 atom% Tyzor TE/Al_2O_3 CAT. WT. : 5.555g

Sample	T °C	P MPa	WHSV hr^{-1}	Conv. %	Adjusted wt.% DEET in products	Raw wt. DEET sel.%	ETA+DEET Sel. %	TOS hr	Comment
33Q	260	2.14	1.76	40	89	54	99	128.56	N_2@260C
33R	260	2.14	1.23	39	85	44	100	134.81	
33S	260	2.14	1.21	25	82	42	100	147.23	
33T	260	2.14	1.26	48	87	44	99	151.15	N_2@260C
33U	260	2.14	1.08	30	90	40	100	158.4	
33V	260	2.14	0.81	35	87	45	100	170.73	
33X	260	2.14	0.86	38	85	58	97	184.06	N_2@260C
33Y	260	2.14	1.08	36	81	58	99	195.98	
33Z	260	2.14	1.28	16	86	59	98	200.56	Air@500C
33ZA	260	2.14	1.10	27	85	62	97	206.98	
33ZB	260	2.14	0.83	29	89	60	99	218.98	

Table B7. RUN NAME: D-34A-F FEED: DEA/MTA/DEET=1/1/0.75 FEED DENSITY 0.9366 g/mL
CATALYST: HEA00, hydroxyapatites, Ca^{2+}/H^{+}=7.9 CAT. WT. : 2.601g

Sample	T °C	P MPa	WHSV hr^{-1}	Conv. %	Adjusted wt.% DEET in products	Raw wt. DEET sel.%	ETA+DEET Sel. %	TOS hr	Comment
34A	260	2.14	5.08	28	88	69	99	4.75	
34B	260	2.14	1.58	40	84	65	99	13.2	
34C	260	2.14	2.30	30	83	66	99	24.03	
34D	260	2.14	5.51	35	87	64	99	27.96	N_2@260C
34E	260	2.14	1.94	38	85	66	99	36.24	
34F	260	2.14	3.67	39	82	63	99	40.57	

Table B8. RUN NAME: D-34G-ZL FEED: DEA/MTA/DEET=1/1/0.4 FEED DENSITY 0.9236 g/mL
CATALYST: HEA00, hydroxyapatites, Ca^{2+}/H^{+}=7.9 CAT. WT. : 2.601g

Sample	T °C	P MPa	WHSV hr^{-1}	Conv. %	Adjusted wt.% DEET in products	Raw wt. DEET sel.%	ETA+DEET Sel. %	TOS hr	Comment
34G	260	2.14	3.94	46	92	62	100	46.82	N2@260C
34I	260	2.14	2.48	37	85	56	100	61.40	
34J	260	2.14	5.43	36	90	56	100	65.33	N2@260C
34K	260	2.14	1.92	36	84	52	100	73.61	
34L	260	2.14	2.27	35	85	56	100	85.89	
34M	260	2.14	4.83	33	85	52	99	89.65	Air@500C
34N	260	2.14	2.31	44	83	54	99	95.39	
34P	260	2.14	2.84	37	88	59	99	119.0	
34Q	260	2.14	4.83	36	86	53	99	122.9	N2@260C
34R	260	2.14	2.24	49	81	51	99	129.7	
34S	260	2.14	2.24	44	81	55	98	141.6	
34T	300	0.78	3.16	62	78	53	99	145.6	N2@300C
34U	300	0.78	2.20	59	80	56	99	152.6	
34V	300	0.78	2.31	63	79	61	99	165.2	
34W	300	0.78	2.98	64	82	59	99	169.7	N2@300C
34X	300	0.78	2.45	63	77	58	99	176.7	
34Y	300	0.78	1.78	68	77	60	98	189.2	
34ZA	300	3.50	3.44	65	55	52	98	194.0	Air@500C
34ZB	300	3.50	2.63	67	59	48	98	200.75	
34ZC	300	3.50	2.24	68	59	53	99	212.13	
34ZD	300	3.50	3.80	46	82	53	99	215.93	Air@500C
34ZE	300	3.50	2.63	56	83	59	99	222.68	
34ZF	300	0.44	2.24	61	81	57	98	234.83	
34ZG	300	0.44	3.20	48	79	56	98	238.83	N2@300C
34ZH	300	0.44	2.63	58	78	57	98	246.08	
34ZI	300	0.44	3.09	59	81	58	98	259.08	

Table B9. RUN NAME: D-34G-ZL FEED: DEA/MTA/DEET=1/1/0.4 FEED DENSITY 0.9236 g/mL
CATALYST: HEA00, hydroxyapatites, Ca^{2+}/H^{+}=7.9 CAT. WT. : 2.551g

Sample	T °C	P MPa	WHSV hr^{-1}	Conv. %	Adjusted wt.% DEET in products	Raw wt. DEET sel.%	ETA+DEET Sel. %	TOS hr	Comment
34ZJ	300	3.50	3.27	53	64	53	98	265.08	Air@500C
34ZK	300	3.50	2.10	49	52	48	99	271.66	
34ZL	300	3.50	1.95	71	53	51	99	282.49	

Table B10. RUN NAME: D-35 FEED: DEA/MTA/DEET=1/1/0.4 FEED DENSITY 0.9236 g/mL
CATALYST: HEA00,, hydroxyapatites, Ca^{2+}/H^{+}=7.9 CAT. WT. : 2.601g

Sample	T °C	P MPa	WHSV hr^{-1}	Conv. %	Adjusted wt.% DEET in products	Raw wt. DEET sel.%	ETA+DEET Sel. %	TOS hr	Comment
35A	300	3.67	3.87	69	59	52	98	4.28	
35B	300	3.67	2.32	76	49	48	97	11.53	
35C	300	3.67	2.17	79	35	46	98	24.43	
35D	300	0.1	3.08	60	84	65	99	28.83	Air@500C
35E	300	0.1	3.33	49	81	61	97	36.10	
35F	300	0.1	2.10	59	82	62	97	49.21	
35G	300	0.1	2.46	52	78	58	98	53.34	N_2@300C
35H	300	0.1	2.14	50	77	61	99	60.77	
35I	300	0.1	1.92	56	77	61	97	73.10	

Table B11. RUN NAME: D-36 FEED: DEA/MTA/DEET=1/1/0.4 FEED DENSITY 0.9236 g/mL
CATALYST: HEA01, hydroxyapatites, Ca^{2+}/H^{+}=6.3 CAT. WT. : 2.614g

Sample	T °C	P MPa	WHSV hr^{-1}	Conv. %	Adjusted wt.% DEET in products	Raw wt. DEET sel.%	ETA+DEET Sel. %	TOS hr	Comment
36A	300	0.1	2.69	61	92	68	100	4.8	
36B	300	0.1	1.80	60	90	62	100	13.01	
36C	300	0.1	2.19	60	89	64	100	24.84	
36D	300	0.1	2.23	56	88	63	100	29.59	N_2@300C
36E	300	0.1	2.33	57	88	63	100	36.59	
36F	300	0.1	2.61	50	86	63	100	48.59	
36G	300	0.1	2.61	54	88	52	100	53.34	Air@500C
36H	300	0.1	1.94	70	90	66	98	61.01	
36I	300	0.1	2.37	57	87	60	99	72.76	
36J	300	0.1	2.08	53	93	65	100	79.51	Air@500C
36K	300	0.1	1.78	64	92	67	100	85.68	
36L	300	0.1	2.47	60	91	64	100	97.26	
36M	320	0.1	2.33	61	91	61	100	101.68	Air@500C
36N	320	0.1	2.37	70	90	62	100	109.15	
36P	320	0.1	2.26	59	85	63	100	120.73	
36Q	320	0.1	2.47	52	83	56	99	125.33	Air@500C
36R	320	0.1	2.23	63	84	61	98	131.81	
36S	320	0.1	2.72	50	80	59	98	143.86	

Table B12. RUN NAME: D-37 FEED: DEA/MTA/DEET=1/1/0.4 FEED DENSITY 0.9236 g/mL
CATALYST: YJ01, 40 wt% HPA/Silica Gel CAT. WT. : 2.575g

Sample	T °C	P MPa	WHSV hr^{-1}	Conv. %	Adjusted wt.% DEET in products	Raw wt. DEET sel.%	ETA+DEET Sel. %	TOS hr	Comment
37A	300	0.1	2.33	69	82	58	97	4.58	
37B	300	0.1	2.12	70	82	65	99	12.33	
37C	300	0.1	2.62	70	82	62	97	23.66	

Table B13. RUN NAME: D-37 FEED: DEA/MTA/DEET=1/1/0.4 FEED DENSITY: 0.9236 g/mL
CATALYST: YJ01, 40 wt% HPA/Silica Gel CAT. WT. : 2.575g

Sample	T °C	P MPa	WHSV hr^{-1}	Conv. %	Adjusted wt.% DEET in products	Raw wt. DEET sel.%	ETA+DEET Sel. %	TOS hr	Comment
37D	300	0.1	3.23	64	86	65	99	28.0	N_2@300C
37E	300	0.1	2.01	63	86	65	98	33.92	
37F	300	0.1	2.26	60	81	62	98	46.62	
37G	300	0.1	2.65	65	84	58	99	50.95	Air@450C
37H	300	0.1	2.8	70	90	63	99	58.62	
37I	300	0.1	2.76	57	85	65	99	70.62	
37J	300	0.1	3.19	63	95	63	100	75.12	Air@450C
37K	300	0.1	4.34	63	97	67	100	82.45	
37L	300	0.1	3.34	62	94	65	99	94.78	
37M	300	0.1	3.23	63	95	69	99	99.96	Air@450C
37N	300	0.1	3.12	68	93	66	99	107.0	
37P	300	0.1	2.87	66	93	67	99	118.8	
37Q	300	0.1	3.69	65	93	68	99	123.2	Air@450C
37R	300	0.1	3.41	66	92	66	97	130.5	
37S	300	0.1	3.19	67	94	66	99	142.7	
37T	300	0.1	3.44	66	94	63	99	147.1	Air@450C
37U	300	0.1	3.55	67	95	64	97	154.4	
37V	300	0.1	4.02	64	95	65	99	167.6	
37W	300	0.1	4.30	66	95	63	99	172.3	Air@450C
37X	300	0.1	4.27	67	96	64	99	179.8	
37Y	300	0.1	4.45	66	94	64	99	190.4	
37Z	320	0.1	4.70	68	92	64	99	194.8	Air@450C
37ZA	320	0.1	4.48	66	92	64	100	201.4	
37ZB	320	0.1	5.09	67	92	65	99	214.1	

Table B14. RUN NAME: D-37 FEED: DEA/MTA/DEET=1/1/0.4 FEED DENSITY: 0.9236 g/mL
CATALYST: YJ01, 40 wt% HPA/Silica Gel CAT. WT. : 2.575g

Sample	T °C	P MPa	WHSV hr^{-1}	Conv. %	Adjusted wt.% DEET in products	Raw wt. DEET sel.%	ETA+DEET Sel. %	TOS hr	Comment
37ZC	300	0.1	4.81	64	93	63	100	219.0	Air@450C
37ZD	300	0.1	4.02	65	97	63	100	226.5	
37ZE	300	0.1	5.09	66	95	61	100	238.1	
37ZF	300	0.1	4.52	57	94	57	100	242.2	Air@450C
37ZG	300	0.1	4.63	65	94	60	100	252.5	
37ZH	300	0.1	4.63	65	94	63	100	261.7	
37ZI	250	0.1	4.41	56	86	32	98	266.7	Air@450C
37ZJ	250	0.1	2.62	55	91	44	99	273.4	
37ZK	250	0.1	4.48	51	93	42	99	284.8	
37ZL	300	0.95	4.27	66	86	47	100	289.2	Air@450C
37ZM	300	0.95	5.24	67	91	55	100	296.0	
37ZN	300	0.95	6.06	64	91	58	100	306.6	

Table B15. RUN NAME: D-38 FEED: DEA/MTA/DEET=1/1/0.4 FEED DENSITY: 0.9236 g/mL
CATALYST: YJ01, 40 wt% HPA/Silica Gel CAT. WT. : 1.390g

Sample	T °C	P MPa	WHSV hr^{-1}	Conv. %	Adjusted wt.% DEET in products	Raw wt. DEET sel.%	ETA+DEET Sel. %	TOS hr	Comment
38A	300	0.1	6.05	70	92	59	99	4.42	
38B	300	0.1	4.99	69	93	61	99	11.9	
38C	300	0.1	6.39	69	92	63	100	22.8	
38D	300	0.1	8.97	61	91	58	99	26.5	Air@450C
38E	300	0.1	7.51	67	86	59	98	33.3	
38F	300	0.1	8.71	68	93	57	99	44.2	
38G	320	0.1	9.31	63	88	58	100	48.2	Air@450C
38H	320	0.1	8.18	68	87	61	99	54.7	
38I	320	0.1	5.72	68	80	59	99	68.3	

Table B16. RUN NAME: D-39 FEED: DEA/MTA/DEET=1/1/0.4 FEED DENSITY 0.9236 g/mL
CATALYST: Davison 57 Silica Gel CAT. WT. : 0.6428 g

Sample	T °C	P MPa	WHSV hr^{-1}	Conv. %	Adjusted wt.% DEET in products	Raw wt. DEET sel.%	ETA+DEET Sel. %	TOS hr	Comment
39A	300	0.1	9.48	46	90	46	100	5.75	
39B	300	0.1	9.6	46	87	54	100	11.45	
39C	300	0.1	10.6	42	87	49	100	23.67	
39D	300	0.1	12.2	52	87	55	100	28.25	Air@450C
39E	300	0.1	10.5	54	80	54	98	34.67	
39F	300	0.1	10.2	57	78	51	100	47.08	
39G	300	0.1	6.3	57	85	52	96	52.08	Air@450C
39H	300	0.1	5.75	55	75	54	100	58.08	
39I	300	0.1	5.60	55	69	54	97	70.58	
39J	250	0.1	6.32	54	72	50	97	75.08	Air@450C
39K	250	0.1	6.47	46	77	46	97	81.58	
39L	250	0.1	6.18	46	77	49	100	94.17	

Table B17. RUN NAME: D-40 FEED: DEA/THN =1/1.6, FEED DENSITY:0.7550 g/mL
CATALYST: Davison 57 Silica Gel CAT. WT. : 0.6428 g

Sample	T °C	P MPa	WHSV hr^{-1}	Conv. %	Adjusted wt.% DEET in products	Raw wt. DEET sel.%	ETA+DEET Sel. %	TOS hr	Comment
40A	300	0.1	11.2	0	0	0	0	6.45	

Table B18. RUN NAME: D-41 FEED: DEA/MTA/DEET =1/1/0.4 FEED DENSITY: 0.9236 g/mL
CATALYST: YJ03, 40 wt.% CsHPA/MCM-41, Cs^+/H^+=2.5/0.5 CAT. WT. : 0.6415 g

Sample	T °C	P MPa	WHSV hr^{-1}	Conv. %	Adjusted wt.% DEET in products	Raw wt. DEET sel.%	ETA+DEET Sel. %	TOS hr	Comment
41A	300	0.1	5.62	62	75	41	100	4.33	
41B	300	0.1	3.31	63	80	54	97	6.5	
41C	300	0.1	9.50	42	85	51	98	11	
41D	320	0.1	5.04	38	86	52	98	17.58	Air@450C
41E	300	1.1	10.1	44	86	54	94	22.5	
41F	300	1.1	6.62	58	43	50	95	27.5	
41G	250	1.1	5.9	55	51	51	97	32.92	
41H	300	0.1	11.1	50	52	52	99	39	Air@450C
41I	300	0.1	8.49	58	52	52	97	43.83	
41J	300	0.1	8.78	50	51	51	98	55.83	

Table B19. RUN NAME: D-43 FEED: DEA/MTA/DEET =1/1/0.4 FEED DENSITY: 0.9236 g/mL
CATALYST: YJ10, 40 wt.% CsHPA/MCM-41, Cs^+/H^+=1/2 CAT. WT. : 0.9 g

Sample	T °C	P MPa	WHSV hr^{-1}	Conv. %	Adjusted wt.% DEET in products	Raw wt. DEET sel.%	ETA+DEET Sel. %	TOS hr	Comment
43A	300	0.1	6.67	52	90	61	98	4.75	
43B	300	0.1	6.67	51	91	64	99	11.7	
43C	300	0.1	6.98	50	93	64	99	21.2	

Table B20. RUN NAME: D-44 FEED: DEA/MTA/DEET =1/1/0.4 FEED DENSITY: 0.9236 g/mL
CATALYST: YJ10, 40 wt.% CsHPA/MCM-41, Cs^{+}/H^{+}=1/2 CAT. WT. : 0.9 g

Sample	T °C	P MPa	WHSV hr^{-1}	Conv. %	Adjusted wt.% DEET in products	Raw wt. DEET sel.%	ETA+DEET Sel. %	TOS hr	Comment
44A	300	0.1	5.03	52	90	61	98	4.28	
44B	300	0.1	6.06	51	91	64	99	16.5	
44C	300	0.1	6.16	42	93	59	98	21	Air@450C
44D	300	0.1	5.64	50	96	61	99	28.67	
44E	300	0.1	6.06	45	94	63	98	40.5	
44F	300	0.1	5.75	44	94	58	99	44.95	N_2@300C
44G	300	0.1	5.44	49	93	57	98	53.68	
44H	300	0.1	5.95	50	97	64	100	64.6	
44I	300	0.1	5.85	48	97	64	100	70.05	N_2@300C
44J	300	0.1	6.06	45	96	58	99	74.55	
44K	300	0.1	6.16	45	97	59	100	86.05	

Appendix C: Calculations for MTA Synthesis

1. No Products in the Primary Feed:

Gas phase calculation:

Calculation of gas molar number N_i(gmols) at 25℃, 1atm from gas meter or measured flow rates.

The total gas molars number:

$$NTG = \sum_{i=1}^{n_i}(N_i)(y_{CO_2,i}) + \sum_{i=1}^{n_i}(N_i)(y_{CO_2,i}) + 8\sum_{i=1}^{n_i}(N_i)(y_{xy})_i$$

The weight of solution in gas:

$$GW = 12\sum_{i=1}^{n_i}(N_i)(y_{CO_2})_i + 12\sum_{i=1}^{n_i}(N_i)(y_{CO})_i + 106\sum_{i=1}^{n_i}(N_i)(y_{xy})_i$$

- If N_i is not measured, it should be estimated from the total gas space above the reactor.

Liquid and solid phase calculation:

Solid weight SW is measured after experiment.

Liquid weight is calculated from the below equation:

$$LW = WT_{m-xylene,t=0} - GW - SW$$

Benzoic acid (BA,99.5%) was used as an internal standard. For MTA feeds, 1.0mL of a 1.0 wt% benzoic acid ethanol/methanol=1/1 solution was added to the 0.1mL product sample before GC analysis.

Let: SL_j=slope of calibration curve of j.

ρ_j=calibration density of j.

A_j=area% of j.

A_{ref}=area% of reference standard (internal standard), benzoic acid.

V_j=volume% of j.

V_{ref}=volume% of reference standard (internal standard), benzoic acid.

ρ_j= calculation density of compound j.

Then the calibration slopes of the various compounds were calculated from the formula:

$$SL_j = \frac{V_j/V_{BA}}{A_j/A_{BA}},$$

where SL_j is the calibration slope of compound j.

Raw liquid weight fraction of the compound j:

$$WL_j = \frac{(SL_j)(A_j)(\rho_j)}{A_{ref}}$$

Raw solid weight fraction of the compound j:

$$WS_j = \frac{(SL_j)(A_j)(\rho_j)}{A_{ref}}$$

So liquid weight fraction of the compound j is:

$$wl_j = \frac{100WL_j}{\sum_j WL_j}.$$

Solid weight fraction of the compound j is:

$$ws_j = \frac{100WS_j}{\sum_j WS_j}.$$

The total weight fraction including the solid and liquid of the compound j is:

$$WT_j\% = (WL_j)(\frac{LW}{LW + SW}) + (WS_j)(\frac{SW}{LW + SW})$$

2. Products Present in the Primary Feed (Adjusted WT% calculation):

If some fraction of products is added into the primary feed and after the contents of all compounds in the feed sample are analyzed except m-xylene, the following equation is used to get the adjusted WT% for every compound except m-xylene.

$$(ADJ.WT\%)_j = (WT\%)_j - (WT\%)_{j,feed}$$

Then the adjusted wt% for the compound j in the product is calculated by the equation below.

$$(ADJ.wt\%)_j = 100 \times (\frac{(ADJ.WT\%)_j}{\sum (ADJ.WT\%)_j})$$

Moles of carbon of reactants or products excluding products added to the feed.

Let:

$$NT = \frac{8(WT.of \quad m- \ XYLENE)_{t=0}}{MW_{XYLENE}}$$

$$NTL = \left[\frac{8(WT.of \quad XLYLENE)_{t=0}}{MW_{XYLENE}}\right] - NTG$$

Then the moles of carbon of the compound j are:

$$(Moles \quad of \quad carbon)_j = \left[\frac{(WT\%)_{LIQ,j}}{MW_j}\right](No. \quad of \quad carbon \quad atoms)_j$$

Then,

$$(ADJ. \quad Moles \quad of \quad Carbon)_j = \left[\frac{(Moles \quad of \quad Carbon)_j}{\sum_j (Moles \quad of \quad Carbon)_j}\right](NTL)$$

Calculation of conversion and selectivity:

$$(Total\%Conversion)_{m-XYLENE} = \left[\frac{NT - (ADJ.\quad Moles\quad of\quad Carbon)_{m-XYLENE} - 8\sum_{i=1}^{n_i} (N_i)(y_{xy})_i}{NT} \right] \times 100$$

$$(\%selectivity)_j = \frac{100 \times (ADJ.\quad Moles\quad of\quad Carbon)_j}{\left[NT - (ADJ.\quad Moles\quad of\quad Carbon)_{m-xylene} - 8\sum_{i=1}^{n_i} (N_i)(y_{xylene})_i \right]}$$

$$(\%selectivity)_{CO_2} = \frac{100\sum_i (N_i)(y_{CO_2})_i}{\left[NT - (ADJ.\quad Moles\quad of\quad Carbon)_{m-xylene} - 8\sum (N_i)(y_{xy})_i \right]}$$

$$(\%selectivity)_{CO} = \frac{100\sum_i (N_i)(y_{CO})_j}{\left[NT - (ADJ.\quad Moles\quad of\quad Carbon)_{m-xylene} - 8\sum_{i=1}^{n_i} (N_i)(y_{xy})_i \right]}$$

- The sum of the selectivity of all compounds should be closed to 100%.

Appendix D: Calculation of Saturation Pressure for DEET Feed

The DEET feed saturation pressures at different temperatures were estimated by treating the feed mixture as ideal, therefore following Raoult's law. The saturation pressures of DEET, MTA and DEA at different temperatures were calculated by the Antoine equation (D-1) (Smith and Van Ness, 1987):

$$Log_{10} P^{sat} = A - \frac{B}{T + C} \qquad (P, \quad bar; T, K) \qquad (D-1)$$

The constants A, B and C for DEET and MTA were determined using 3 data points. Antoine constants for DEA were found from a standard reference (NIST Chemistry WebBook, 2001). The estimated vapor pressures were compared with some actual experimental pressures. The % error was found to be less than 10%.

The experimental data for DEET saturation pressures are given in Table D.1. After solving the three parameter equation to get A, B and C, the Antoine equation of DEET is given as equation (D-2).

Table D.1. Three experimental points, DEET saturation pressure

Tempreature, K	298.15	384.15	433.15
Saturature Vapor Pressure, Bar[1]	2.226×10^{-6}	0.001333	0.02533
Reference	MGK, 1998	MGK, 1998	MGK, 1998

[1] 1 bar=0.1MPa

$$Log_{10} P^{sat}_{DEET} = 15.5364 - \frac{12087.33}{T + 272.306} \qquad (P, \quad bar; T, \quad K) \qquad (D-2)$$

The three experimental saturation vapor pressures for DEET are given in Table D.2. After solving the three parameter equation to get A, B and C, the Antoine equation of MTA is given as equation (D-3).

Table D.2. Three experimental points of MTA saturation pressure

Temperature, K	298.15	384.15	536.15
Saturation Vapor Pressure, Bar[1]	3.14563×10^{-7}	0.001333	1.013
Reference	Colomina, M. et al., 1986	2	Aldrich, 1990

[1] bar=0.1Mpa

[2] Information Handling Services. Material Safety Data Sheets Service. Microfiche Ed. Bimonthly Updates. August/September 1990. #5833-655, B-12.

$$Log_{10}P^{sat}_{MTA} = 3.08236 - \frac{1131.20}{T - 168.493} \qquad (P,bar;\quad T,K) \qquad (D-3)$$

The Antoine equation for DEA is given as equation (D-4) (Bittrich and Kauer, 1962). The estimated saturation vapor pressures were compared with the experimental values and summarized in Table D.3.

$$Log_{10}P^{sat}_{DEA} = 2.86193 - \frac{559.071}{T - 132.974} \qquad (P,bar;\quad T,K) \qquad (D-4)$$

TableD.3. Error% of Estimated Vapor Pressures to Experimental Values

Temperature, K	293.15	298.15	328.65
Estimated values, bar	0.23537	0.3	1.011
Experimental values, bar	0.2559	0.3159	1.013
Error%	-8.0	-5.0	-0.2

DEET Feed Vapor Pressure

From the above equations, DEET feed vapor pressures at different temperatures were estimated and summarized in Table D.4.

Table D.4. DEET Feed Saturation Vapor Pressure at Different Temperatures

T, ºC		245	250	260	300	320
T, K		518.15	523.15	533.15	573.15	593.15
Feed A [1] P^{sat}	bar	10.09	10.65	11.88	18.55	27.22
	MPa	1.009	1.065	1.188	1.855	2.722
Feed B[2] P^{sat}	bar	11.31	11.88	13.11	18.73	25.77
	MPa	1.131	1.188	1.311	1.873	2.577
Pure DEET	bar	1.76	2.19	3.39	17.36	37.15
	MPa	0.176	0.219	0.339	1.736	3.715

[1]Feed A, $P^{sat}=(P^{sat}_{DEA}+P^{sat}_{MTA}+0.75P^{sat}_{DEET})/2.75$.

[2]Feed B, $P^{sat}=(P^{sat}_{DEA}+P^{sat}_{MTA}+0.4P^{sat}_{DEET})/2.4$.

Appendix E: Vapor Pressure of m-Xylene

Table E.1. The relationship between temperature and vapor pressure of m-xylene

T (˚C)	P (Mpa)	T (˚C)	P (Mpa)
80	0.0149	165	0.191
85	0.0180	170	0.214
90	0.0217	175	0.240
95	0.0259	180	0.267
100	0.0308	185	0.297
105	0.0363	190	0.330
110	0.0427	195	0.365
115	0.0500	200	0.403
120	0.0582	205	0.444
125	0.0674	210	0.489
130	0.0778	215	0.536
135	0.0894	220	0.587
140	0.102	225	0.641
145	0.117	230	0.700
150	0.133	235	0.762
155	0.150	240	0.828
160	0.170		

Appendix F: Kinetics of p-Xylene Oxidation

The rate constant ratios for m-xylene oxdation to p-xylene oxidation can be used to determine the relative efficiency of different catalyst systems. The kinetics of p-xylene are from Cao and Servida (1994). Their homogeneous catalytic oxidation system is summarized in Table F-1.

Table F-1 Catalytic oxidation system for p-xylene

Catalyst[1]	Solvent	Promoter
$Co(NA)_3$, 104 ppm based on p-xylene	Methyl benzoate / p-xylene = 1/1 mol ratio	p-tolualdehyde/p-xylene = 31.4mmol/mol

[1] NA, naphthenate.

By taking into account only the reactions leading to the most important intermediate and final products, the following lumped kinetics scheme for PX oxidation to PTA was proposed:

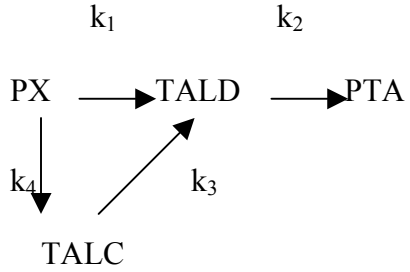

Based on lumping the complex chain mechanism of the oxidation process, the oxidation reactions were assumed to be zeroth-order with respect to oxygen and first-order with respect to the liquid reactant if the oxygen flux entering the liquid bulk was sufficient to sustain the reaction. Their kinetics data are summarized in Table F-2.

Table F-2 Data for p-xylene oxidation, Cao and Servida (1994).

T, C	1/(T+273)	k1,1/min	k2,1/min	k3,1/min	k4,1/min	(k1+k4),1/min
80	0.002833	0.000137	0.00488	0.0018495	5.07E-05	0.00018769
90	0.002755	0.000233	0.00764	0.0035183	9.55E-05	0.00032853
100	0.002681	0.000404	0.01426	0.0091304	0.000246	0.00065044
105	0.002646	0.000654	0.02139	0.0130146	0.000327	0.000981
110	0.002611	0.000794	0.02946	0.0203264	0.000556	0.0013498
120	0.002545	0.00125	0.05138	0.029625	0.00095	0.0022

These data were regressed to Arrhenius form. The plots of temperature vs. rate constants are given below.

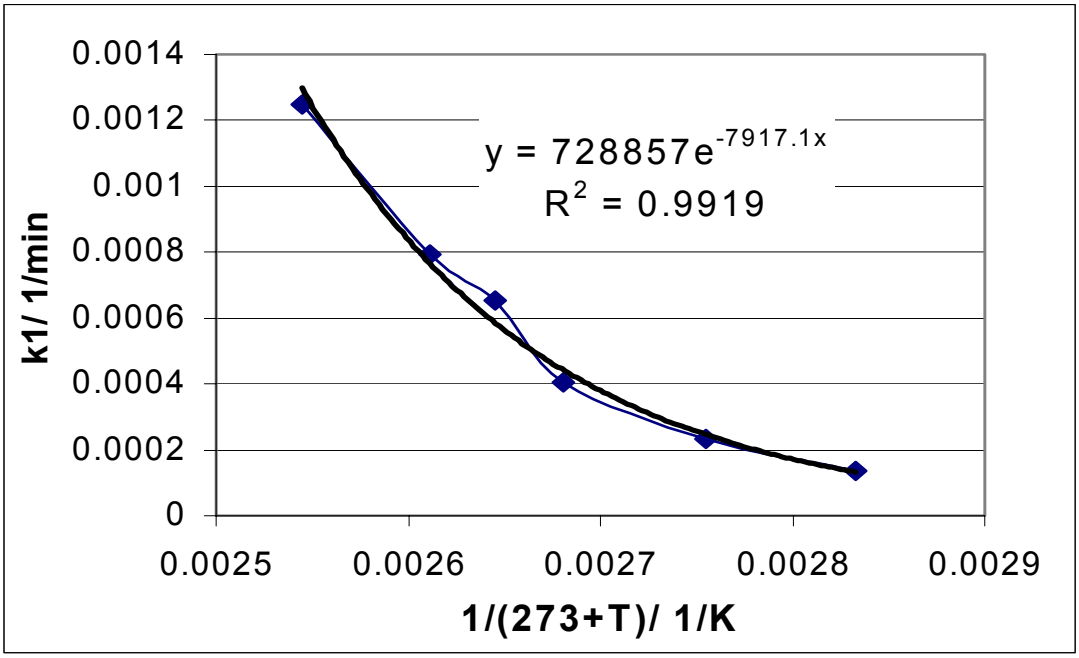

Fig. F-1 Arrhenius fit for k_1

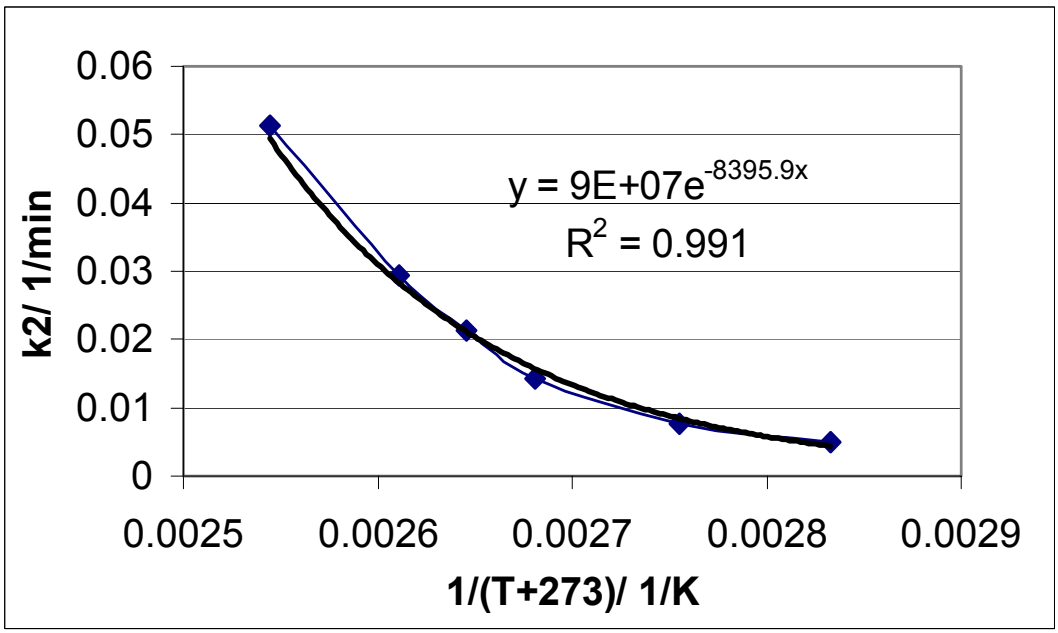

Fig. F-2 Arrhenius fit for k_2

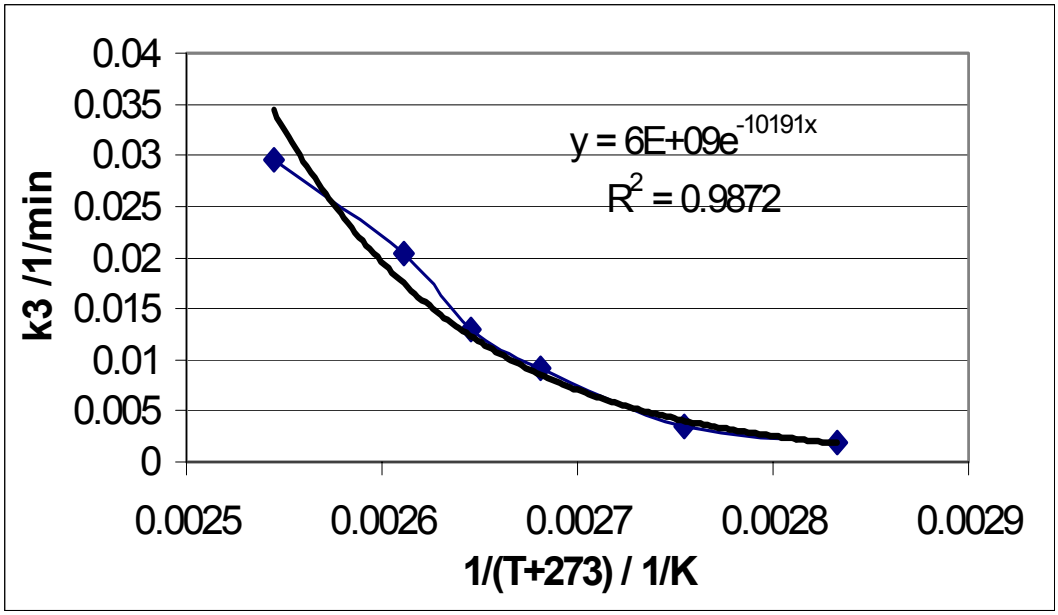

Fig. F-3 Arrhenius fit for k_3

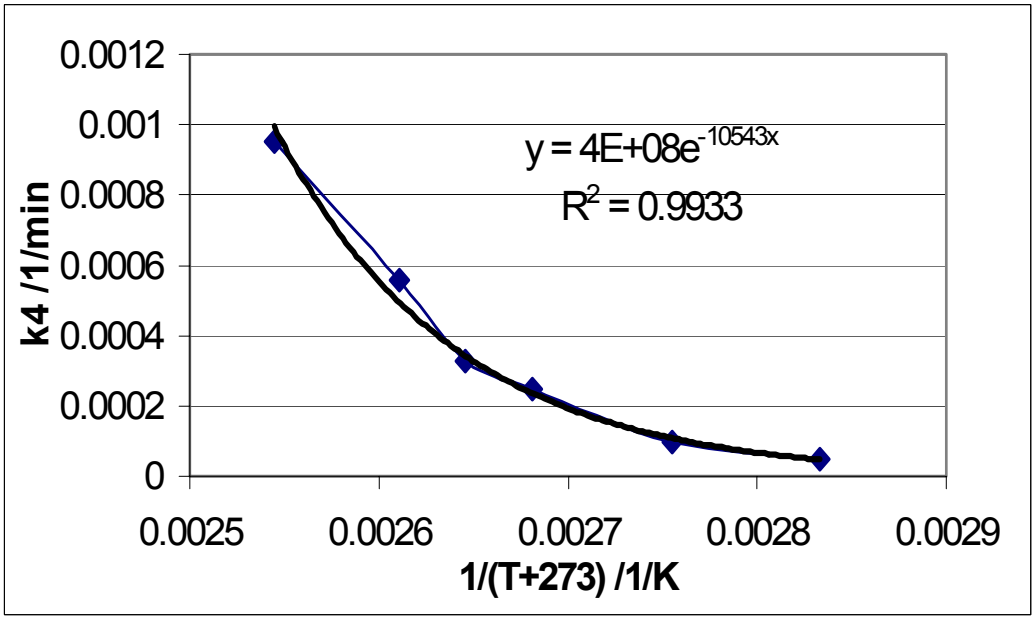

Fig. F-4 Arrhenius fit for k_4

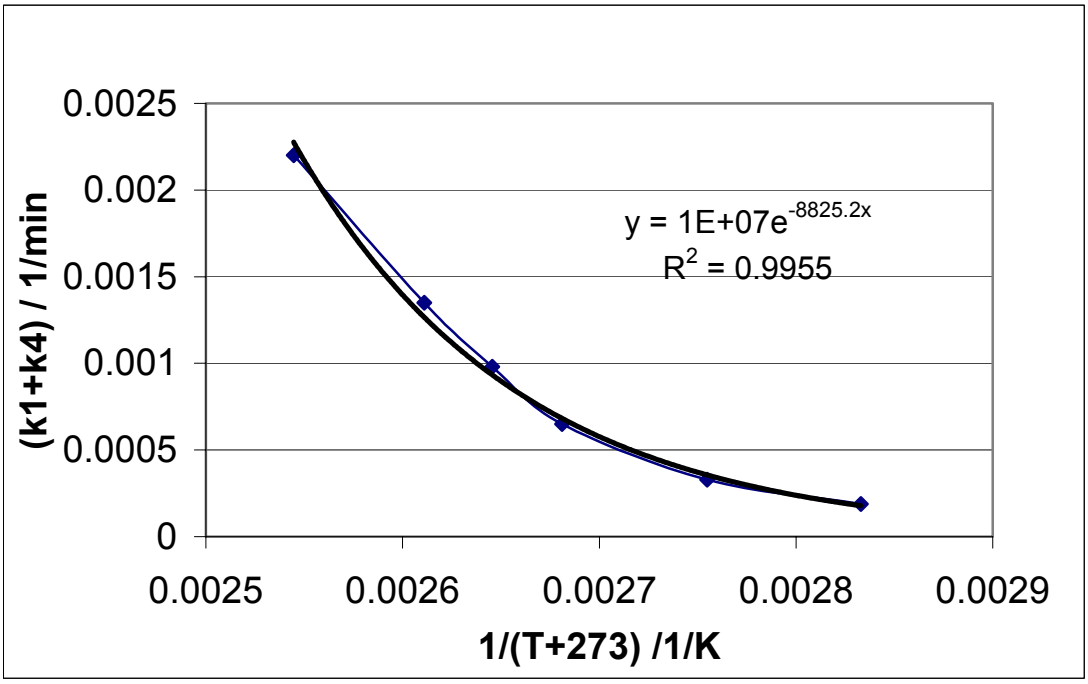

Fig. F-5 Arrherius fit for (k_1+k_4)

In order to compare the results for different catalysts, the values ($k_1 + k_4$) were adjusted for catalyst usage in the reaction, with the amount of catalyst used by Cao and Servida (104 ppm) as the baseline. The adjusted $(k_1+k_4)_{adj}$ was computed as follows.

$$(k_1 + k_4)_{adj} = (k_1 + k_4) \exp\left[-8825.2\left(\frac{1}{T_{adj}} - \frac{1}{T} \right) \right] \left(\frac{C_{base}}{C_{cat}}\right) \qquad (F-1)$$

Here, T_{adj} = 393 K, T in K. C_{base} is the catalyst concentration that Cao and Servida used (0.19 mmol/mol p-xylene). $C_{cat.}$ is the metal catalyst concentration in our experiments (mmol/mol m-xylene).

Appendix G: TGA Results and Co Content Calculation for Co(salen)

TGA results for supported Co(salen) are summarized in Table G.1.

Table G.1. TGA Results for supported Co(salen)

Catalysts	First Peak			Second Peak			Co% mmol/g Calculated	Co%, mmol/g stoichiometric
	T, ^{o}C	Original wt%	Final wt %	T, ^{o}C	Original wt%	Final wt %		
Co(salen)	114~260	99.4	95.1	304~498	94.8	81.6	0.511	0.516

Assuming the following reaction at high temperature, the Co% can be calculated approximately according to the TGA data.

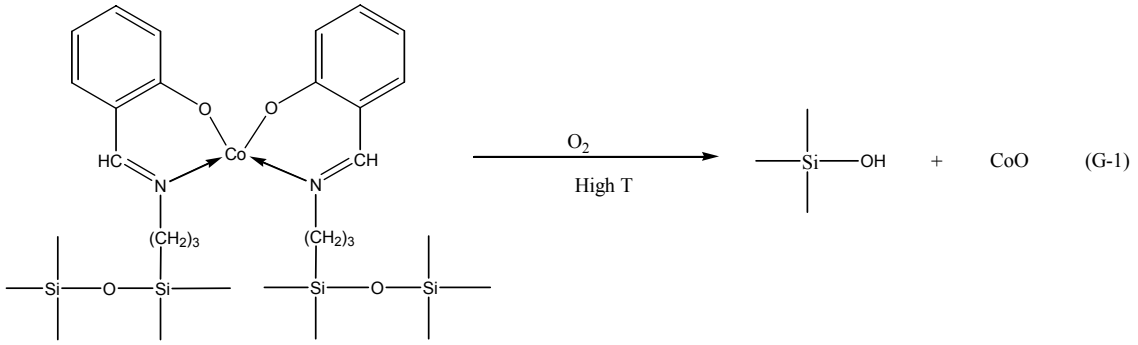

The first peak, from 114-260 ^{o}C, represents the weight loss of residual EtOH, ethoxide and other solvents. The second peak represents the decomposition of the complex.

Based on the second peak, the actual wt% loss is 13.2/0.948 (%)=13.9 (%). From the above reaction at high temperature at air, the molecular weight change per Co complex is (381-109) = 272, Co content will be 10*13.9/272 = **0.511 mmol/g (30110 ppmCo/g cat.).** The stoichiometric molecular weight of the original Co(salen) complex is (381+56) = 437, the weight is 437 g/mol*0.006 mol = 2.62 g. With 150 mmol TEOS, we can get 9.0 g SiO_2 (0.150 mol*60 g/mol = 9.0g). Therefore, the stoichiometric Co content, assuming all complexes reacted with SiO_2, is 6/(2.62+9.0) = **0.516 mmol/g.**

Vita

Yujun Song was born on April 2, 1971, to Mr. and Mrs. M. Song of Henan, People's Republic of China. Song graduated with his degree of Bachelor of Science in polymer chemical engineering in 1992 at Nanjing University of Chemical Technology. After several years' work and study, Song entered the graduate program at Louisiana State University in Baton Rouge, Louisiana, in 2000. This thesis completes his requirements to receive the degree of Master of Science in Chemical Engineering, which will be awarded in December 2002. After that, Song will continue his doctoral studies in the Department of Chemistry of Louisiana State University.